Die approbierte Originalversion dieser Diplom-/Masterarbeit ist in der Hauptbibliothek der Technischen Universität Wien aufgestellt und zugänglich.
http://www.ub.tuwien.ac.at

The approved original version of this diploma or master thesis is available at the main library of the Vienna University of Technology.
http://www.ub.tuwien.ac.at/eng

TECHNISCHE UNIVERSITÄT WIEN
Vienna University of Technology

MEDICAL UNIVERSITY OF VIENNA

DIPLOMA THESIS

Conditioning of Posterior Root Reflexes by Single-Joint Voluntary Motor Tasks

Supervised by

Ao. Univ.-Prof. Dipl.-Ing. Dr. h.c. Dr. Winfried Mayr

INSTITUTE OF MECHANICS AND MECHATRONICS, VIENNA UNIVERSITY OF TECHNOLOGY
CENTER FOR MEDICAL PHYSICS AND BIOMEDICAL ENGINEERING, MEDICAL UNIVERSITY OF VIENNA

&

Dipl.-Ing. Dr. Matthias Krenn

CENTER FOR MEDICAL PHYSICS AND BIOMEDICAL ENGINEERING, MEDICAL UNIVERSITY OF VIENNA

Submitted by

Cosmin Tabacariu, BSc
Hütteldorferstraße 155/31
1140, Wien

Vienna, February 2016

Acknowledgements

My gratitude goes first to Dr. Matthias Krenn, who guided me step-by-step through the whole project. I thank Dr. Winfried Mayr for his inspiring vision, that arouse my interest on this field of research. I appreciate Dr. Milan Dimitrijevic for his constructive impulses and his humorous way of teaching. Thanks to my colleagues for assistance during the measurements!

Above all, I want to thank my family, and my fiancée Jana Bremicker, who supported and encouraged me through these intensive months, and blessed me with a joyful life throughout my studies, visions and goals.

Abstract

Electrical stimulation of the human lumbosacral posterior roots is used to evoke spinal reflexes and to neuromodulate altered sensory-motor function following spinal cord injury. The posterior roots can be depolarized by epidural as well as transcutaneous electrical stimulation. Here we present preliminary results of conditioning of the reflex pathway using volitional motor tasks.

The posterior root reflexes (PRR) were elicited by transcutaneous stimulation at the T11-T12 vertebral level. The conditioning input was generated by unilateral dorsi- and plantar flexion in supine position. First tSCS was demonstrated to evoke effectively short-latency reflexes, in all recorded leg muscle groups. The reflex nature was proved by attenuation of reflex responses when stimuli were applied in close succession (inter-stimuli interval 35 ms). Test responses, elicited at a stimulation rate of two pulses per second were inhibited in ipsilateral triceps surae during dorsiflexion, compared to rest. When conditioned by plantar flexion, responses in hamstrings, tibialis anterior, and triceps surae showed facilitation accompanied by muscular contraction. Due to functional equivalence, observed PRR modifications can be interpreted by previous studies of H reflex modification, particularly by the mechanisms of reciprocal Ia-inhibition and monosynaptic Ia excitation.
Overall, the presented new methodology is a first step to assess spinal networks in healthy and disabled subjects. In further studies, the supraspinal influence to the lumbosacral network can be analyzed in more detail by using this work as a starting point.

Glossary and Abbreviations

Action potential electrical impulse transmitted through neurons, fundamental unit of information

Agonist contracting muscle that causes a movement to occur

Antagonist opposing muscle to agonist

Antidromic conduction of an action potential opposite of the normal direction

Axon long process of a nerve cell that conducts action potentials from the cell body

Cauda equina bundle of spinal nerves, consisting of nerve pairs from the second lumbar segment to the coccygeal segment

Contralateral on the opposite side of the body

Common peroneal nerve (CNP) nerve fiber descending obliquely along the lateral side of the popliteal fossa, innervates lateral and anterior lower leg muscles

Crosstalk undesired effect that a measured signal transmitted on one channel creates in another channel

Dorsiflexion backward flexion of the foot

Dura mater cerebral membrane surrounding the spinal cord

Electromyography (EMG) electrodiagnostic technique of recording electrical potential generated by muscle cells

Epidural outside the dura mater, within the spinal canal

Hamstrings (H) muscle group of three knee flexor muscles

Homonymous affecting the same part

Ipsilateral on the same side of the body

Isotonic at unchanged tension

Plantar flexion downward flexion of the foot

Posterior root reflex (PRR) spinal reflex elicited by electrical stimulation of posterior roots

Quadriceps (Q) muscle group of four knee extensor muscles

Reciprocal affecting the opposite part

Spinal cord cylindrical part of the central nervous system within the spinal canal

Spinal cord stimulation (SCS) stimulation of spinal cord nerves with electrodes

Spinally evoked potential electrical signal generated by the nervous system in response to a sensory stimulus at the spinal cord

Synergist muscle that perform the same set of joint motion as the agonist

Tibialis anterior (TA) medial muscle of the anterior lower leg, induces dorsiflexion

Transcutaneous applied through the skin

Triceps surae (TS) pair of muscles located at the calf, induces plantar flexion

Vertebra a spinal column segment

Contents

1

Introduction

Electrical spinal cord stimulation (SCS) in patients suffering spinal cord injury has been used in the past decades for intervention and assessment. Over the last years, SCS was also used to improve or augment motor functions in paraplegic individuals, which has been demonstrated in various remarkable case studies (Dy et al., 2010; Gerasimenko, Roy, & Edgerton, 2008; Hofstoetter et al., 2013). Dimitrijevic et al. (1998) activated spinal networks in patients with complete spinal cord injury using electrodes that were surgically placed in the epidural space of the lumbar spinal cord. The evoked movements were rhythmical and/or stepping-like. These movements indicate a human spinal locomotor pattern generator within the spinal circuits, which can be activated even when the spinal segments are isolated from brain control.

Next to epidural SCS also, transcutaneous SCS (tSCS) is capable of activating afferent fibers of large diameters within the posterior roots (Minassian et al., 2004; Murg, Binder, & Dimitrijevic, 2000). Minassian et al. (2007a), demonstrated that the same afferent structures are depolarized transcutaneously compared to stimulation by implanted epidural electrodes. Therefore, the electrodes were placed above the lumbar spine and on the abdomen to generate a trans-spinal electrical field. This non-invasive technique eliminates the need of a cost-intensive surgery, related infection and compatibility risks, as well as recovery time.

The elicited spinal reflex responses can be modified by various mechanisms that involve inhibiting and facilitating spinal interneurons (Figure 1.1). Lundberg (1970) suggested the existence of Ia inhibitory interneurons that hinder contraction of antagonist during

activation of agonists, by experiments on the cat spinal cord. This hypothesis was confirmed by human experiments, where a reflex in soleus muscle that was elicited by stimulation of the common peroneal nerve, could be inhibited during volitional dorsiflexion (Crone, Hultborn, Jespersen, & Nielsen, 1987; Iles, 1986; Nielsen, Kagamihara, Crone, & Hultborn, 1992; Nielsen, Sinkjær, Toft, & Kagamihara, 1994; Shindo, Harayama, Kondo, Yanagisawa, & Tanaka, 1984).

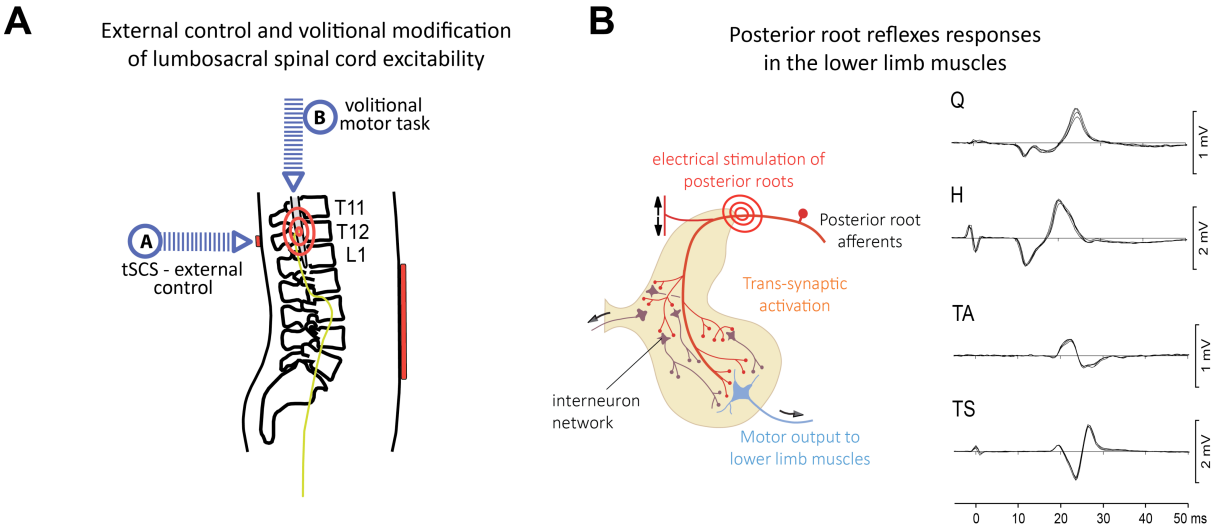

Figure 1.1: (A) Depolarization of afferents of thigh and leg muscles by tSCS, and additional modification of reflex responses by volitional motor tasks. (B) The reflex circuit at stimulation of posterior root afferents, and recorded reflex responses in quadriceps (Q), hamstrings (H), tibialis anterior (TA), and triceps surae (TS).

1.1 Research Aim and Hypothesis

The aim of the present study was to investigate how reflex responses in the lower limbs that are evoked by tSCS can be modified by voluntary dorsi- and plantar flexion. Additionally, challenges and limitations to the applied method were addressed.

First, the appropriate stimulation site and stimulation intensity were determined for each subject, to elicit distinct responses bilaterally in quadriceps, hamstrings, tibialis anterior and triceps surae. Therefore, a single stimulus of rectangular shape and duration of 1 ms per phase was applied to the T11-T12 inter-spinous space and reflex responses were measured with pairs of surface electrodes on the muscle belly. Recruitment curves were recorded by gradually increasing stimulation current (in 5 mA increments) to the level of saturation or the level that started to cause moderate discomfort to the subject.

For the preparation of the conditioning-test paradigm, the reflex nature of responses was verified by application of a second stimulus with an inter-stimuli interval of 35 ms.

Sustained tSCS at a stimulation rate of 1 pps and/or 2 pps was applied in resting state, and during unilateral volitional dorsi- and plantar flexion.
Additionally, the posterior root reflex (PRR) responses were compared at different isotonic dorsiflexion with different contraction forces. It was assumed that the responses were more affected by high muscle tones and also the temporal evolvement would be different.

1.2 Overview

In the chapter "Physiological Background" an anatomical overview of the human spine is given. Then the nervous structures of the spinal cord are presented including the peripheral sensory and motor systems. Finally, the mechanisms and roles of spinal reflexes are addressed.
In the chapter "Methods" subject's data is given, and the applied stimulation set-up and recording procedure is described. A study protocol of each experimental paradigm is given as well as the utilized methods of data analysis.
The chapter "Results" is divided into two sections. In the first one results of experiments are summarized, where single stimuli or pairs of stimuli were applied. In the second section results to the application of sustained stimulation, especially under reflex modification by motor tasks are presented.
These results are interpreted and compared to previous studies in the chapter "Discussion". Additionally, challenges and limitations to the method of tSCS are addressed there. The chapter "Conclusion" gives a brief summary of the discussed findings.
In the chapter "Appendix", the Matlab code, which was written and used for visualization and analysis of all datasets, is presented.

2

Physiological Background

2.1 The Neuron and Action Potentials

The neuron is the fundamental signaling component of the nervous system. It responses to and transmits electrical signals called action potentials. Neurons are composed of a cell body called soma and several processes. Multiple short dendrites extend the receiving surface of the neuron while a single axon conducts nerve impulses to other neurons or muscle cells (Brodal, 2010). Large axons are wrapped in a myelin sheath, which increases the speed of impulse propagation. The myelin sheath is interrupted by the nodes of Ranvier. The traveling action potential is regenerated at these nodes.

The synapse is the site of contact between an axon of a neuron and the next neuron. When an action potential reaches the synapse, it releases chemical substances called neurotransmitters to pass the signal to the adjacent neuron.

The cellular membrane of a neuron contains a high amount of ion channels. These ion channels enable the membrane to regulate the exchange of certain ions between the cell and its surrounding selectively. At rest, the ion concentration difference generates a potential difference of about -70 mV between inside and outside the nerve cell. When the neuron is stimulated and thus depolarized above the threshold of around -55 mV, sodium ion channels are opened, and an action potential is generated. The action potential then propagates along the axon to the synapses.

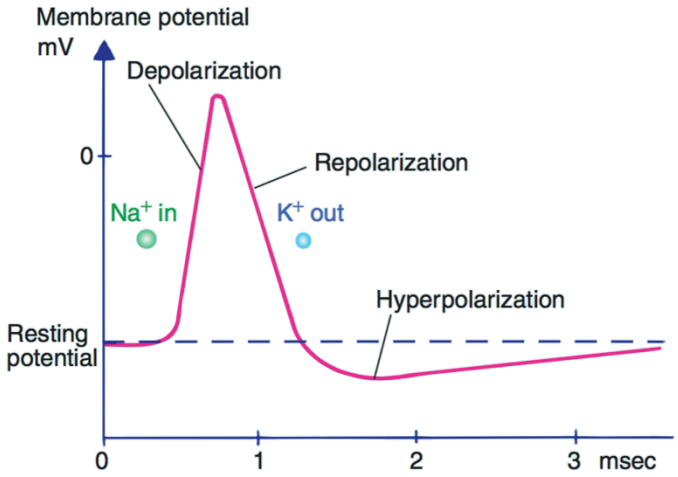

Figure 2.1: Schematic action potential. Sodium channels open when the cell membrane is depolarized above the threshold. Time-delayed potassium channels open, repolarizing the membrane. The membrane then restores the original ion distribution via ion pumps. Reprinted from Brodal (2010).

2.2 Anatomy of the Spinal Column

The human spinal column has three main functions: Support of the body, protection of the spinal cord and nerve roots and movement of the trunk (Dramer, 2014). The spinal column consists of 33 interlocked, bony vertebrae together with the soft tissues surrounding these bones.

Bone Structure of the Spine

The superior seven cervical vertebrae (C1 to C7, Figure 2.2) support the weight of the head. The first and second cervical vertebrae have the greatest range of motion due to a ring- and peg-shaped axis. The thoracic spine (T1 to T12) holds the rib cage and protects heart and lungs. The lumbar spine (L1 to L5) rests on the bony sacrum, which is made of five fused segments. The sacrum connects the spine to the hip bones (iliac bones). The iliac bones and the sacrum form the pelvic girdle. The spine ends with 3-5 partly fused bones of the coccyx (Dramer, 2014).

The spine develops four anterior to posterior curves: two kyphoses and two lordoses. The latter curves become apparent postnatal and more clearly at the stage of sitting and standing upright.

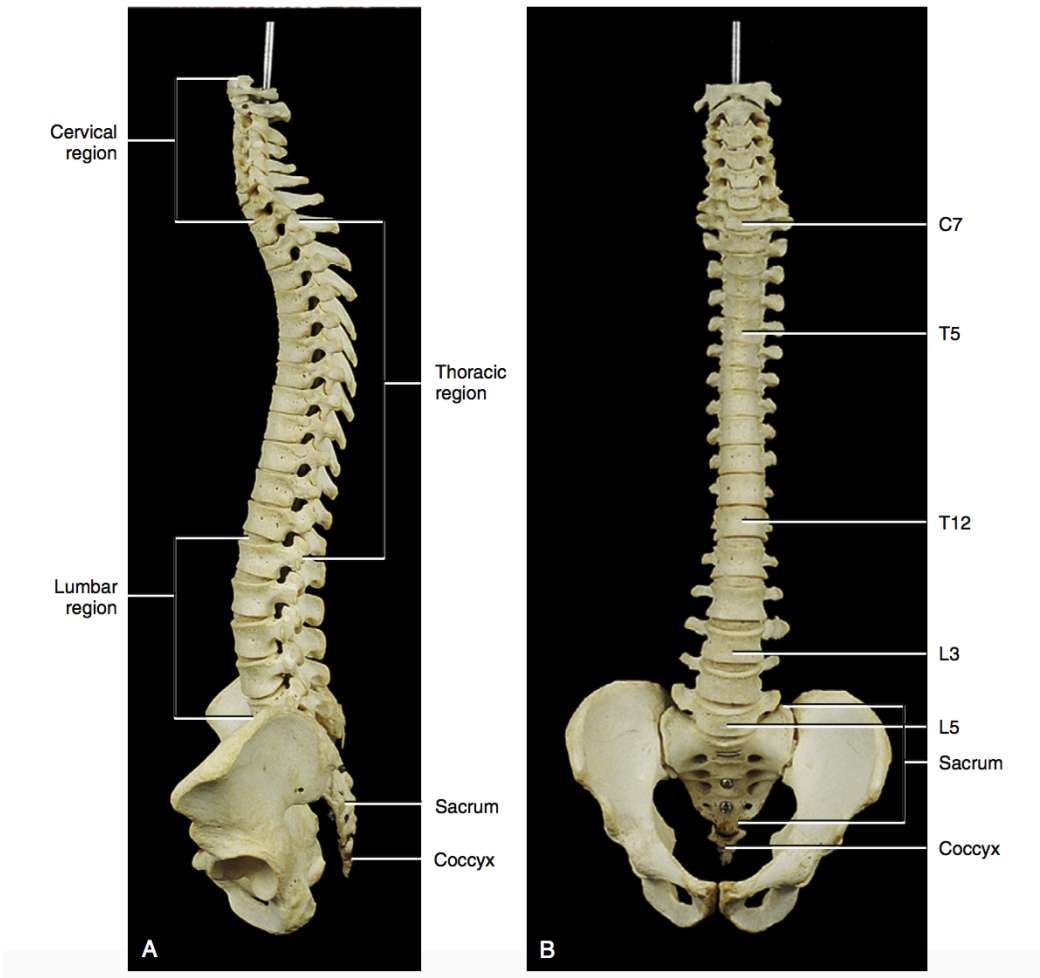

Figure 2.2: Lateral (A) and anterior (B) view of the human vertebral column, showing the cervical, thoracic, lumbar and sacral regions. The lateral view also shows the cervical and lumbar lordosis, and the thoracic and sacral kyphosis. Reprinted from Dramer (2014, p. 17).

A typical *vertebra* consists of two basic regions: a vertebral body and a vertebral arch. Both of them are composed of an outer compact bone layer and an inner trabecular bone.

Skedros et al. (1994) found that the trabeculae in vertebrae are oriented parallel to the lines of greatest stress. The trabeculae withstand not only axial compression but also are strong at the pedices that connect to the vertebral body, to allow transmission of high loads during rotation and anterior to posterior movement (bending) of the spine (associated with walking). The compact bone layer is thin on the discal surfaces of the vertebral body and thicker in the vertebral arch and its processes. Such a microarchitecture is optimally suited to provide the greatest amount of strength with the least amount of bone mass.

Osteoporosis is associated with a decrease in trabecular bone mass. More precisely osteoporosis is diagnosed by measuring the bone mineral density and distribution of trabeculae. A loss of mineral density together with the rearrangement of trabeculae lead to a loss of elasticity in the bone and an increase in bone fragility (Mosekilde, 1989).

Osteoporosis has been associated with aging and particularly with menopause (Ribot et al., 1988).

The *vertebral bodies* (VB) have various shapes depending on the region of the spine. Cervical vertebral bodies are rectangular; thoracic VBs are heart-shaped and lumbar VBs are kidney-shaped. Fibro-cartilaginous intervertebral discs (IVDs) connect adjacent vertebral bodies. Together they serve as a "pillar" to support the weight of the head and trunk. The vertebral bodies as well as the IVDs increase in diameter from C2 to L3, probably because of the successive addition of load from the neck to the sacrum.

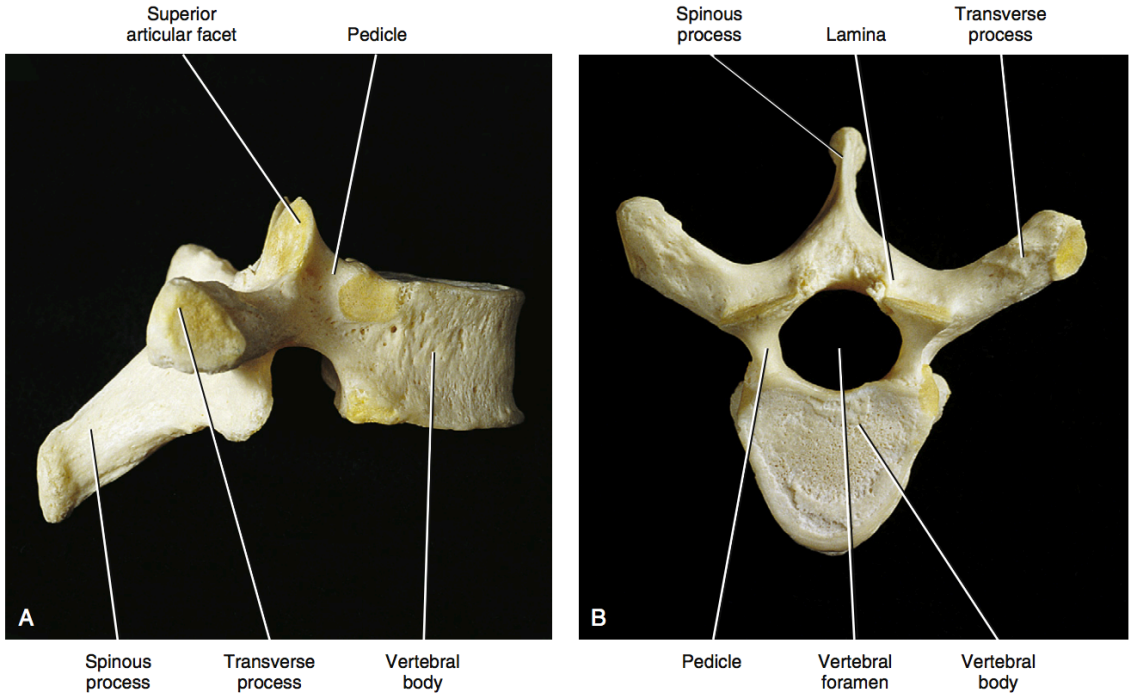

Figure 2.3: Photo of a thoracic vertebra. Lateral view (A) and superior view (B). Reprinted from Dramer (2014, p. 21).

Vertebral bodies have predominantly vertical trabeculae that are supported by horizontal trabeculae. Animal studies (Issever et al., 2003) showed, that horizontal, as well as vertical trabeculae in vertebrae increase in number after prolonged and increased loading by superior-inferior compression.
Relatively large arteries branched from the segmental artery (SA) pierce the vertebral bodies along their circumference. Inside the vertebral bodies, they branch into a large number of small arteries reaching the superior and inferior margins of the vertebral bodies. The veins in turn converge to the basivertebral vein (occasionally there are two basivertebral veins in the same vertebral body).

The *vertebral arch* consists of several structures including the pedicles, laminae and different processes (Figure 2.3).

The pedicles are short, rounded portions of the vertebral arch, attached to the posterior and lateral aspects of the vertebral body. They are smaller than the vertebral body, leaving an upper and a lower groove, called the vertebral notches.
The composition of the bone material in the pedicles varies from one region of the spine to another. For regions that are exposed to more motion, such as the cervical and the middle lumbar region, the pedicles contain a higher percentage of compact bone than for regions of little motion (Pal, Cosio & Routal, 1988).
The laminae are flattened from anterior to posterior and complete the vertebral foramen. The vertebral foramina compose the vertebral canal that houses the spinal cord, nerve roots, and many vessels. The laminae unite with the spinous process posterior. Laminae and pedicles serve to protect the spinal cord.
The spinous processes are the palpable posterior spikes of the spine. They serve as levers for muscles for posture and of active movement. These attaching muscles usually extend the spinal column and also perform rotations. On the lateral sides of the spinous processes, there are the vertebral grooves. They are gutters for the deep back muscles that course the entire length of the spinal column.
The transverse processes project laterally from the laminae. In the cervical region they project obliquely anteriorly, in the thoracic region they project obliquely posteriorly. There they also articulate with the ribs. The transverse processes act as lever arms for muscles of posture, of rotation and lateral flexion.
The superior and inferior articular processes (zygapophyses) project superiorly (inferiorly respectively) from the junction of the laminae and the pedicles. They end with articular surfaces or facets. The superior facets are inclined posteriorly and build the zygapophysial joints (Z joints) with the inferior facets of the adjacent vertebrae.

Soft Tissue of the Spine

The following section gives an overview of the cartilaginous tissue and the ligaments related to the spine. In particular, their anatomical structure and their mechanical function will be discussed.

The *intervertebral discs* are the pads between the vertebral bodies. They are located between adjacent VBs from C2 to the joint between L5 and the first sacral segment. There is also a small disc between the sacrum and the coccyx, and occasionally a small disc remains between the fused sacral segments or the first and the second coccygeal segments. A disc is usually named by referring to the vertebrae that surround it, for example, the C2-C3 disc.
The shape of an IVD is determined by the shape of the two attaching vertebral bodies. The discs are thicker in the lumbar region and thinnest in the thoracic region (Standring, 2008). In the cervical and the lumbar region, the discs are thicker anteriorly than

posteriorly, contributing to the lordoses of these regions. In total, the IVDs comprise 20% to 33% of the height of the spinal column (Coventry, Ghormley & Kernohan, 1945).
The intervertebral discs maintain the changeable space between adjacent vertebral bodies and avoid friction between the bones. They allow flexibility of the spine is ensuring that only a reasonable amount of motion occurs between vertebrae. Furthermore, the IVDs absorb compressive loads and work as dampers.
Intervertebral discs consist of three regions: the anulus fibrosus, the nucleus pulposus and the vertebral end plate (Humzah & Soames, 1988). The main difference between the anulus fibrosus and the nucleus pulposus is their different fibrous structure.
The anuli fibrosi consist of several criss-crossing fibrocartilaginous lamellae. The lamellae are formed mostly by collagen type I, and a few elastic fibers. The outer lamellae directly anchor themselves to the vertebral body, while the inner lamellae are connected to the cartilaginous end plates. They withstand tension stresses in all directions under various movements of the spine.
The nucleus pulposus is the viscoelastic cartilaginous tissue within the center of the IVD. It contains 70% to 90% water and a high amount of proteoglycans and less collagen type I than the anulus fibrosus (Coventry et al., 1945). The nucleus pulposus absorbs the majority of the fluid received by the IVD. When the nucleus pulposus is compressed and water is extruded, it retains sodium and potassium ions. Therefore, an osmotic gradient is created, that rapidly rehydrates the tissue when it is relaxed. This osmotic system is responsible for the viscoelastic properties of the nucleus pulposus. Depending on the rate and magnitude of loading, the nucleus pulposus acts as a fluid or solid.
The vertebral end plates limit the IVD superiorly and inferiorly, except for the most peripheral rim of the disc (Figure 2.4). The end plates are connected both to the compact bone and to the disc. The side facing the bone contains hyaline cartilage whereas the IVD-facing side contains fibrocartilage. The end plates assist in preventing the vertebral bodies from suffering pressure atrophy. They also keep the anulus fibrosus and the nucleus pulposus within their normal anatomic borders. Another important feature of the end plates was found by Humzah et al. (1988), regarding nutrition of the disc. The porous structure of the end plates allows for fluid flow into and from the nucleus pulposus by osmotic action. In the adult organism, the IVDs are entirely avascular and are nourished only through the intruding fluid.

The *zygapophysial joints*, or facet joints, interconnect the vertebral arches of the spine. They determine the directions and limitations of relative movement of the vertebrae. The articular processes are covered with a 1-2 mm-thick layer of hyaline cartilage. The Z joints are encapsulated in connective tissue and covered by the ligament flavum on the anterior and medial side.

Synovial folds are extensions of the Z joint capsule that protrude into the joint space and cover a part of the hyaline cartilage. These folds have been found in different sizes and shapes in the different regions of the spine. They are thought to aid the lubrication of the Z joints and also to protect the margins of the cartilaginous joints (Uhrenholt et al., 2008).

The role of the *spinal ligaments* is to enable smooth motion, with the least amount of resistance and maximum conservation of energy, within the spine's full normal range of motion. The ligaments also help to provide protection to the spinal cord, by limiting too much motion and absorbing a significant amount of the loads placed on the spine during trauma (Dramer, 2014).
Many spinal ligaments attach to processes of adjacent vertebrae, for example the interspinous or the intertransverse ligaments (Figure 2.4). The anterior and the posterior longitudinal ligament attach to the sacrum and successively to the vertebral bodies up to the occiput (the anterior longitudinal ligament ends at the C2).
All spinal ligaments have a similar load-deformation curve. While they resist highest tensile stress along the direction in which their fibers run, they buckle when subjected to compression. There is a sharp increase in stiffness as soon as full physiological motion has been attained. Tensile loading beyond the physiological motion range leads to ligament sprain.

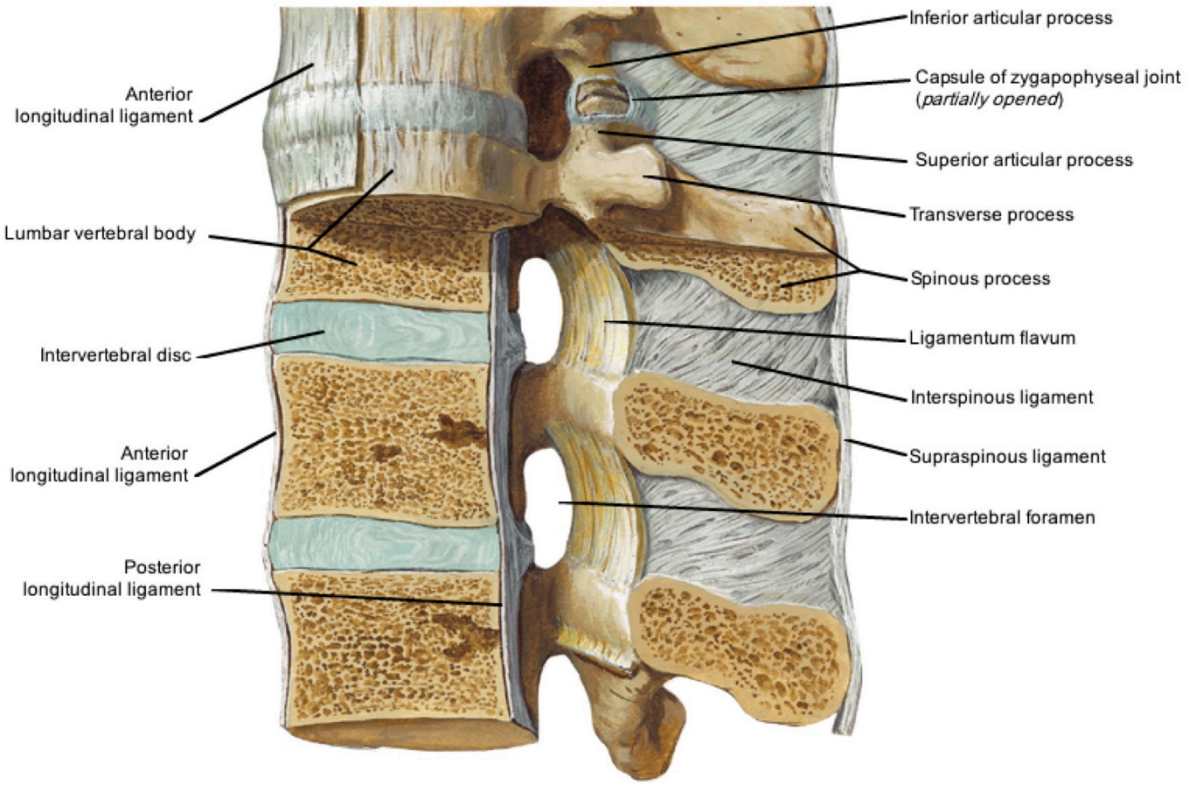

Figure 2.4: The spinal ligaments in the lumbar region seen from the side. Reprinted from Netter (2006, p. 158).

2.3 Neuroanatomy of the Spinal Cord

In humans, the spinal cord is a 40-45 cm-long cylinder of nervous tissue of approximately the same thickness as a little finger. It extends from the lower end of the brain stem (at the level of the upper end of the first cervical vertebra) down the vertebral canal to the upper margin of the second lumbar vertebra (Brodal, 2010) and is covered by a protective layer, called dura mater. The cauda equina is a bundle of nerve roots in the extension of the spinal cord reaching to the sacral segments of the spine.
The spinal cord is flattened in the anteroposterior direction. The thickness decreases caudally, but there are two enlargements, at the cervical and the lumbar region. These enlargements supply extremities with sensory and motor nerves.
There is a longitudinal fissure along the anterior aspect, called the anterior median fissure. There is a corresponding, but shallower fissure on the posterior side called the posterior median fissure.

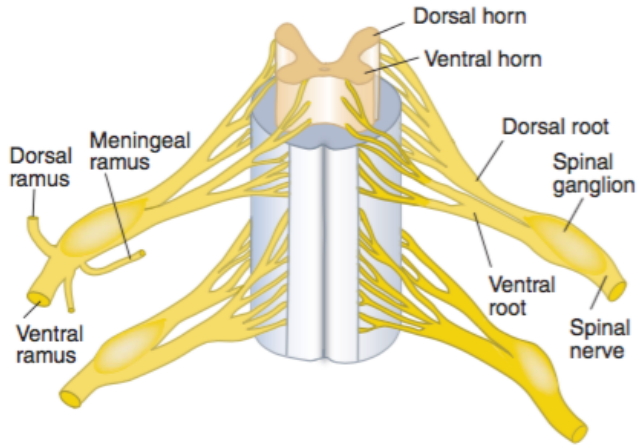

Figure 2.5: Two segments of the thoracic spinal cord, as viewed from the ventral aspect. Small rootlets combine into the dorsal and the ventral roots. The dorsal and ventral roots are forming together the spinal nerve. Reprinted from Brodal (2010, p. 75).

Internal Organisation of the Spinal Cord

Nerve fibers mediating communication between the central nervous system (CNS) and other parts of the body through the spinal cord are called the *spinal nerves*. The axons of the spinal nerves enter and leave the spinal cord in small bundles, or rootlets (Figure 2.5). These rootlets combine into nerve roots. In this way, rows of nerve roots arise along the dorsal and ventral aspects of the spinal cord. Each dorsal root has a swelling, the spinal ganglion that is located in the intervertebral foramen. Furthermore, in the foramina a dorsal and a ventral root join to form a spinal nerve.
Altogether, 31 pairs of spinal nerves leave the spinal cord through the intervertebral foramina on each side. Each pair of spinal nerves is numbered by the vertebra above the nerves. The cervical nerves are an exception to this nomenclature, because there are

eight cervical nerve pairs, with the first pair leaving the spine above the first cervical vertebra.

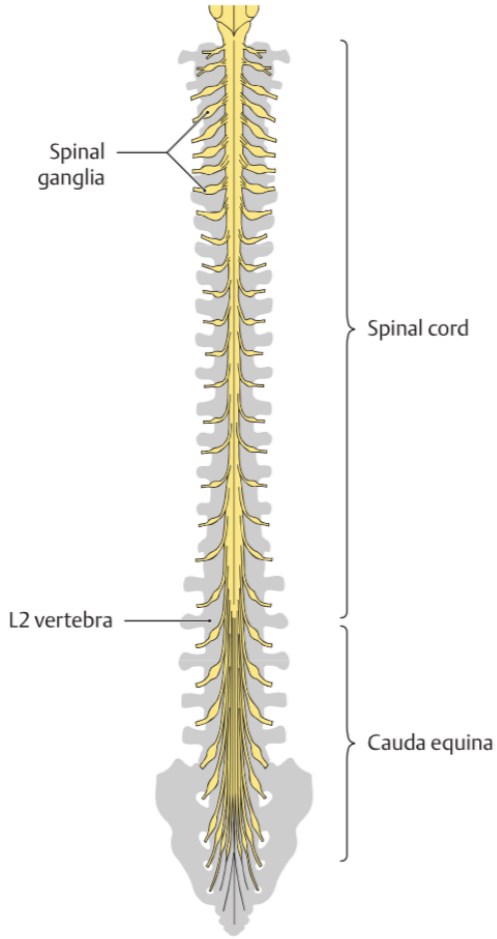

Figure 2.6: Spinal cord and spinal ganglia in situ. The longitudinal growth of the spinal cord lags behind of that of the bony vertebral column. Also note the cervical and the lumbar enlargement. Reprinted from Ebrall (2007, p. 266).

Whereas the upper spinal nerves pass approximately horizontally from the cord through the intervertebral foramina, the lower ones have to run obliquely downward the spinal canal to reach the corresponding intervertebral foramen. This shift between the site of exit from the cord and the site of exit from the spinal canal increases steadily. Therefore, although the spinal cord reaches only down between the vertebrae S1 and S2, there are nerve roots reaching to all five sacral segments and the first coccygeal segment (cauda equina).

When the spinal cord is cut transversely, an outer zone of white matter and a central, H-shaped zone of gray matter can be distinguished. The arms of the H-shape zone extend dorsally and ventrally and are called the dorsal and ventral horn, respectively. The structure and functions of the white matter and its neural tracts will be discussed first, followed by an overview of the structure and function of the gray matter.

The White Matter

The white matter contains myelinated and unmyelinated axons, of diameters in the range between 1 and 10 μm. The myelinated sheets of the fibers give the whitish appearance of the external part of the cord.

The white matter consists of four regions: the dorsal funiculus (column) between the dorsal horns, the ventral funiculus between the ventral horns, and two lateral funiculi. There are found tracts, or fasciculi in each of these regions. Ascending tracts transfer sensory information to higher centers and descending tracts transfer signals from higher centers to the cord. Other axons interconnect cord segments at various levels.

In general, three different groups of *ascending tracts* are described. One group of tracts transmits information about the type, location, and intensity of a stimulus. Another group of tracts transmit information about the initiation of reflexes, and the third group of tracts transmits information about the unconscious monitoring and control of motor activity, such as posture and movement (Benarroch, 1993).

Ascending tracts transmit information that originates from a stimulated peripheral receptor located in the skin, muscles, tendon, joints, or viscera. They proceed to a higher center like the cerebral cortex for conscious awareness of the stimulus, or the cerebellar cortex for regulation of motor patterns. In the first step of the process of information transfer, the stimulated receptor transmits an action potential via the sensory (afferent) nerve fibers to the CNS. These fibers are called the first-order neurons. Some of the first-order neurons synapse on neurons in the gray matter of the spinal cord, while others branch into the gray matter and into an ascending arm reaching the nuclear gray matter in the caudal medulla of the brain stem (Figure 2.7). Second-order neurons transmit the input from the gray matter of the cord or the medulla to higher centers. In the case of consciously perceived sensory information, the second-order neurons synapse with third-order neurons in the thalamus, which is located in the diencephalon of the brain. The thalamus is an oval area of gray matter, which not only passes sensory information on, but also modulates the information depending on excitatory and inhibitory input from other centers. So the thalamus works as a gatekeeper for the cerebral cortex by modulating its output based on the immediate needs of the individual (Amaral, 2013). From here the third-order thalamic neurons lead to the cerebral cortex, thus completing the chain.

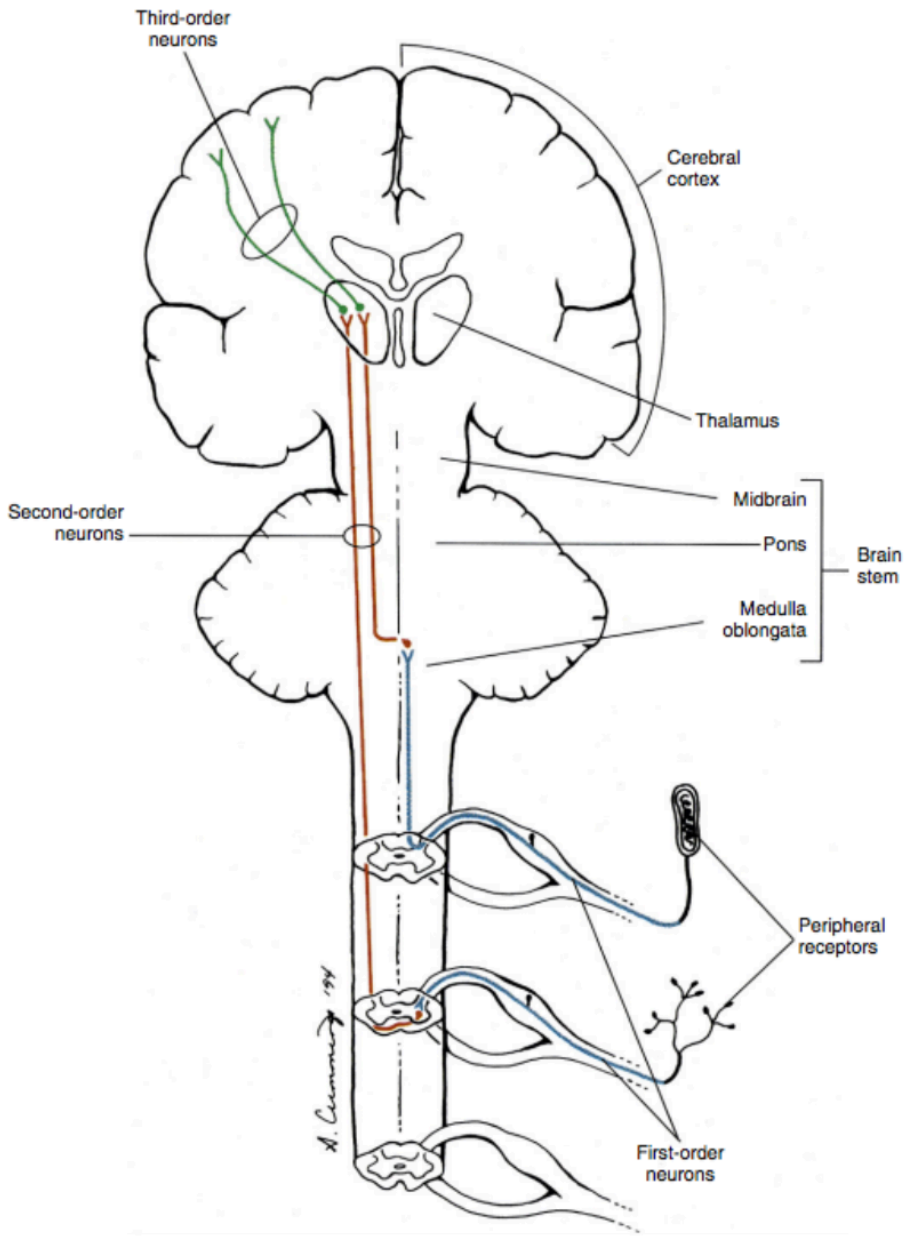

Figure 2.7: Neuronal organization of ascending information to higher centers. The first-order neuron (blue) cell body is located in the dorsal root ganglion. The second-order (red) cell body is located in the gray matter of the cord or the medulla of the brain stem. The third-order neuron (green) crosses the cerebral cortex. Reprinted from Dramer (2014, p. 360).

Descending tracts convey information from higher centers to motor neurons and interneurons. Thereby we can distinguish between three major motor areas. The first area is the spinal cord, supplying muscles directly or forming local circuits that mediate reflexes (see chapter Spinal Reflexes). These circuits are influenced excitatory or inhibitory by descending inputs from higher centers. The second area is the brain stem, which receives information from ascending tracts and other sensory organs and sends information back to the cord. The cerebral cortex is the third motor area, projecting to the brain stem or directly to the cord. There are two additional higher centers, the basal

ganglia and the cerebellum, which project to the cortex or the brain stem and thus are involved with planning, coordinating and correcting motor activities.
Although most descending tracts are involved with somatic control, some influence primarily sensory afferents and autonomic functions.
The largest descending tract is the corticospinal or the pyramidal tract (CST, Figure 2.8). It transmits mostly information concerning voluntary motor activity. The majority of the fibers originate in the motor cortex of the frontal lobe. The CST descends within the ventral portion of the brain stem and at the caudal level of the medulla 80% to 90% of the fibers cross, forming the pyramidal decussation. Then the crossed fibers course as the lateral CST in the lateral funiculus of the spinal cord. In the cervical region, 55% of the fibers leave the tract and synapse on neurons in the gray matter (supply of upper extremities, which can perform highly skilled movements). 20% of the fibers synapse in the gray matter of the thoracic cord and the rest synapse in the lumbar and sacral gray matter.

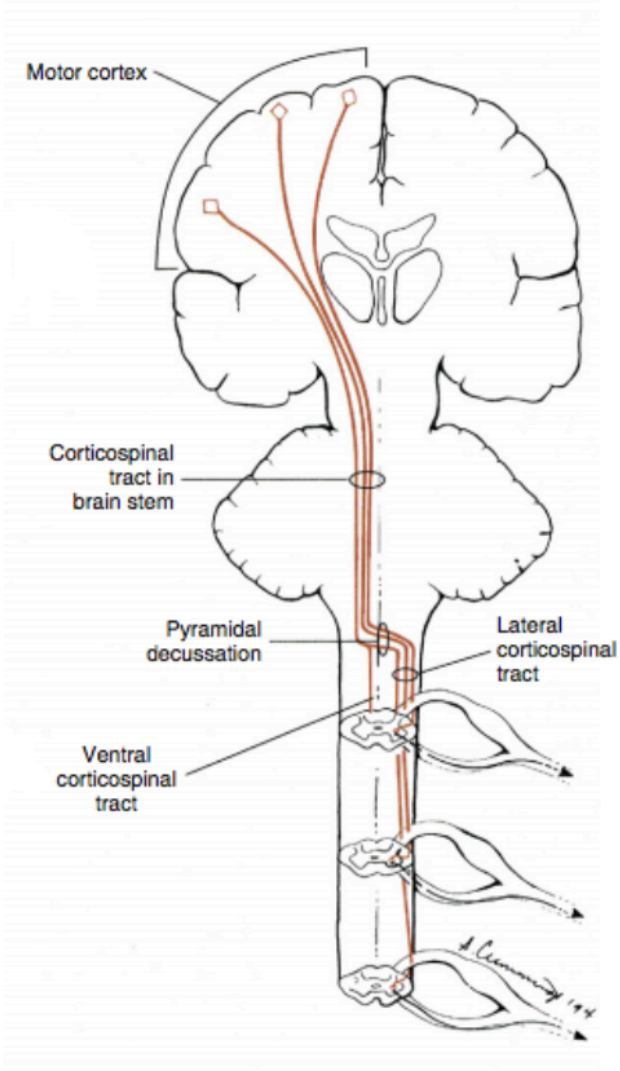

Figure 2.8: Corticospinal tract (CST). The fibers in the medulla become very compact and cross from the left to the right side and vice versa. Reprinted from Dramer (2014, p. 364).

The Gray Matter

The gray matter of the spinal cord is a dense region of neuron cell bodies, cell processes and their synapses, glia cells and capillaries. In general, the dorsal horn of the gray matter receives the afferent sensory input, and the ventral horn is involved in motor functions and houses the cell bodies of motor neurons (innervating skeletal, smooth and cardiac muscles, glands). Other cells of the gray matter are the tract neurons, which are mentioned in the previous two sections, interneurons, which have short processes and propriospinal neurons. The latter neurons communicate between cord segments and are not only involved in the coordination of somatic motor activity, but also with the autonomic innervation of sweat glands, smooth muscle of the vasculature, and viscera such as the bladder and bowel (Standring, 2008).

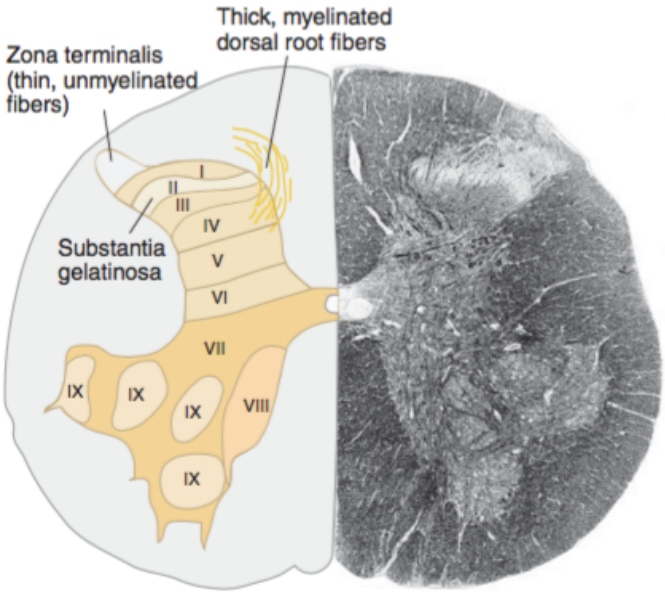

Figure 2.9: Cross section of a lumbar spinal cord segment. Left: The borders between the Rexed's laminae. Right: Photomicrograph of a section stained to show myelin and neuronal cell bodies. Reprinted from Brodal (2010, p. 79).

The gray matter is organized in 10 layers, or *laminae* (Figure 2.9). These laminae were first proposed by Rexed (1952) in a study of feline spinal cords.

The laminae I to IV are the main termination sites of cutaneous afferent fibers. Lamina I and II are also known as the superficial dorsal horn and are involved with the processing of nociception. Lamina V receives fibers from the skin, muscle and viscera. Lamina VI receives proprioceptive and some cutaneous fibers. So the dorsal horn comprising the first six laminae is the major receiving area for sensory input.

Lamina VII of the ventral horn receives proprioceptive fibers and its lateral neurons are involved in regulation of posture and movement. Latter neurons have ascending and descending connections to the cerebellum and midbrain. The medial part of the lamina VII has mostly interconnecting neurons and is associated with reflexes. Lamina VIII is

also located in the ventral horn. Descending fibers synapse in the Lamina VIII on interneurons and propriospinal neurons. These interneurons excite gamma motor neurons, which in turn influence alpha motor neurons (discussed in the section 'Nervous Structure in the Periphery'). Interneurons may also synapse on alpha motor neurons directly. Lamina IX provides the axons that innervate the epaxial muscle groups (deep back muscles) and the hypaxial muscle groups (vertebral muscles, intercostal and anterior abdominal wall muscles). The lateral group of the cervical and lumbar lamina IX innervates the muscles of the upper and lower extremities, respectively. The central group, particularly at C4, known as the phrenic nucleus, innervates the diaphragm. Lamina X forms the area between the two halves of the gray matter and consists of interneurons.

2.4 Nervous Structure in the Periphery

After a description of the neural architecture of the spinal cord in the previous chapter, the nervous structure in the periphery will be discussed in the following sections. We distinguish between the somatosensory system, including the sense organs and their neural connection to the CNS, and the somatic motor system, especially the peripheral motor neurons (also called lower motor neurons), which send their axons to skeletal muscles. Furthermore, an overview of the lumbosacral spinal nerves will be given.

The Peripheral Parts of the Somatosensory System

All sensations about the body can be attributed to the somatosensory system. The cells, where sensory signals originate, are called sense organs, or receptors. These receptors are either terminal branches of axons (skin, joints, muscles) or separate cells, where nerve fibers synapse (retina, taste buds, inner ear). A sensory unit refers to a sensory neuron with all its ramifications to the CNS and in the CNS.

We can distinguish between exteroceptors, which capture information from our surroundings and are located in the skin and proprioceptors, which are located in the muscles and joints. Another group, which won't be discussed, are enteroceptors. They are located in the internal organs, like the intestinal tract, the heart, and the lungs.

We can also classify receptors by their adequate stimulus as mechanoreceptors, thermoreceptors and chemoreceptors. A receptor transduces the adequate stimulus into an action potential, which is the language of the CNS. Furthermore, receptors can be divided into rapidly adapting, and slowly adapting receptors. Slowly adapting receptors respond continuously to a sustained stimulus, while rapidly adapting receptors respond only to a change in stimulus strength. The rapidly adapting Meissner corpuscle, for

example, produces action potentials, when the pressure on them is increased until the pressure becomes constant.
Four characteristics are given by a stimulus to a receptor: modality, stimulus intensity, duration, and location of the stimulus. In a stimulated receptor, a generator potential occurs across its membrane and leads to an action potential, which in turn propagates along the sensory neuron to the CNS. First, the classes of sensory neurons will be discussed, followed by the cutaneous exteroceptors and finally the proprioceptors.

The cell bodies of *sensory neurons* are located in the dorsal root ganglia. Their dorsal processes lead to the sense organs, while their central processes enter the CNS through the dorsal roots of the spinal cord. The dorsal processes have various conduction velocities, depending on their diameters. The thicker an axon is, the faster it conducts an action potential. There is a classification for cutaneous nerve fibers, based on their diameter (Tabelle1). Thick, fast fibers are classified Aα, and conduct the signal from rapidly adapting mechanoreceptors. Aβ fibers are associated with slowly adapting mechanoreceptors. Aδ and C fibers route signals from nociceptors (pain signals) and thermoreceptors.
Table 1.1 also shows the classification of afferent fibers from the skeletal muscles and articular receptors (type I to IV). In addition, type I has subgroups of Ia, associated with the muscle spindles, and Ib, associated with the Golgi tendon organ. These mechanoreceptors will be discussed subsequently.

Table 2.1: Summary of the classification of peripheral fibers. Adapted from Dramer (2014, p. 342).

Fiber Diameter (µm)	Efferent Fibers	Afferent Fibers (from Cutaneous Receptors)	Afferent Fibers (from Skeletal Muscle and Articular Receptors)	Myelination
12-20	A-alpha (skeletomotor)	A-alpha (from mechanoreceptors) (rapidly adapting)	Type I (from mechanoreceptors)	Heavily myelinated
6-12		A-beta (from mechanoreceptors) (slowly adapting)	Type II (from mechanoreceptors)	Myelinated
3-8	A-gamma (fusimotor)			Myelinated
1-6		A-delta (from nociceptors and thermoreceptors)	Type III (from mechanoreceptors and nociceptors)	Thinly myelinated
1-3	B (preganglionic autonomic fibers)			Myelinated
0.2-1.5	C (postganglionic autonomic fibers)	C (from nociceptors and thermoreceptors)	Type IV (from nociceptors)	Unmyelinated

One prominent group of receptors are the *nociceptors*. (Figure 2.10). They are found not only in the skin but also in all other tissues from which painful sensations can be evoked (therefore not all of them are exteroceptors). Nociceptors can be defined as the

receptors, which are activated, by stimuli that produce tissue damage, or would do so, if the stimulus continued. Morphologically they are free nerve endings. Some cutaneous nociceptors respond to intense mechanical stimulation, as pinching, cutting or stretching. Other nociceptors respond also to mechanical stimuli, but additionally to warming of the skin and to chemical substances, which are liberated by tissue damage and inflammation. They are called polymodal nociceptors. The last group contains the silent nociceptors, which are responsive only to chemical substances released in inflamed tissue. Silent nociceptors are usually activated after a stimulation duration of 10-20 minutes. Thereafter they continue firing for hours. They contribute to the regulation of the immune system and to the sickness behavior of an individual.
Nociceptors tend to be sensitized by prolonged stimulation. Inflammatory products up-regulate Na channels, so that even weak stimuli cause high response to the sensory neuron. That is why even non-noxious stimuli, as touching, may feel painful, when the skin is inflamed.

Thermoreceptors are responsible for the perception of heat and cold. Cold receptors respond with increasing firing frequency to cooling of the skin. They stop firing at very low temperatures and do also fire at very high temperatures (cold sensation at the beginning of a hot shower). The signals of cold receptors are conducted via thin, myelinated Aδ fibers. Warm receptors respond to temperature increase up to 35 °C and their signals are transmitted through unmyelinated C fibers.
At steady temperature thermoreceptors send action potentials with low frequency. Even a small change in the temperature of the tissue, which surrounds the receptors, elicits a significant change in the firing frequency. Therefore, thermoreceptors do not objectively measure the actual skin temperature, but detect temperature changes, and thus help the body to adjust appropriately to the environment.

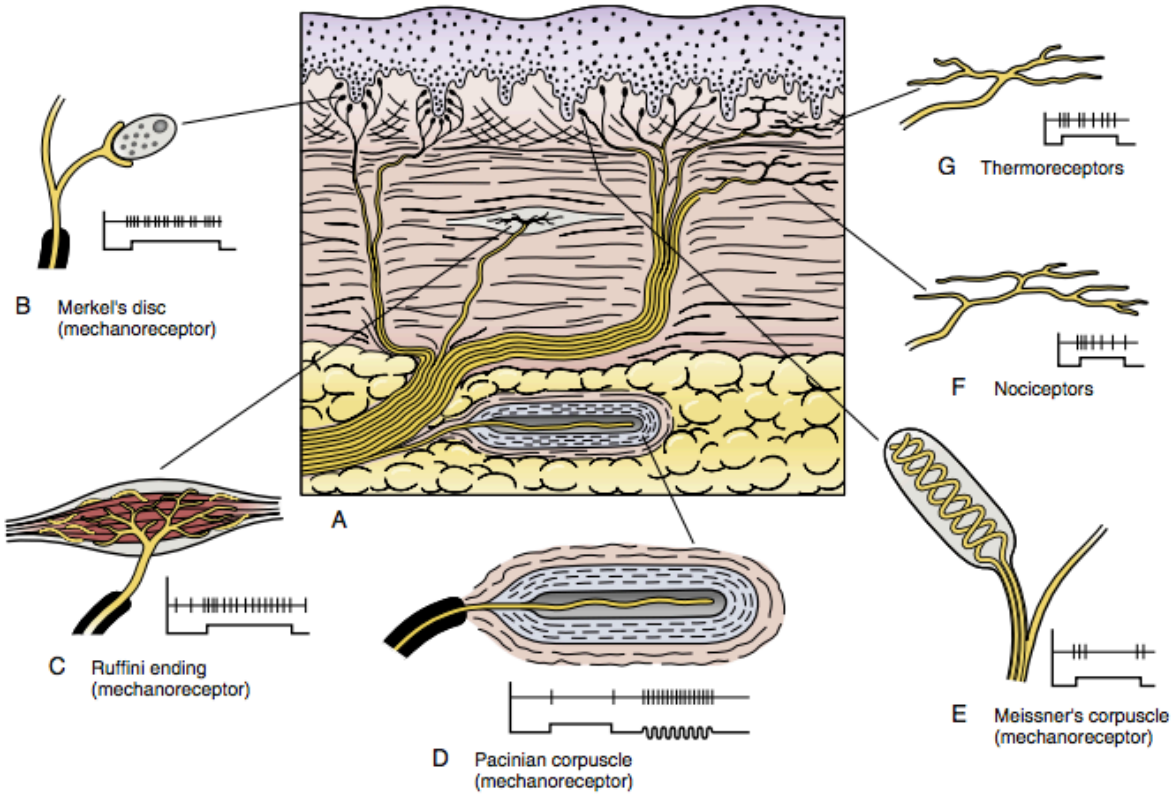

Figure 2.10: Types of cutaneous receptors. Receptors D and E are rapidly adapting. Receptors B, C, F, and G are slowly adapting. The tracings illustrate that the slowly adapting receptors fire continuously throughout the stimulus and the rapidly adapting receptors fire at the onset and offset of the stimulus. Reprinted from Dramer (2014, p. 343).

Mechanoreceptors, or more precisely low-threshold mechanoreceptors are found in the skin, ranging from free to encapsulated receptors. Some adapt slowly, while others adapt very rapidly. Receptors close to the roots of hairs, for example, adapt very fast. Even slight bending of the hair activates them, but when the hair is held in the new position, the sensation disappears immediately.

The superior sensory abilities of the palm of the hand and the sole of the feet are attributed to the encapsulated receptors, which are found abundant in these regions.

One such receptor is the Meissner corpuscle, which transmits information about touch. It is an oval body located in the dermal papillae just beneath the epidermis and is therefore the closest receptor to the skin surface. It is a highly sensitive, rapidly adapting receptor, firing on the onset and the offset of a mechanical stimulus. Meissner corpuscles are, among others, responsible to detect the direction and velocity of objects moving on the skin.

Another important mechanoreceptor is the Ruffini corpuscle. It is composed of a bundle of collagen fibrils and a sensory axon branching between the fibrils. It is a slowly adapting receptor, thus firing continuously for a long time at the presence of a stimulus. Ruffini corpuscles respond to stretching of the skin in the direction of their collagen fibrils. They deliver information about the magnitude and direction of stretch.

Another slowly adapting mechanoreceptor is the Merkel disk. It is located in the basal layer of the epidermis and in close contact to epithelial cells. Merkel disks are found particularly in the distal parts of the extremities, the lips and the external genitals. They react to touch and provide information about the form and surface of objects.
Finally, the Panician corpuscle is a mechanoreceptor found between the dermis and the subcutaneous layer. It has a big oval body (up to 4 mm long) and consists of a thick axon, which is surrounded by numerous lamellae and fluid-filled spaces. Panician corpuscles are very rapidly adapting and fire only one or two action potentials at the onset and the offset of a mechanical stimulus. Therefore, adequate activation is extremely rapid indentation of the skin, achieved by vibration with frequencies of 100 Hz to 400 Hz. Meissner corpuscles, in contrast, are sensitive to vibration of frequencies up to 100 Hz.

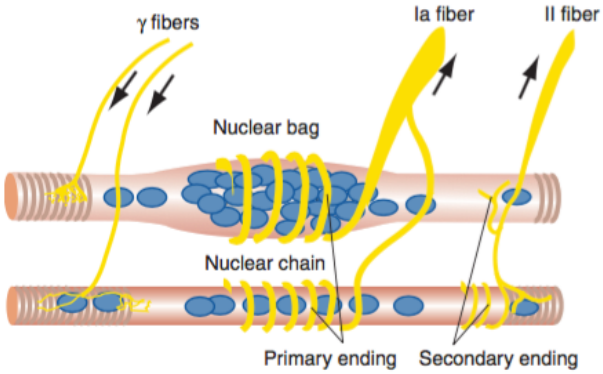

Figure 2.11: The muscle spindle and its innervations. The cross-striated ends are innervated by γ motor fibers and are able to contract. Reprinted from Brodal (2010, p. 175).

Muscle spindles, which are located within the muscles, are part of the proprioceptive sensory system. They are specialized thin muscle fibers, encapsulated in connective tissue (Hunt, 1990). Their capsule is approximately 5 mm long. The muscle fibers of a spindle are called intrafusal fibers and are cross-striated only at their ends that are the contractile segments of the spindle. The intrafusal fibers can be further divided into nuclear bag fibers, which have their nuclei all collected in the middle part of the muscle fiber, and nuclear chain fibers, which have their nuclei equally distributed along the muscle fiber.
A thick Ia sensory fiber surrounds the middle portion of a nuclear bag fiber in a spiraling course (primary sensory ending). Additionally, a thin II sensory fiber attaches to a nuclear chain fiber (secondary sensory ending). The muscle spindles are unique among peripheral receptors in that they also have a motor innervation. This innervation controls the contraction of the ends of the intrafusal fibers, also called fusimotor and is a γ-type motor fiber (Table 1.1).
The nuclear bag fiber is sensitive to the rate of change of the intrafusal fiber length, and is a rapidly adapting receptor (Figure 2.12). It responds to muscle stretch with a burst of

action potentials, and to shortening with a dramatic decrease of firing. This property is called dynamic sensitivity and gives information about length change of the muscle, as well as the velocity of the length change. On the contrary, the nuclear chain fibers are slowly adapting and reach a steady-state firing of action potentials that reflects the overall length of the muscle. This property is referred to as static sensitivity.
The fusimotor preserves muscle spindle sensitivity over the wide range of physiological muscle lengths. During voluntary contraction of the muscle, the fusimotor is contracted too, to keep tension on the muscle spindle, and thus allows it to continue to sense changes in the muscle length that might occur.

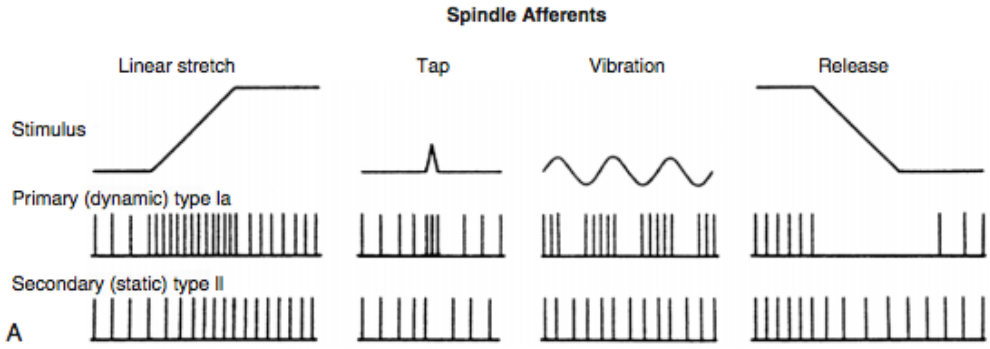

Figure 2:12: Muscle spindle afferent functions. The primary Ia receptor is a rapidly adapting receptor that responds to transient length change of the muscle. The secondary II receptor is a slowly adapting receptor. Its firing rate reflects the overall length of the muscle but does not respond well to transient length change. Reprinted from Dramer (2014, p. 390).

The *Golgi tendon organ* is a proprioceptor found at the junction of the muscle and its tendon. It is an encapsulated, slowly adapting receptor of about 0.5 mm length. A tendon organ is innervated by a large afferent fiber of the type Ib, which is entwined in collagen fibers. The intrafusal fibers of the muscle spindle are parallel to the muscle fibers, can accurately detect muscle length changes, but not tension. On the contrary, the tendon organ is in series with the muscle fibers and detects tension, but no length change.
The output of the Golgi tendon organ increases dramatically for voluntary contraction of a muscle, compared to passive stretch of the muscle. Structurally the tendon organ is attached to a few muscle fibers. The contraction of some of these fibers produces a much higher tension in the tendon organ than the passive stretch of the entire muscle.

Joint receptors are nerve endings in the joint capsules and in the ligaments around the joints. They can be divided into 4 types. The first three types are encapsulated mechanoreceptors and resemble the mechanoreceptors of the dermis. They provide information about the position and the movement velocity of the joint. Type 4 consists of free nerve endings and mediate nociception.

The Peripheral Motor Neurons and Motor Coordination

The lower motor neurons innervate skeletal muscles. They constitute the final and only connection between the CNS and the muscles. For this reason, the British neurophysiologist Sir Charles Sherrington introduced the term "final common path" (1906) of CNS activation. Interruption in these axons leads to paralysis of the corresponding muscles. Motor coordination is the function of linking the contraction of many independent muscles, so that they act synergistically and can be controlled as a single unit. Spinal reflexes, as discussed in the chapter "Spinal Reflexes", achieve this task.

First the types of motor neurons will be addressed, followed by the motor unit and the muscle fiber types.

The α motor neurons are the largest type of peripheral *efferent neurons*. They innervate all skeletal muscles, or, more precisely, all extrafusal muscle fibers. The intrafusal muscle fibers of the muscle spindle are innervated by thinner γ motor neurons, which are also called the fusimotor neurons. The axons of both types of motor neurons are connected to the spinal cord through the ventral roots. In the gray matter of the cord the motor neurons are collected in groups, which form Rexed's lamina IX. But they also synapse into lamina VII. Groups of motor neurons that supply axial muscles (muscles of the back, neck, abdomen, and pelvis) are located medially within the ventral horn, while motor neurons, that supply muscles of the extremities are found more laterally.

The cell bodies of α and γ motor neurons are not segregated within the spinal cord but are mixed together to form groupings called pools. One neuron pool generally innervates one particular muscle, so that the CNS controls pools instead of individual motoneurons.

At the end of a α motoneuron on the site of the innervated muscle, the axon branches and each of the branches innervates one muscle cell only. The branches end approximately at the middle part of the muscle cells, forming the motor end plate. At the end plate the branch divides into about 50 boutons, which synapse with muscle cell. The boutons release acetylcholine, which bind to the acetylcholine receptors of the postsynaptic membrane and provoke a depolarization of the whole muscle cell. A single action potential elicits a brief contraction of the muscle cell. If the muscle cell receives repeated action potentials, the tension is upheld and increases. This effect is called summation of single twitches. External electrical stimulation of motoneurons with 30 Hz produces a fused muscular tetanus (Kandel et al., 2000).

The *motor unit* is defined as the smallest functional unit of the motor system. It consists of one α motoneuron and all the muscle cells that it innervates (Kandel et al., 2000). One

α motoneuron innervates a couple of muscle cells, and no muscle cell is innervated by more than one α motoneuron.
The number of muscle fibers that are innervated by a motor neuron determines its innervation ratio and the size of the motor unit. The large motor units of the gastrocnemius muscle, for example, have an innervation ratio of 2000:1 (Dramer, 2014). The small muscles in the hand generally have an innervation ratio of 10:1. Therefore, small motor units are used in muscles for precise motor skills, while large motor units are common in muscles that generate high forces with less control. Furthermore, large motor units are innervated by motor neurons with large cell bodies and thick axons, and accordingly, small motor units are innervated by motoneurons with small cell bodies and thin axons.

We can distinguish between two types of striated *muscle fibers*, based on their biochemical properties. Some fibers appear reddish, because of their high content of the oxygen-transporting protein myoglobin. They contain many mitochondria, which are responsible for aerobic ATP production. These fibers contract rather slowly and do not develop high forces, but have a high endurance. They are known as the oxidative, or slow motor units and are classified as type 1. The firing rate to stimulate fibers of type 1 is slow, because they have a large hyperpolarizing afterpotential.
Other fibers appear whitish and contain less myoglobin and mitochondria. They produce ATP anaerobic through glycolytic metabolic pathways. They can contract very rapidly and generate high forces, but also fatigue rapidly. These fibers are known as the fast glycolytic or fast fatigable motor units and are classified as type 2. Type 2 fibers generally have the greatest cross-sectional area.
Moreover, fibers of type 2 can be subdivided into type 2A, type 2B and type 2X. Type 2A resemble the type 1 fibers in having a relatively high oxidative capacity, while type 2B and type 2X have the lowest oxidative capacity and fatigue the fastest (Rhoades & Bell, 2012).
Individual muscles contain varying proportions of all types of muscle fibers. The proportion of fiber types corresponds to the functional needs of the respecting muscle. Postural muscles have a high amount of type 1 fibers, whereas strength muscles have a large proportion of type 2. Furthermore, athletes engaged in endurance sports have a high percentage of type 1 fibers, while athletes engaged in sports requiring explosive force have a high proportion of type 2 fibers.
Motor units are stimulated, or recruited in a fixed order within the gray matter of the spinal cord. First the weak type 1 muscle fibers are recruited, since their motor neuron has as small cell body with high membrane resistance, so that the threshold for an action potential is easily reached by a few excitatory synapses. With increasing input to the motor neuron pool the larger motor neurons are stimulated above their threshold and

thus the strong type 2 muscle fibers are recruited. The American neurophysiologist E. Henneman et al. demonstrated this "size principle of recruitment" (1965).

The Lumbosacral Spinal Nerves

The branches of the lumbosacral spinal plexus innervate the lower extremities and are thus of major importance for the present work. The lumbosacral spinal plexus is composed of the spinal nerves L2 through S2. These nerves leave the spinal cord at the level of the vertebrae T11 and T12.

The major branches of the lumbosacral plexus are the femoral, obturator, gluteal, sciatic, common fibular, and tibial nerves (Dramer, 2014). The obturator and the femoral nerve (L2 to L4) innervate the adductor muscles of the thigh and its anterior and lateral muscles (e.g. quadriceps). The sciatic nerve (L4 to S3, Figure 2.13) has motor branches in the posterior thigh, which innervate the hamstring muscles. Furthermore, the sciatic nerve branches into the common fibular (peroneal) and the tibial nerve. The peroneal nerve divides into the superficial and the deep fibular (peroneal) nerve. While the superficial peroneal nerve innervates the lateral leg muscles for eversion of the foot, the deep peroneal nerve innervates the anterior leg muscles, which enable dorsiflexion of the foot and extension of the toes. The tibial nerve innervates the posterior leg muscles providing plantar flexion of the foot.

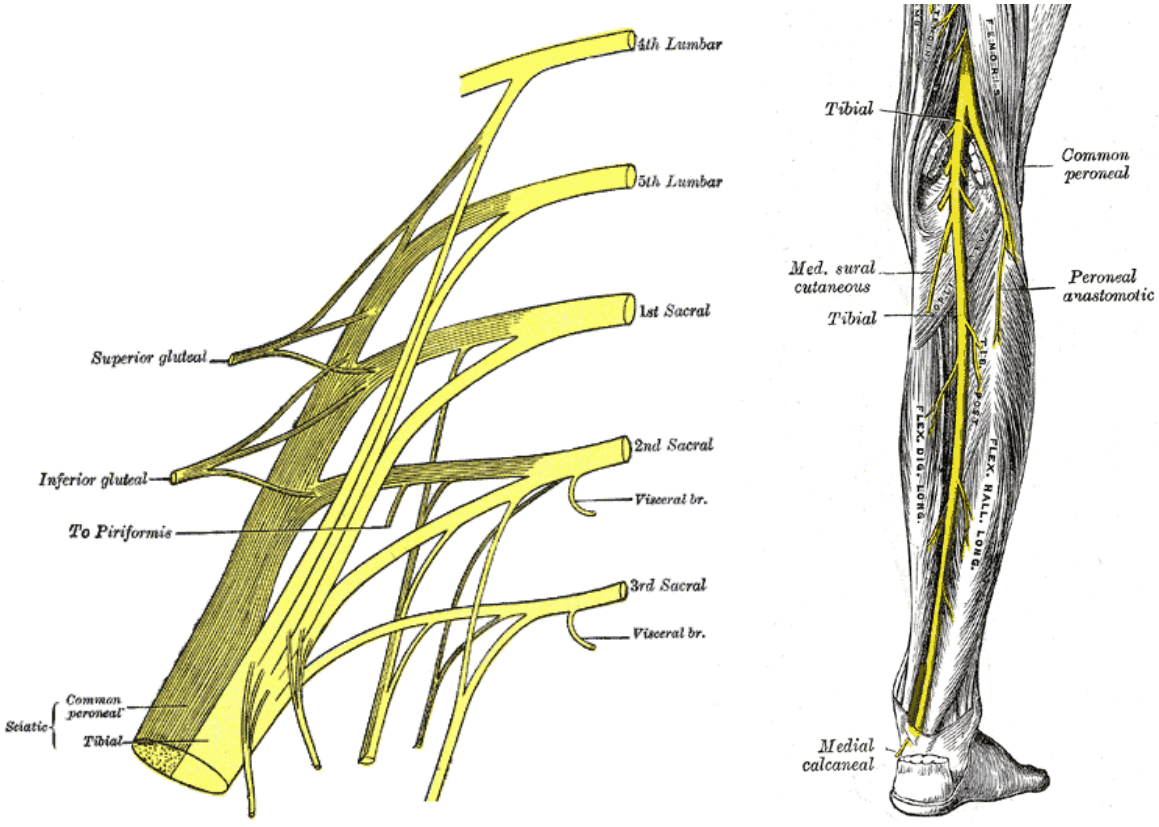

Figure 2.13: Origin and branches of the sciatic nerve. The sciatic nerve arises from the spinal cord segments L4 to S3 (left) and branches into the common peroneal and the tibial nerve (right). Adapted from Gray (1918).

2.5 Spinal Reflexes

Before discussing the generation of voluntary movement, which is presented in the next chapter, we address to the role of the spinal cord as executer of reflexes. Many tasks of the nervous system are carried out intrinsically, without conscious or brain interaction. However, there is no clear border between fully automatic movements and fully conscious movements. Many reflexes can be modeled with relatively simple neural circuits. Nevertheless, the reflex pathways are under control of descending pathways to generate more complex motor actions.

The simple basis of a reflex is a reflex arc. It consists of a receptor, an afferent sensory neuron, a reflex center, an efferent motoneuron and an effector, like a skeletal muscle, heart, or smooth muscles in the walls of vessels and visceral organs. Next to spinal the spinal cord, the pathway center may be also in the brain stem (medulla, pons or mesencephalon) or in the cerebral cortex. Here, we will confine our discussion to the spinal reflexes, having the reflex center in the spinal cord.

In the gray matter of the spinal cord afferent and efferent nerve fibers are interconnected to neural circuits. In simple circuits only one synapse is intercalated between the afferent and the efferent link. Such reflexes are called monosynaptic. Most reflexes, however, include links of several coupled interneurons. Therefore, these reflexes are called polysynaptic.

The most prominent monosynaptic reflex is the patellar reflex, which is commonly tested clinically. There, a tap on the patellar tendon leads to a quick length change in the quadriceps muscle. Afferent Ia neurons of the muscle spindles signal the sudden length change and transmit the action potentials through monosynaptic connections in the gray matter directly to motoneurons that contract the quadriceps muscle. This monosynaptic stretch reflex (also called myotatic reflex) can be elicited in most skeletal muscles.

Other reflexes employ spinal interneurons between the afferent and efferent link. These interneurons will be discussed in the following. Then some examples of preprogrammed movements will be shown and Hoffmann's reflex will be discussed.

Spinal Interneurons

Spinal interneurons interconnect nerve afferents with efferents in the gray matter of the spinal cord to form reflex arches. Some interneurons also connect descending neurons to the reflex circuits. Three main types of interneurons are discussed below.

Ia inhibitory interneurons were first described by John Eccles et al. (1962). He analyzed the monosynaptic stretch reflex and found that the Ia muscle spindle afferents not only excite α motoneurons of the stretched muscle and of synergistic muscles, but also activate inhibitory interneurons that inhibit the α motoneurons of the antagonist muscle

group (Figure 2.14). Thus the agonist muscle group contracts freely, with less resistance. This process is known as reciprocal inhibition and the responsible interneurons are called Ia inhibitory interneurons. These interneurons also receive descending information from coordination centers of voluntary movement as well as information from other spinal interneurons. They are also extensively connected to the central pattern generators (CPG) (McCrea & Rybak, 2008).

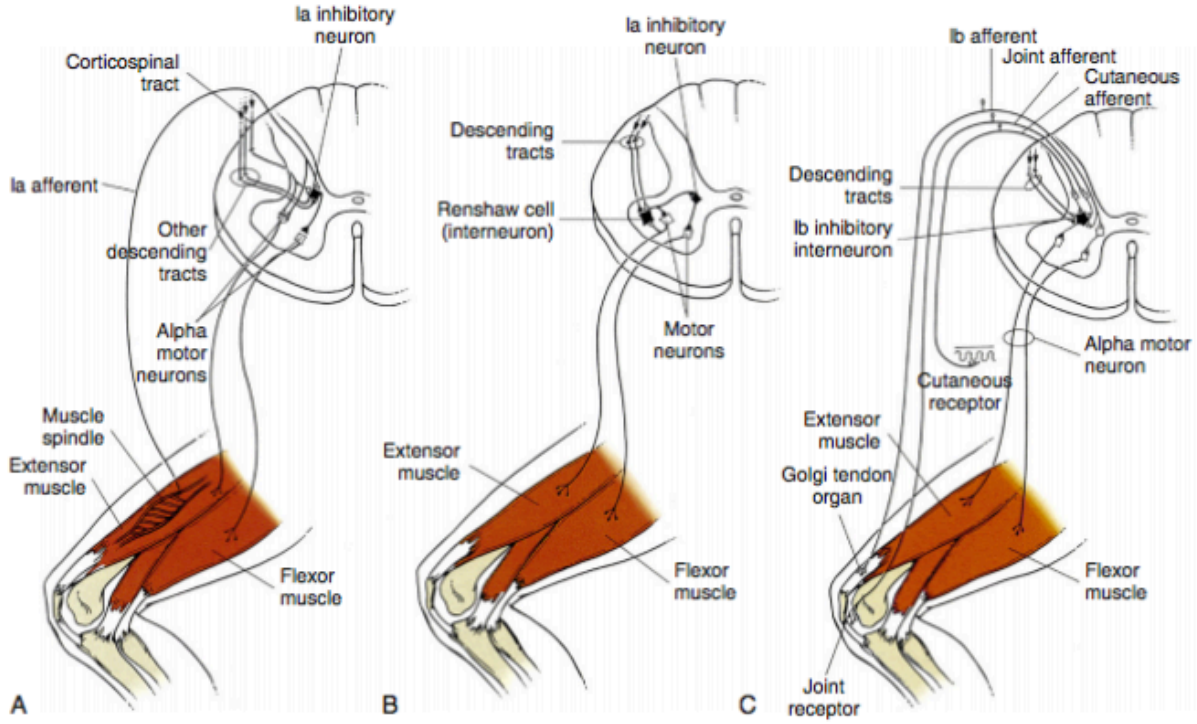

Figure 2.14: Reflex circuitry in the spinal cord. A, The Ia afferent link from the muscle spindle directly synapses on a motoneuron innervating the agonist muscle, but also on a Ia inhibitory interneuron, which inhibits the motoneuron innervating the antagonist muscle. B, The Renshaw cell receives input from a collateral branch of a motoneuron and from higher centers. Its effect is to inhibit the agonist motoneuron pool and thus shortens or reduces the motor neuron's response. Additionally, Renshaw cells can disinhibit the antagonist motoneuron via the connection to Ia inhibitory interneurons. C, The Ib inhibitory interneuron receives signals from the Golgi tendon organ, joint receptors, cutaneous receptors, and by descending pathways. Its effect is to inhibit the motoneuron to the homonymous muscle. It also disinhibits the antagonistic motoneuron (Δ, Excitatory; ▲, inhibitory.). Reprinted from Dramer (2014, p. 391).

The second type of inhibitory interneuron of the spinal cord is the *Renshaw cell*. The α motoneurons inhibit their own activity via Renshaw cells. Before leaving the ventral horn the α motoneurons send off collaterals that supply the Renshaw cells. These, in turn, synapse on the same motoneurons and on other α motoneurons that supply agonist muscles. This process is called recurrent or feedback inhibition. Renshaw cells are also extensively connected to descending neurons, so that their inhibitory effect is regulated in accordance with the overall plan of a voluntary movement.

Furthermore, Renshaw cells are connected to Ia inhibitory interneurons, influencing the strength of reciprocal inhibition. If a voluntary co-contraction of agonist and antagonist

is desired, the Renshaw cells suppress the reciprocal inhibition (also called disinhibition).

A third type of inhibitory interneuron in the spinal cord is the *Ib inhibitory interneuron*. It receives input from the Golgi tendon organs, joint receptors, pain receptors and general somatic afferents from the joint, which is affected by the concerning motor neuron pool. It has a powerful inhibitory connection to the agonist muscle and synergistic muscles but also excitatory connections to antagonistic motoneurons through trisynaptic pathways (Eccles et al., 1962).

Preprogrammed Movements and Muscle Tone

Groups of spinal interneurons function together to build stereotyped or *preprogrammed movements*. One example is the flexion withdrawal reflex. Nociceptors trigger this reflex, which leads to extension of the contralateral limb, followed by flexion of the ipsilateral limb. The withdrawal reflex involves coordinated contraction of numerous muscle groups, reciprocal inhibition and the opposite response in the contralateral limb (crossed extension reflex). The extending limb provides support of the body weight, during withdrawal of the affected limb. The magnitude and location of the sensory input determines the magnitude and speed of the reflex. The flexion withdrawal reflex is also involved in coordination of certain voluntary movements.
The choice of the adequate movement among many stereotyped movements depends on the type of stimulus perceived. Stimulation of the sole of the foot, for example, can trigger various reflexes, depending on the strength and type of the stimulus. When the sole is stroked with a blunt object (simulation slipping), a plantar flexion is elicited (in order to regain grip). When pressure is applied on the entire sole, the extensor thrust reflex is triggered (which is crucial for standing). When a painful stimulus is applied to the sole, the flexion withdrawal reflex is activated.

The normal *muscle tone* has three major roles. It helps to maintain posture, to store energy (for example during gait) and to dampen jerky movements. Muscle tone arises from the cooperation of the viscoelastic properties of muscles and tendons, and controlled contraction of muscle groups. These contractions are controlled primarily through feedback mechanisms, were the monosynaptic stretch reflex plays a major role. The muscle spindles constantly measure and counteract the length changes in muscles, by activating or deactivating motoneuron pools and thus contracting or relaxing the muscles. However, the muscle tone is not only regulated by stereotyped cord responses, but also by the ongoing activity of different peripheral sensors and descending input (Davidoff, 1992).

Hoffmann's Reflex

Hoffmann's reflex is commonly used to assess the excitability of defined groups of interneurons at rest and during voluntary movement in man (Crone, 1993). It was first described by Hoffmann 1918 as a reflex response in calf muscles following electrical stimulation of the tibial nerve in the popliteal fossa.

H reflexes are the electrical equivalent of myotatic reflexes such as the Achilles' reflex or the patellar reflex. Instead of a muscle stretch, an electrical stimulus applied on the Ia afferents elicits a reflex response in the associated muscle. A small stimulus evokes APs only in thick Ia afferents and thus elicits the H reflex, whereas a strong stimulus also stimulates adjacent, thinner α motoneurons, which can be seen as M wave in the EMG recording of the respective muscle. At further increase of stimulation intensity, a small F wave can be seen, produced by backfiring of motoneurons from antidromic conduction in motor fibers.

2.6 Posterior Root Reflex

Electrical stimulation of nerve afferents in the dorsal roots of the spinal cord elicits reflexive responses in the muscles that send these afferents. These posterior root reflexes (PRR) are the functional equivalent of the H reflex (Figure 2.15). Both are initiated by sensory fibers of muscle spindles, and trigger via a monosynaptic reflex arch motoneurons that innervate agonist muscle groups. Whereas the H reflex is evoked by stimulation of afferents in the peripheral nerves, the PRR is elicited by stimulation of similar afferents at proximal sites, adjacent to the spinal cord (Minassian et al., 2007).

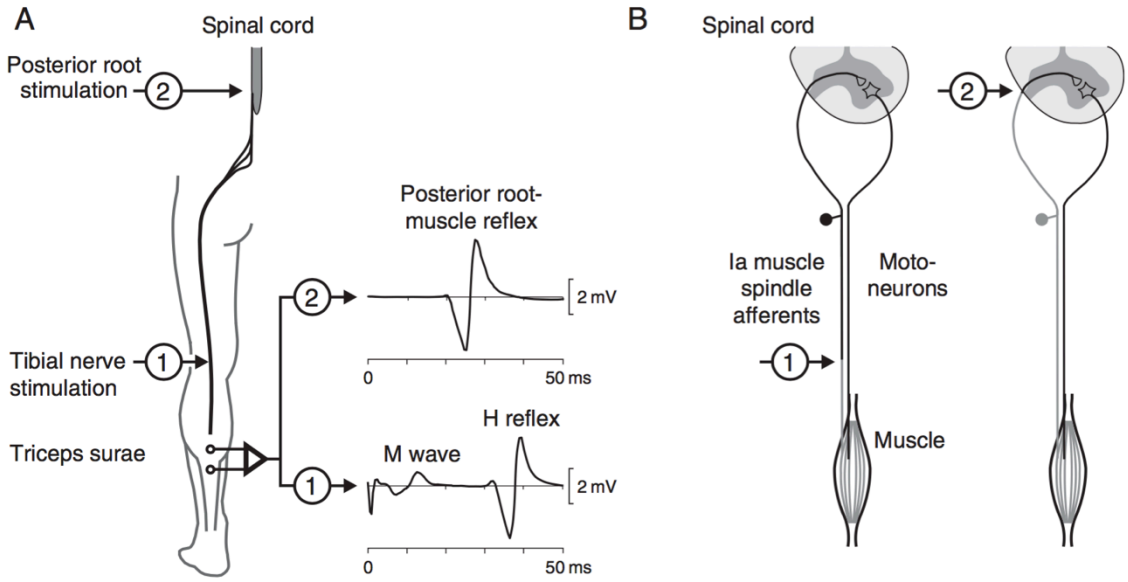

Figure 2.15: Comparison of elicitation of the H reflex and posterior root reflex. (A) The H reflex is evoked by stimulation of the posterior tibial nerve in the popliteal fossa. PRR is elicited by the same group of sensory fibers, but close to the spinal cord. Recordings of H reflex show a preliminary M wave of direct activation of motor fibers. Reprinted from Minassian et al. (2012, p. 240).

The PRR can be evoked in several muscles of the lower limbs by appropriate stimulation of dorsal roots at lumbosacral cord levels. This can be achieved through epidural spinal cord stimulation (eSCS), where an epidural lead is surgically placed over the dura mater on the posterior aspect of the spinal cord. Epidural spinal cord stimulation is generally associated with the treatment of chronic neurogenic pain conditions (Krames et al., 2009) and epidural electrodes are positioned at various spinal cord levels. In order to elicit a PRR in the lower limb muscles, the epidural lead is placed between the L2 and the S2 cord segment.

Minassian et al. (2007) demonstrated that transcutaneous spinal cord stimulation (tSCS), as a non-invasive technique, can also elicit PRR in all muscle groups of the lower limbs. Simulation studies (Danner et al., 2011; Ladenbauer et al., 2010) confirmed clinical findings, that there are two 'hotspots' for electrical stimulation: the sites where the fibers enter the cord, and the sites where the root fibers exit the spinal canal at the interface between cerebrospinal fluid and epidural fat. Roy et al. (Roy, Gibson, & Stein, 2012) described the best location for targeting efferent or afferent roots.

2.7 Generation of Movement

In the following, the generation of voluntary movements and the associated centers of the CNS will be discussed. Voluntary movements differ from reflexive movements in many ways. For voluntary, movements motor systems use different strategies in different situations to achieve the same results (also called motor equivalence). They improve in effectiveness by learning and experience. Voluntary movements are independent of external stimuli and can dissociate the content of movement from the initiation of movement.
The generation of voluntary movements can be divided into three steps: identification of an action that will be performed, planning of the action, and execution of the planned action. From this point of view, the motor centers will be discussed.

The *posterior parietal cortex* is associated with the identification of an action. It integrates visual, auditory and somatosensory information and has a motivational component. It is also influenced by the state of attention and the limbic system. The posterior parietal cortex provides the motor regions with information about the overall body position and the subject's intentions for a specific action.

The *premotor cortex* receives input from the posterior parietal cortex and is of major importance in the planning step of a desired movement. The lateral part is involved in conditional motor tasks, i.e. motor tasks based on external cues (reaching an object, for example). In macaque monkeys, areas of the lateral premotor cortex began to fire already at the appearance of a cue (Purves et al., 2001), encoding for the intention to perform a particular movement. It seems that the lateral premotor cortex is particularly involved in the selection of a movement, based on external events. The medial part of the premotor cortex also mediates the selection of movements.

The individual neurons of the *primary motor cortex* excite motoneurons all over the body directly or indirectly through brain stem centers. Penfield (1950) showed, that the primary motor cortex has distinct regions, which can be matched to different muscle groups of the body (Figure 2.16). A disproportionally large region is devoted to control the hand, lips and tongue, while very small parts contain neurons that control muscles of the back and abdomen. The variety and precision of movements seems to determine the amount of cortical neurons that are concerned with the respective body part.

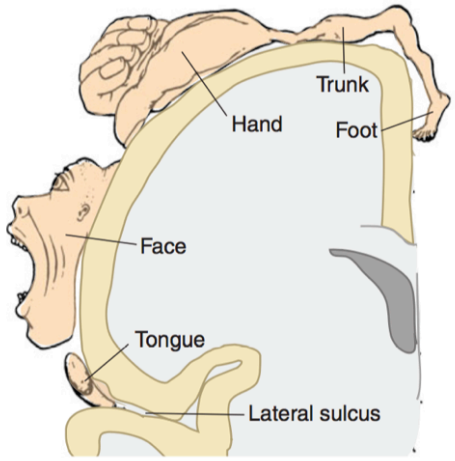

Figure 2.16: Topographic map of movement in the primary motor cortex according to Penfield et al. (1950). Reprinted from Brodal (2010, p. 316).

Graziano et al. (2005), however, applied stimulation on regions of the primary motor cortex of monkeys with stimulation trains of 2 pulses per second and suggested that the topographic representations of movement in the motor cortex are organized around ethologically relevant categories of motor behavior. For example, microstimulation of a specific area in the hand region of the motor cortex often invoked movements of the arm that brought the monkey´s hand to a central space (to inspect and manipulate a held object). Stimulation of more lateral sites often led to hand-to-mouth motions. Interestingly, the output of the stimulated cortical neurons encodes not simply the trajectory of motion, but also the final position of the arm.

The flowchart in Figure 2.17 shows the cooperation of the spinal cord and various higher centers in order to generate a voluntary movement. The movement has to be first formulated in the cerebral cortex. This “idea”, together with current proprioceptive information, is transmitted to the premotor cortex to develop an action plan. The basal ganglia are also involved in planning and receive input from virtually all cortical regions, like sensory, motor, and limbic connections. The premotor cortex and supplementary motor cortices then relay this plan to the primary motor cortex. Latter encodes force, velocity, and direction of the appropriate motor neurons through corticospinal pathways to the spinal cord. Additionally, the planned movement is stored in the cerebellum. Recticulospinal and vestibulospinal pathways provide the spinal cord with postural adjustments in order to hinder loss of balance. Ascending nerve fibers from proprioceptive sensors send collaterals to the cerebellum. It acts as comparator, comparing the planned movement with the actual ongoing movement. It can correct the ongoing movement by modifying the output of corticospinal pathways. The cerebellum can also influence the motor cortex via the thalamus, in order to alter the plan of the movement. Furthermore, the corticospinal pathways can be modified by spinal

interneurons, such as pain pathways, which alter or modify movements in response to sensed pain.

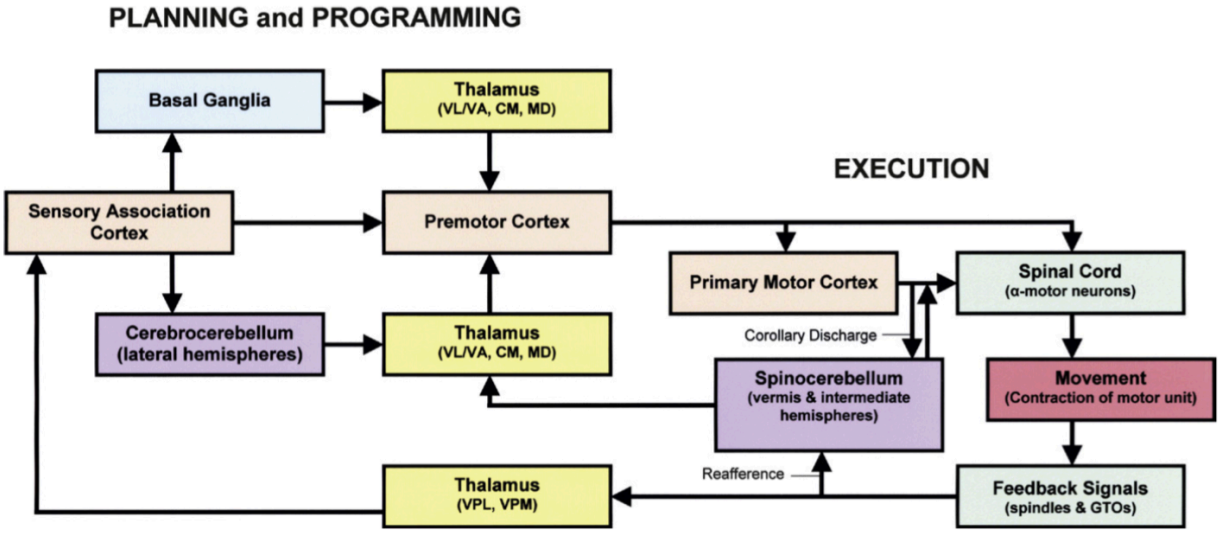

Figure 2.17: Flowchart of motor system components. Motor areas of the cortex (tan) can influence motor neurons in the spinal cord (green) directly or indirectly via the brain stem. The motor system is also influenced by two subcortical systems: the basal ganglia (blue) and the cerebellum (purple). The cerebellum influences both planning (cerebrocerebellum) and execution (spinocerebellum) of a movement. Reprinted from Dramer (2014, p. 399).

3

Methods

3.1 Subjects

Experiments were conducted in six healthy subjects, four males and two females. The mean values and standard deviation (SD) of age, height and weight were 26.5 ± 5.4 yrs, 182.3 ± 12.6 cm and 70.3 ± 14.5 kg, respectively. None of the participants had any history of neurological or orthopedic disorders. The study was performed at a clinical center with permission.

Table 3.1: Subject data of the six subjects group.

Subject number	Subject ID	Sex	Age	Height [cm]	Weight [kg]
S1	MT	M	27	197	88
S2	AM	M	25	182	64
S3	EG	F	24	173	61
S4	ES	F	24	166	50
S5	MK	M	37	179	76
S6	MS	M	22	197	83

3.2 Electrical Stimulation Set-Up

Electrical stimulation was performed using commercially available self-adhesive transcutaneous electrical neural stimulation electrodes (STIMEX, Schwa-medico GmbH,

Ehringshausen, Germany). One stimulating electrode with a diameter of 5 cm was placed over the T11-T12 vertebral processes. A pair of rectangular electrodes (8 cm x 13 cm each) was placed longitudinally over the abdomen, one on either side of the umbilicus. The two abdominal electrodes were inter-connected to function as a single electrode.

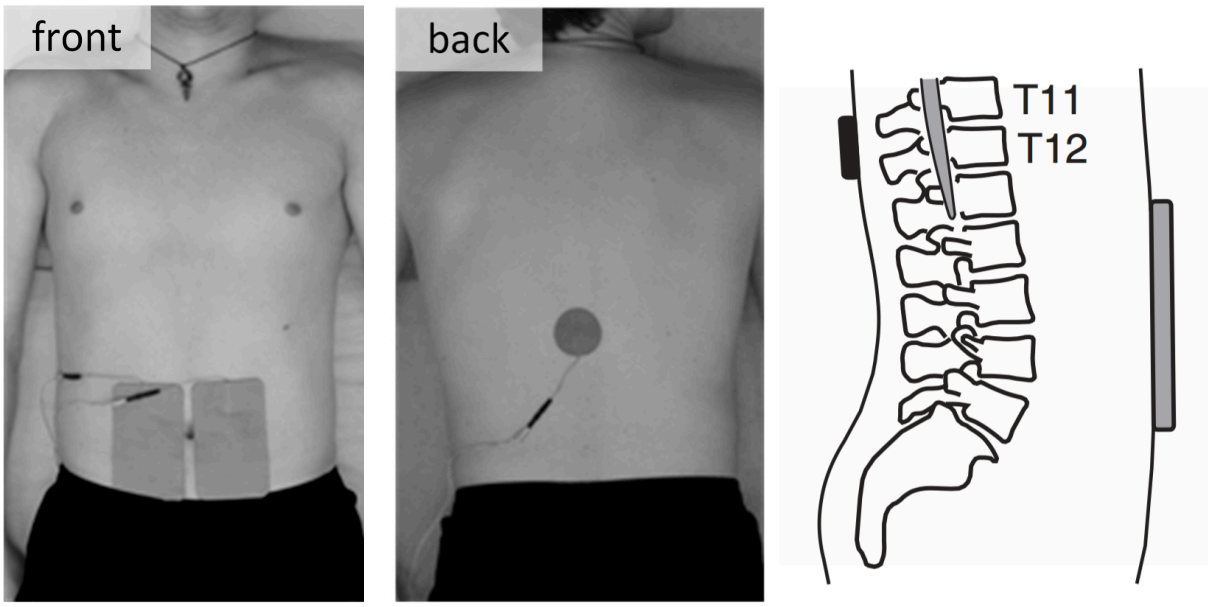

Figure 3.1: Placement of the indifferent electrodes on the abdomen (left) and the stimulating electrode on the back (middle). Scheme of the electrode placement (right).

A constant-current stimulator (Stimulette r2x, Dr. Schuhfried Medizintechnik GmbH, Vienna, Austria) was used to deliver monophasic rectangular pulses. The stimulus had a pulse duration of 1 ms. The stimulation pattern was different for each protocol. First, pairs of stimuli with an inter-stimuli interval of 35 ms were applied with a repetition time of 8 s. Secondly, trains of stimuli between 1 and 80 pulses per second (pps) were applied. The stimulation intensity was increased up to 120 mA. The paravertebral electrodes acted as cathode, with the abdominal electrodes as anode.

3.3 Recording Procedure

Electrode Position and Skin Preparation

The electromyographic (EMG) activity of the quadriceps, hamstrings, tibialis anterior, and triceps surae in both legs was recorded with pairs of silver-silver chloride surface electrodes (Intec Medizintechnik GmbH, Klagenfurt, Austria). Therefore, electrode pairs were placed bilaterally on the muscle belly of the rectus femoris, biceps femoris and tibialis anterior with an inter-electrode distance of 2-3 cm, and oriented along the long axis of the muscles (Figure 3.2). The electrodes for the triceps surae were placed between the two heads of the gastrocnemius and slightly below on the soleus muscle.

The positive polarity of each bipolar pair was oriented proximal. Reference electrodes were placed on the fibular head for each leg.

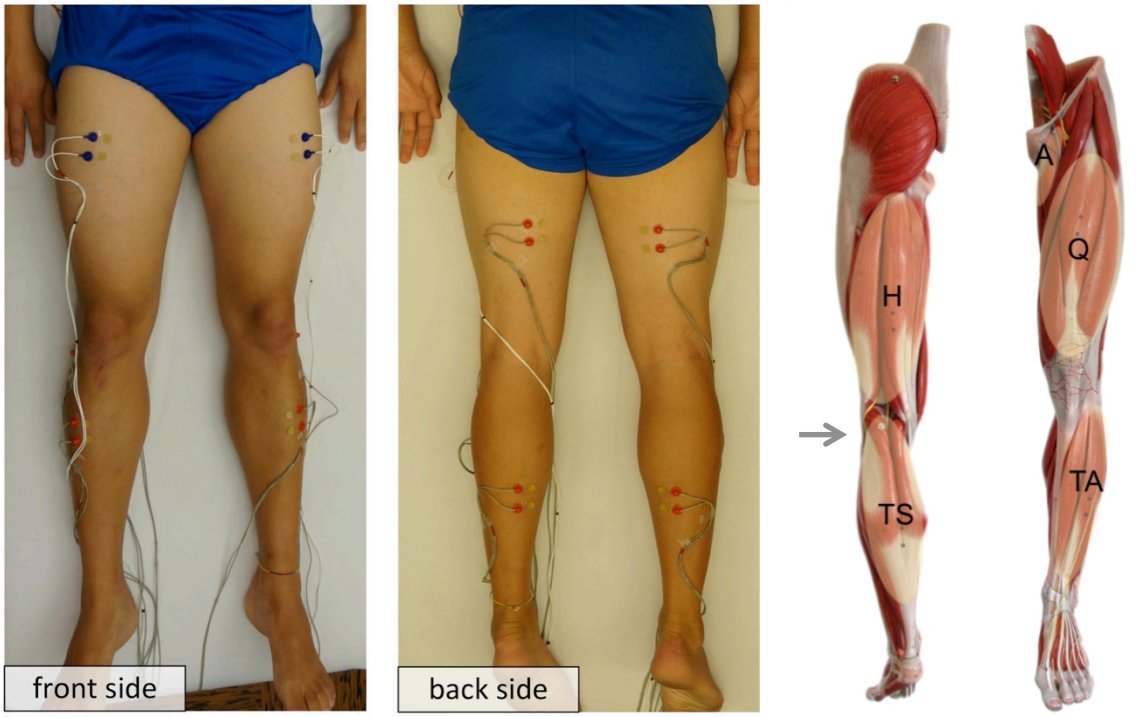

Figure 3.2: Electrode positioning on the lower extremities (left, middle) and main lower limb muscles (right). Adductor (A), quadriceps (Q), hamstring (H), tibialis anterior (TA) and triceps surae (TS). Grey points indicate the placement of the recording electrodes. For each electrode pair, the cranially oriented electrode acted as anode. The grey arrow indicates the placement of the reference electrode on the fibular head.

For synchronization with the stimulator, a pair of electrodes was placed slightly below and lateral to the heart, and oriented obliquely in medio-caudal direction. This electrode pair functioned as trigger for the recording software, and additionally for monitoring the heart rate.

To obtain low electrode impedance, the skin was abraded using abrasive cream (Nuprep, Weaver and Company, Inc., Aurora, CO, USA) and the gel-filled electrodes (Signa-Gel, Parker Laboratories, Inc., Fairfield, NJ, USA) were mounted on the prepared spots.

Amplification and Digitalization

The EMG signals were amplified with a gain of 600 and a bandwidth of 10-600 Hz and digitized at 8000 samples per second (S/s) using a USB-NI 6261 data acquisition card (National Instruments, Inc., Austin, TX, USA). The data was stored and preprocessed with Dasylab 11.0 (Measurement Computing Corporation, Norton, MA, USA) and analyzed using Matlab R2013b (The MathWorks, Inc., Natick, MA, USA) and Microsoft Excel 14.2.3 (Microsoft, Redmond, WA, USA).

3.4 Study Protocol

The study protocol was conducted with the subjects in a relaxed, supine position. Subjects were instructed to focus on a spot on the ceiling, and were kept awake during the measurements. They were called attention, if undesired muscle tone was measured.
First, stimulation was delivered as a 1 ms, monophasic, rectangular pulses, with increasing stimulation intensity to assess the recruitment behavior in thigh and lower leg muscles. If necessary, the stimulating electrode placement was adjusted in the cranial-rostral direction.

Recording of Recruitment Curves

For a given stimulation intensity below reflex threshold intensity, one pair of stimuli (34 ms inter-stimuli interval) and two single stimuli were triggered, with a recovery interval of 8 s. Then stimulation current was gradually increased in 5 mA increments until saturation or to the level that started to cause moderate discomfort to the subject. This discomfort was due to local contraction of paravertebral muscle groups. Recruitment curves were constructed by plotting the peak-to-peak (PTP) amplitude of spinally evoked potentials at increasing stimulation intensities. The resulting Recruitment behavior was used to select appropriate stimulation intensity in order to elicit PRR responses in all recorded leg muscles.

Identification of the Nature of Muscle Responses

In the course of recording of recruitment curves at each stimulation intensity pairs of stimuli with an inter-stimuli interval of 35 ms were applied. Analysis of each pair of stimuli then showed attenuation in the second response, compared to the first response (Figure 3.3). This attenuation reveals a prolonged refractory period, which indicates the reflex nature of the first response. This refractory behavior of the second response would not be expected for direct electrical stimulation of efferent nerve fibers.

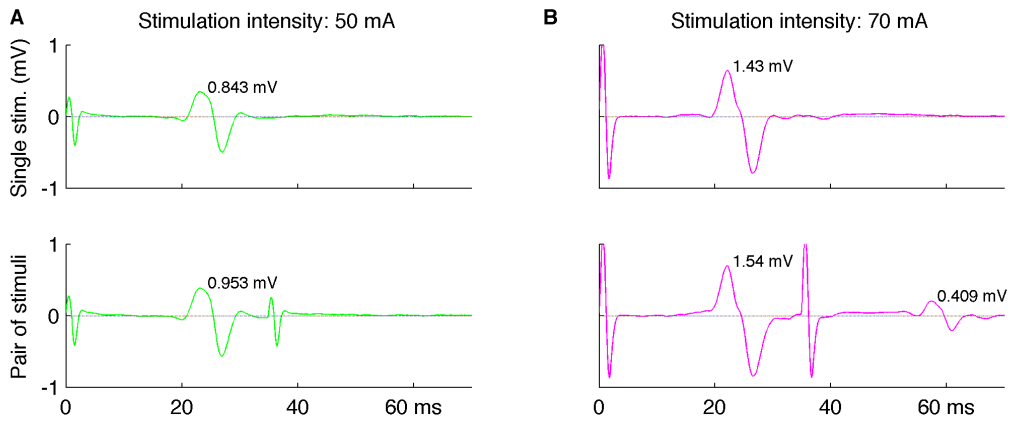

Figure 3.3: Comparison of single stimuli and pairs of stimuli. PRR recorded from the left tibialis anterior in subject S2. The reflex was elicited once by a single stimulus and once by a pair of stimuli with an inter-stimuli interval of 35 ms. At stimulation intensity of 50 mA (a) no response to the second stimulus was seen. At 70 mA (b) attenuated responses were detected. Inserted values are peak-to-peak amplitudes of the responses.

Conditioning-Test Paradigms to Sustained Stimulation

Before the measurement started, the subject was told to completely relax. After a resting phase of 2 minutes, trains of stimuli were applied at 1 or 2 pps. Recordings started with elicitation of control reflexes for 10 s, followed by responses elicited under volitional unilateral dorsi- or plantar flexion.

Subjects performed a motor task pattern of contraction (approx. 2 s), holding (3 s), and fast-release. Thus phases of dorsi- or plantar flexion were held for at least 5 s. The movement was tagged using a marker that generated a rectangular signal and was recorded synchronously with the EMG signals. After each phase of dorsi- or plantar flexion control responses were recorded for at least 5 s.

In order to alter contraction force of dorsiflexion, a spring balance was mounted to the ball of the foot. During dorsiflexion the balance was kept at the desired tension, and such that the ankle stayed in moderate flexed position.

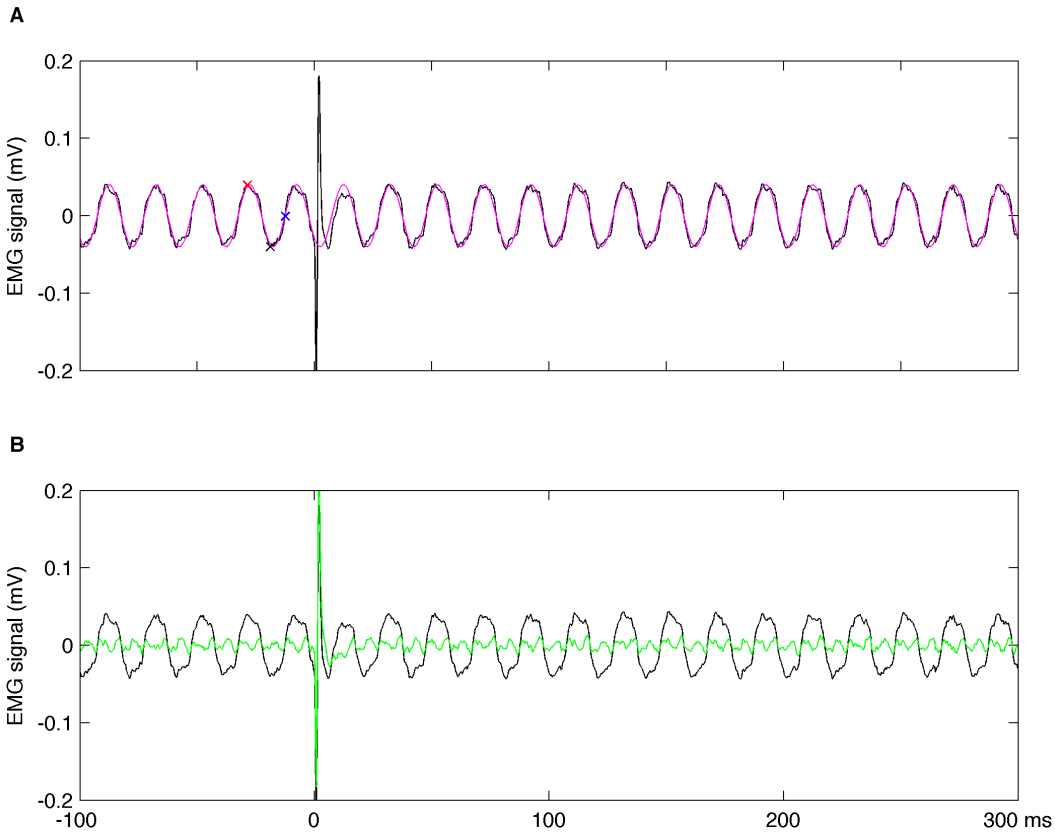

Figure 3.4: Subtraction of fitted sine function. (A) Minimum (black x), maximum (red x), and zero crossing (blue x) were determined in a time frame of -40 ms to -10 ms from the recorded signal (black). From these data points a sine function (magenta) was generated and subtracted. The corrected signal is plotted in green color (b).

3.5 Data Analysis of Responses

Analysis of Responses to Single Stimulus and Pairs of Stimuli

With the recording software Dasylab 11.0 a digital stimulation trigger was defined, that triggered, when the peak-to-peak EMG amplitude measured with the trigger electrodes exceeded an appropriate threshold. With the aid of this digital trigger, datasets of -100 ms to 300 ms (related to stimulation at time point 0) were recorded and read in Matlab R2013b.

The power-line interference in the signal baseline was reduced by subtraction of a fitted sine signal having a fixed frequency of 50 Hz. Therefore, the minimum, maximum, and zero crossing of the interfered signal baseline was determined within the time frame of -40 ms to -10 ms prior to stimulation pulse (Figure 3.4). From these data points a sine function P(t) was generated and subtracted. The following equation shows the fitted power-line interference signal:

A … difference of maximum to minimum, t … time, t_0 … time point of zero crossing, f … frequency of 50 Hz.

$$P(t) = A * \sin((t - t_0) * 2\pi f)$$

EMG response latencies were measured from the onset of the stimulus pulse to the onset of the elicited PRR response. The onset of a PRR signal was defined as the first deflection from the baseline, that was larger than 100 µV. EMG response latencies of all subjects at a stimulation intensity of 55 mA were averaged and Pearson's correlation coefficients comparing subject height with the latency of the response were calculated (with x, y, height and response latency):

$$r = \frac{\sum_i (x_i - \bar{x})(y_i - \bar{y})}{\sqrt{\sum_i (x_i - \bar{x})^2 * \sum_i (y_i - \bar{y})^2}}$$

For the *standard recruitment curves*, peak-to-peak PRR response amplitudes were averaged for each stimulation intensity (Figure 3.5). Then the averaged amplitudes were plotted against the stimulation intensity. Additionally, for paired stimuli, the peak-to-peak amplitude of the response to the second stimulus was calculated and plotted against the stimulation intensity.

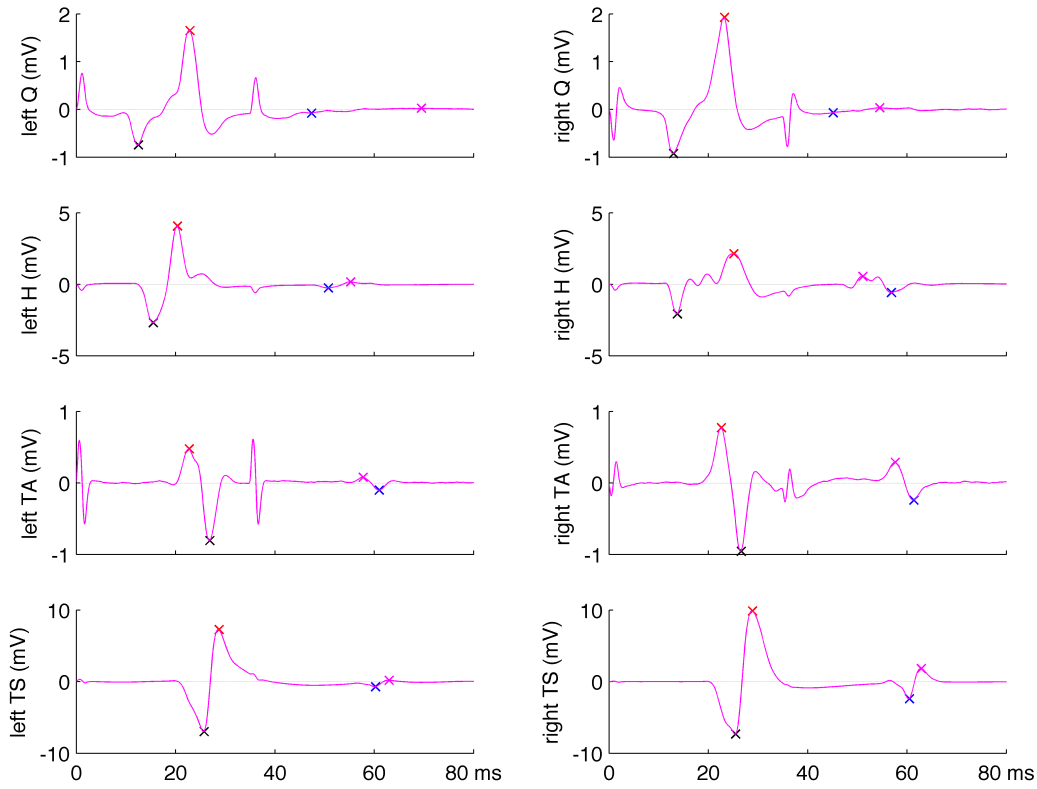

Figure 3.5: Calculation of peak-to-peak values of PRR responses. Minima (black, blue) and maxima (red, magenta) were post-processed in time frames of 10 ms to 33 ms and 45 ms to 80 ms.

Standard recruitment curves were calculated for all subjects and for each muscle group. To compare recruitment in different subjects and muscle groups, threshold stimulation intensities that were necessary to elicit reflex responses in respective muscles were determined. Reflex responses were considered, if their peak-to-peak amplitude exceeded 100 µV. All subject's threshold intensities were then presented as bar plot.

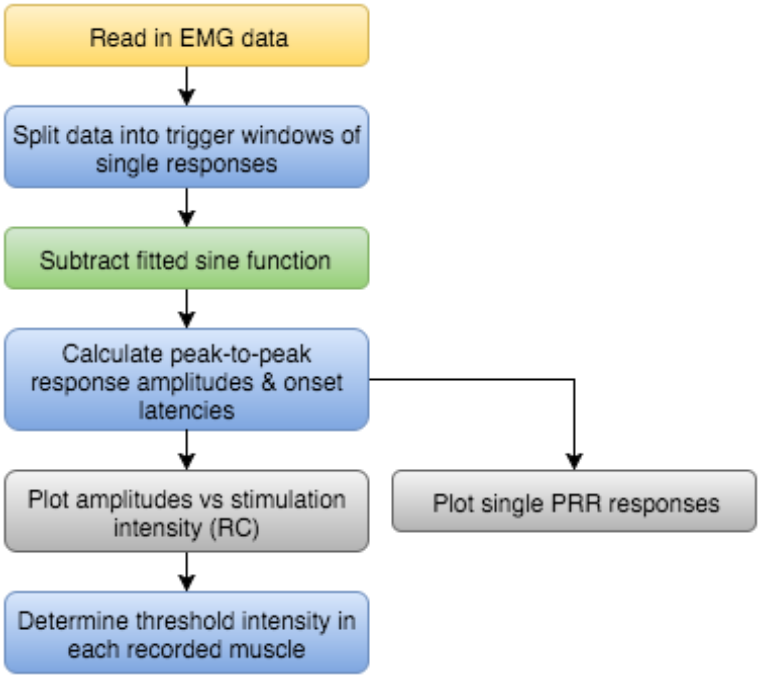

Figure 3.6: Flowchart of the analysis of PRR responses to single stimuli and pairs of stimuli.

Analysis of the Conditioning-Test Paradigms to Sustained Stimulation

Recorded data of experiments with sustained stimulation were first visualized (signals of all channels versus time) and the section of interest was cut out. The conditioning *marker signal* was obtained from the recorded signal of the marker, or adjusted afterwards manually by matching to the periods of continuous EMG activity of the respective muscle (Figure 3.7). In this way, all responses could be labeled, to distinguish if they were elicited at unconditioned state, or elicited during conditioning by dorsi- or plantar flexion.

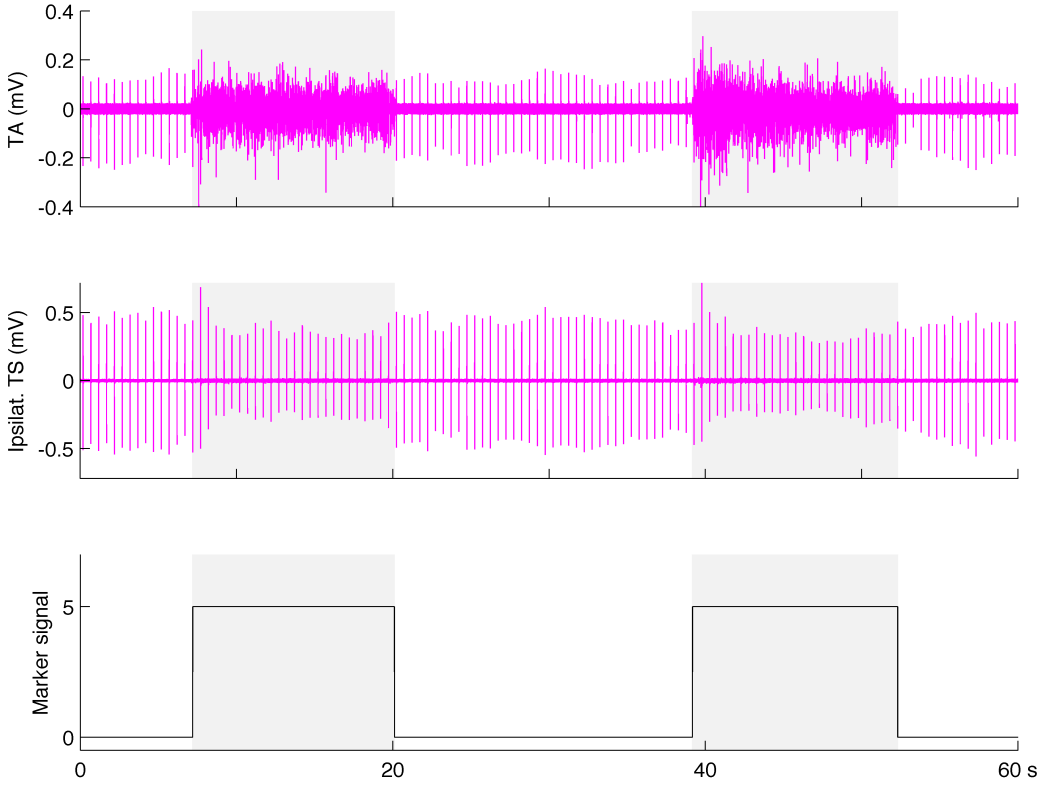

Figure 3.7: Marker signal to unconditioned and conditioned responses. The marker was set to a value of 5 at onset and hold of dorsiflexion (grey). Thus responses of conditioned reflexes were labeled for further analysis.

In this case, the power-line interference could not be removed by subtraction of a fitted signal because of the long measurement time. Therefore, an appropriate notch filter was applied to remove baseline noise. In some cases, the notch filter was not applied when calculating PTP response amplitudes due to distortion of stimulation spikes.

Time points of stimulation were defined through the stimulation artifacts that were recorded with the trigger electrodes in the chest area. These stimulation artifacts were considered only, if they exceeded an appropriate threshold value, to distinguish them from baseline noise and signals of the heartbeat. In order to obtain accurate stimulation time points, they were defined at the rising slope of the absolute value of the artifact (to consider the negative deflection, Figure 3.8). The next stimulation time point was sought after a refractory period of 80% of the inter-stimuli period derived from the stimulation rate.

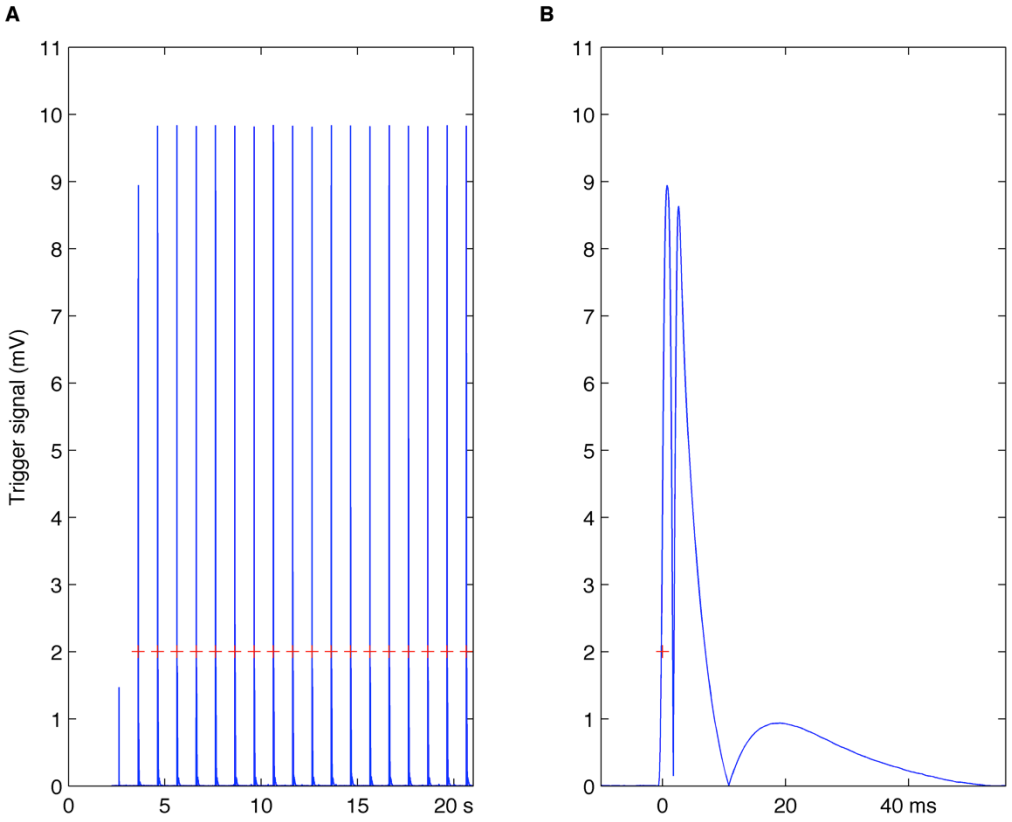

Figure 3.8: (A) Definition of stimulation time points (red crosses). Stimulation artifacts (blue) were measured at level below the heart. Stimulation time points were defined at threshold 2 mV on the rising slope of the absolute value of the stimulation artifact signal (b). The measuring apparatus limited the recorded signal to max. 10 mV.

Then all EMG data set was split into triggered windows of -5 to 50 ms related to the stimulus artifact at time point zero. For each muscle and for each conditioning-test paradigm the respective trigger windows were overlaid and a mean curve and standard deviation was calculated.

In order to visualize exclusively responses to PRR (without stimulation artifacts), the values of EMG data between -2 to 8 ms related to stimulus at time point 0 were set to zero (based on latency measurements as described above). Figure 3.9 shows a section of EMG signal and corrected signal by removing of the stimulation artifact.

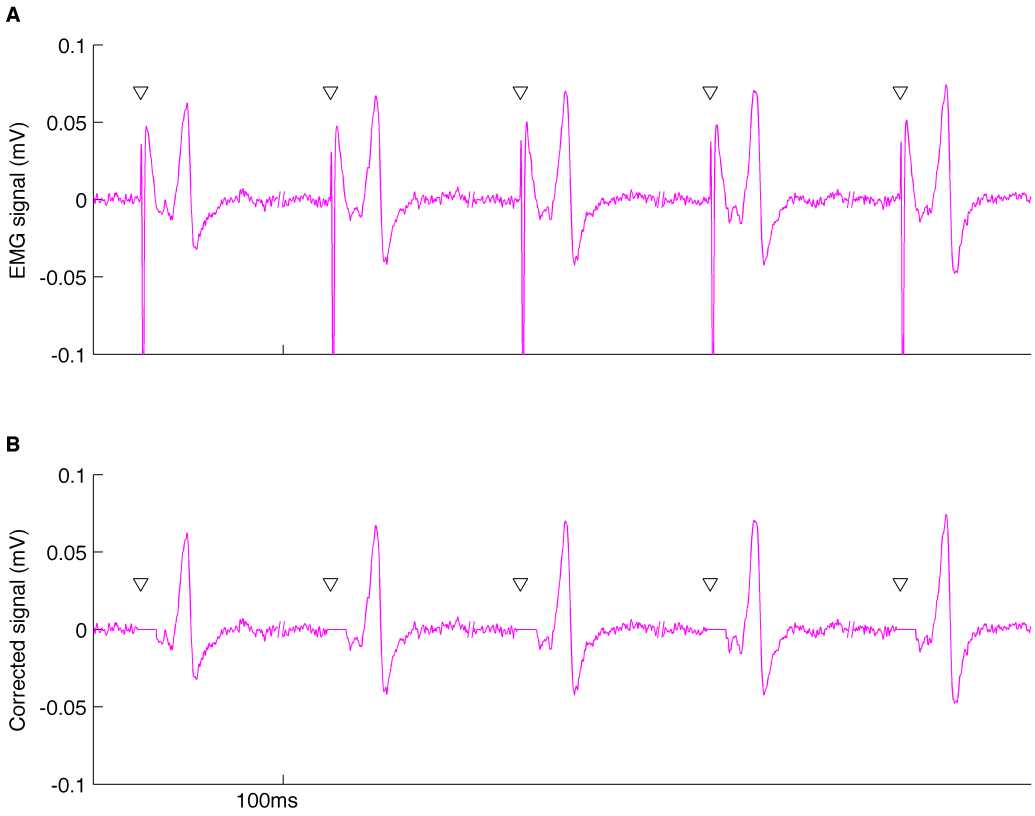

Figure 3.9: Example of recorded EMG activity (a) and with removed stimulation artifact in an interval between -2 ms and 8 ms with regard to stimulation (b). Frames of -25 ms to 75 ms are shown. Black triangles indicate the stimulation.

Calculation of *mean values of PTP amplitudes* turned out to be a delicate task. While responses to unconditioned stimuli could easily be determined from the extreme values of a mean curve (averaging each point of the signal curves), responses to volitional contraction were superimposed by muscular EMG activity, especially during weak contraction (Figure 3.10). For this reason, PTP amplitudes of PRR responses were calculated from each signal curve separately, and then averaged over all signal curves. The choice of the interval for determination of PTP amplitude had great significance for the mean value, as seen in the bar plot in Figure 3.10. For further calculations an appropriate interval was chosen, that corresponded to the response time frame in unconditioned case.

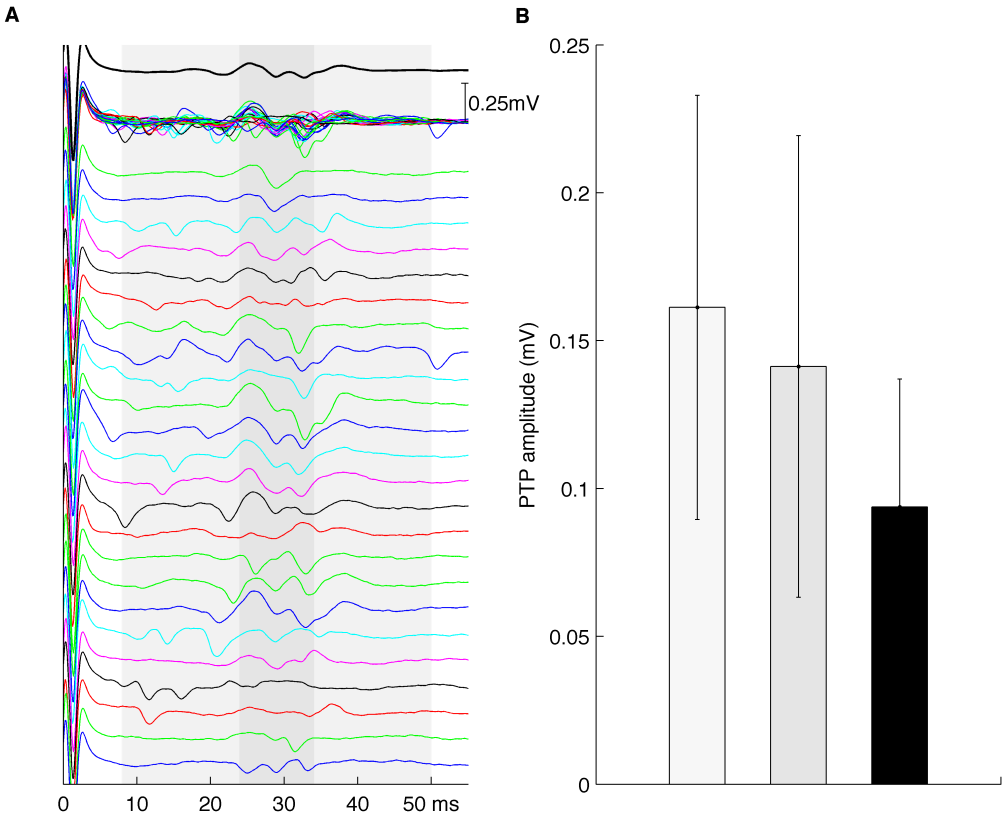

Figure 3.10: Calculation of mean PTP response amplitudes during weak volitional contraction of the recorded muscle. The mean curve (thick black, a) was obtained by point-by-point averaging of superimposed signal curves (multicolored). The black bar (b) shows PTP amplitude of the mean curve. The light grey bar indicates the averaged value of PTP amplitudes from individual signal curves within the interval 8 ms to 50 ms. The dark grey bar represents the same value within the interval 24 ms to 34 ms (corresponding to the response interval in unconditioned case).

Group results were obtained as follows:
For each subject peak-to-peak responses of conditioned PRR were calculated, averaged and normalized to the averaged unconditioned response (for ipsilateral and contralateral side separately). The normalized values were averaged over all measurements and presented as bar plots. Error bars represent the standard deviation among the measurements.

For analysis of PRR responses at different muscular contraction forces and to evaluate, if other muscle groups co-contract at unilateral dorsi- or plantar flexion, EMG signal of muscular contraction was measured by determination of the root mean square (RMS) curve of all superimposed signal curves.

$$RMS(t) = \sqrt{\frac{1}{n}\sum_{i} x_i^2(t)}$$

The RMS curve was calculated for a defined time window (t_1-t_2), where EMG signal of voluntary contraction was seen. This time window could be shortly before stimulation, or after the silent period that was seen after each response. Then a mean RMS value was determined by averaging over time.

$$\overline{RMS} = \frac{1}{T}\int_{t_1}^{t_2} RMS(t)\,dt$$

Signal baseline noise contributes to the RMS and in some cases of muscular contraction (especially co-contraction of antagonist during plantar flexion), the noise predominated EMG activity of voluntary contraction. Therefore, a control RMS was calculated in a selected time frame, where no contraction was seen.

Figure 3.11 presents a flowchart of processing steps underlying every evaluation of EMG signals that were recorded with application of sustained stimulation.

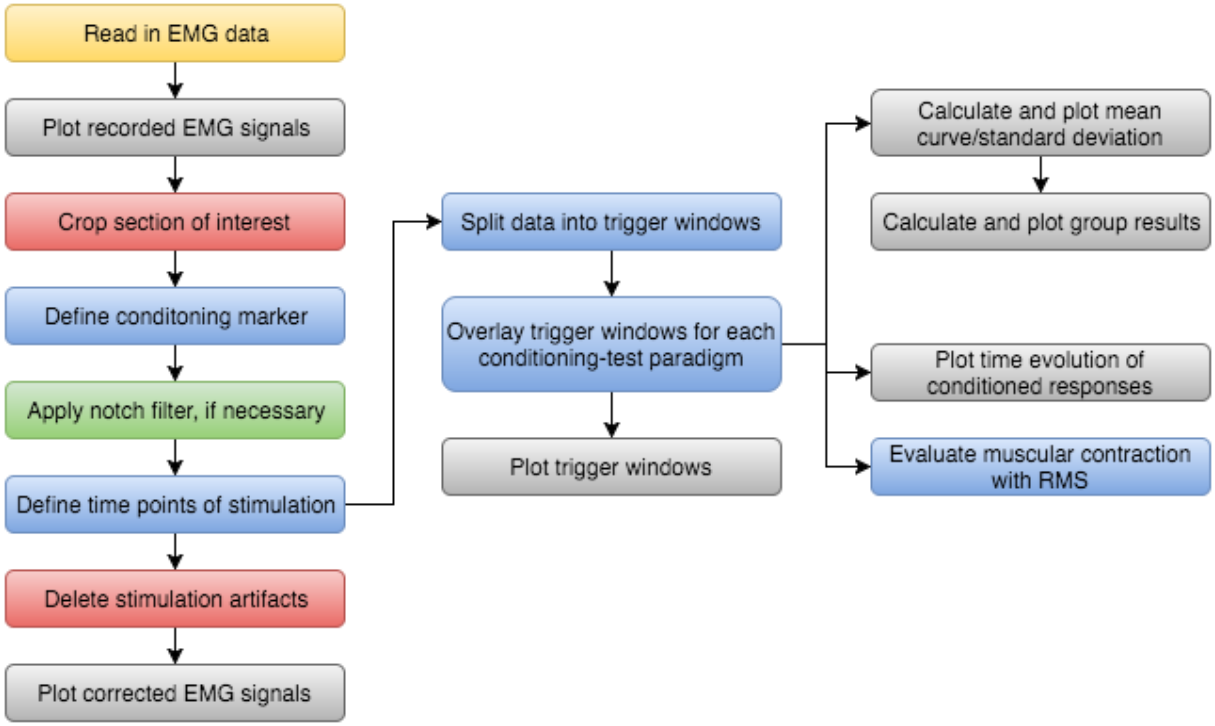

Figure 3.11: Flowchart of analysis of PRR responses to sustained stimulation at 1 pps or 2 pps.

4

Results

4.1 Posterior Root Reflexes

Sample Responses in all Recorded Muscle Groups

PRR were evoked in all recorded muscles by transcutaneous electrical stimulation of the lumbosacral cord in five measurements. Figure 4.1 shows representative EMG recordings in the left and right quadriceps (Q), hamstrings (H), tibialis anterior (TA), and triceps surae (TS) elicited by a single pulse. Three subjects showed a preference side in the lower leg, with lower threshold intensity than on the contralateral side. The common stimulation threshold intensity was in average 51 ± 4 mA. This threshold was defined to elicit responses bilaterally in TA, and TS exceeding a PTP amplitude of 100 µV. Figure 4.2 presents the threshold stimulation intensities of each subject. Subject S5 was measured on two different days and only TA and TS responses were recorded. Additionally, the stimulating electrode was placed 5 mm offset to the left related to the longitudinal axis of the spine.

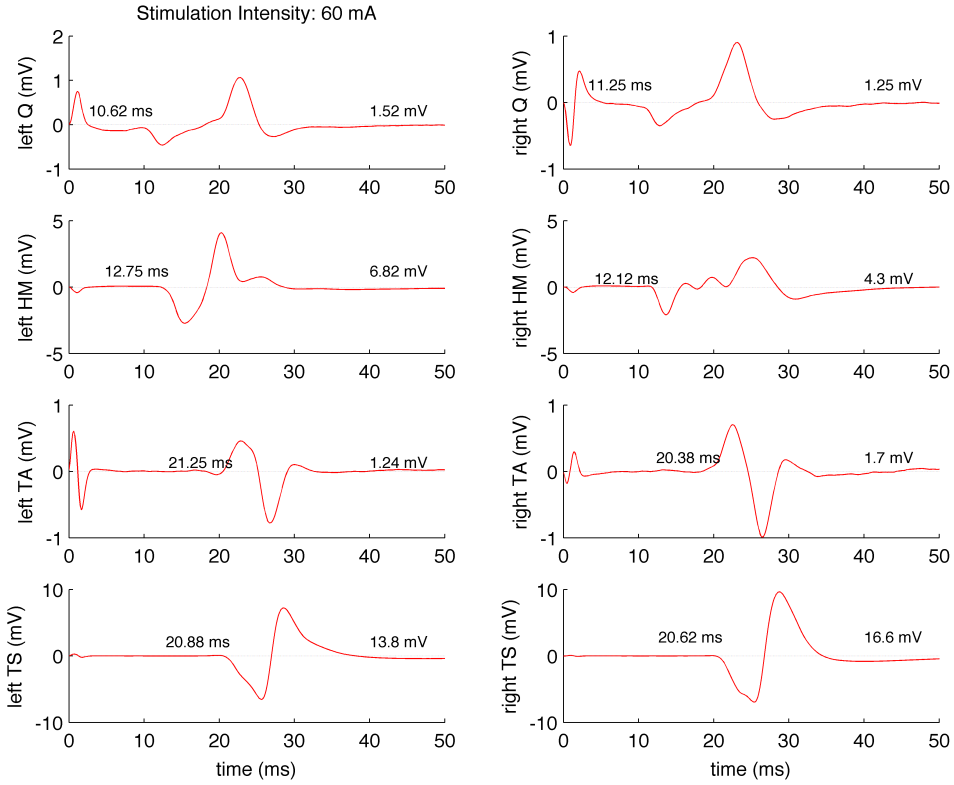

Figure 4.1: PRR simultaneously recorded from the left and right quadriceps (Q), hamstrings (HM), tibialis anterior (TA), and triceps surae (TS) in subject 2. Stimulation site: T11-T12 interspinous space. Inserted values are onset latencies and peak-to-peak amplitudes of PRR responses

The mean and SD values of the response latency at 55 mA were in Q 12.3 ± 0.8 ms, H 13.0 ± 0.5 ms, TA 22.0 ± 1.6 ms, TS 21.1 ± 1.2 ms. Pearson's correlation coefficients comparing latency and subject height were 0.97 and 0.87 for the left TA and left TS, respectively.

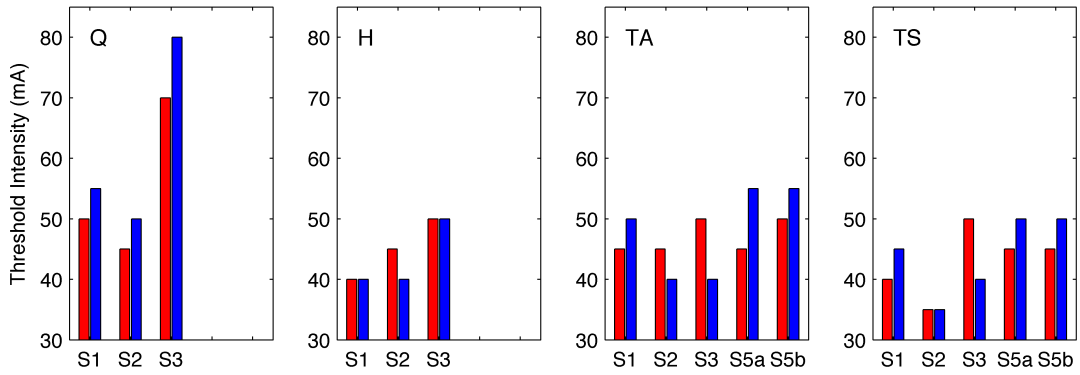

Figure 4.2: Comparison of threshold stimulation intensity values to lumbosacral cord stimulation. Threshold intensity was defined as the intensity that evoked a PTP response < 100 µV. Responses in quadriceps (Q), hamstrings (H), tibialis anterior (TA), and triceps surae (TS) were recorded. Red: muscles of the left leg. Blue: muscles of the right leg. Subject S5 was measured on two days, quadriceps and hamstrings were not recorded and the stimulating electrode was placed 5 mm offset to the left.

Paradigm of Pairs of Stimuli

Responses to a second stimulus applied with an inter-stimuli interval of 35ms, were depressed in all muscles. Figure 3.3 shows EMG recordings in the left tibialis anterior, elicited by single stimuli and by pairs of stimuli for two different stimulation intensities. Table 4.1 reports PTP values of responses to pairs of stimuli in all recorded muscle groups.

In quadriceps of subject S3 the applied stimulation intensity was below threshold to elicit PRR responses with peak-to-peak amplitudes > 100 µV.

Table 4.1: Peak-to-peak values of a response to pairs of stimuli (stimulation intensity 60 mA) bilaterally in quadriceps (Q), hamstrings (H), tibialis anterior (TA), and triceps surae (TS). The inter-stimuli interval was 35 ms. Peak-to-peak amplitudes of EMG responses are presented in mV.

		S1		S2		S3		S5a		S5b		Mean (SD)	
		L	R	L	R	L	R	L	R	L	R		
Q	1. PTP	1.63	0.78	1.86	1.87	0.08	0.05	NM	NM	NM	NM	1.54	0.52
	2. PTP	0.07	0.11	0.10	0.11	0.09	0.04	NM	NM	NM	NM	0.10	0.02
	Ratio	4.5%	14.2%	5.5%	5.7%	103.6%	85.5%	NM	NM	NM	NM	7.5%	4.5%
H	1. PTP	4.71	4.96	6.69	4.23	0.53	2.28	NM	NM	NM	NM	3.90	2.17
	2. PTP	0.49	0.43	0.42	1.14	0.04	0.07	NM	NM	NM	NM	0.43	0.40
	Ratio	10.3%	8.7%	6.3%	26.9%	7.2%	3.1%	NM	NM	NM	NM	10.4%	8.4%
TA	1. PTP	0.64	0.47	1.25	1.70	0.98	0.69	1.13	0.32	0.85	0.23	0.83	0.45
	2. PTP	0.05	0.02	0.18	0.53	0.06	0.02	0.06	0.05	0.02	0.03	0.10	0.16
	Ratio	8.1%	5.0%	14.3%	31.0%	5.9%	3.6%	5.0%	14.1%	2.2%	12.6%	10.2%	8.5%
TS	1. PTP	6.34	3.90	13.95	16.53	2.68	7.48	9.18	2.94	8.94	2.56	7.45	4.84
	2. PTP	0.28	0.21	0.90	4.22	0.04	0.15	0.60	0.13	0.53	0.14	0.72	1.26
	Ratio	4.4%	5.5%	6.5%	25.5%	1.5%	2.0%	6.6%	4.5%	5.9%	5.3%	6.8%	6.8%

NM … not measured

Recruitment Curves

Figure 4.3 shows the standard recruitment curves of all recorded muscles in subject S2. Increasing lumbosacral cord stimulation resulted in recruitment curves of similar shapes for all recorded muscles. The stimulus-response curve grows initially with moderate slopes, then more steeply until a plateau is reached.

When pairs of stimuli were applied, responses to the second pulse could be seen only at stimulation intensities of over 120% of respective threshold intensities for PRR elicitation. The peak-to-peak response amplitude of the second pulse increased linearly and did not reach a plateau for the intensities that were applied in this study.

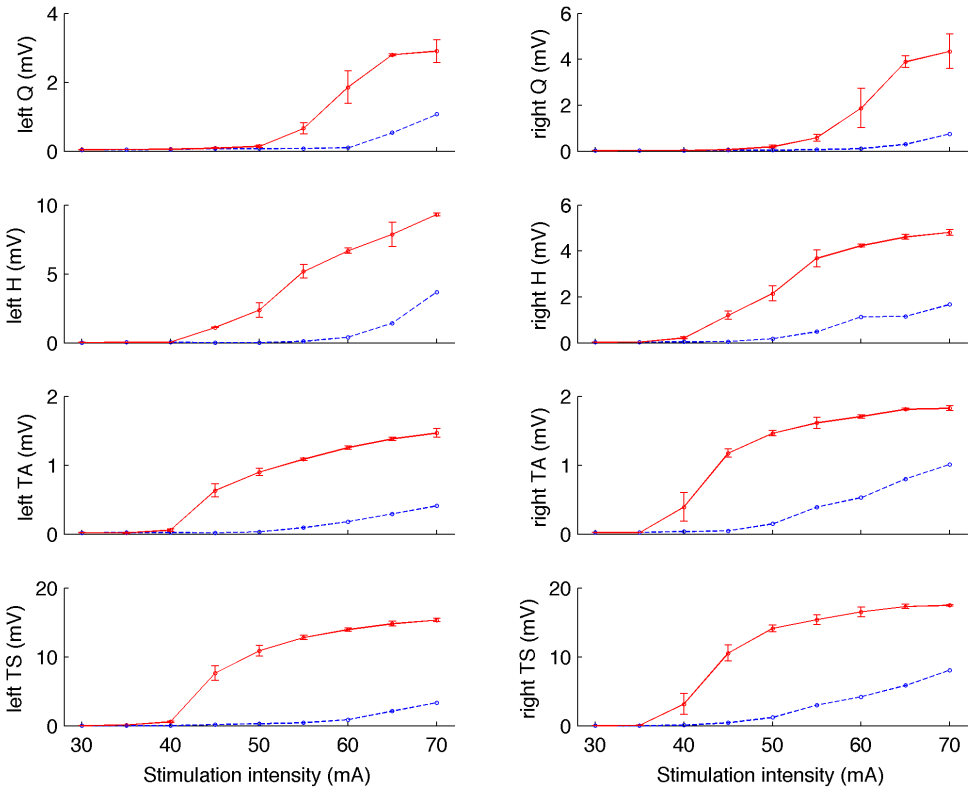

Figure 4.3: Standard recruitment curve of a subject (S2). For every stimulation intensity between 30 mA and 70 mA, a pair of stimuli followed by two single stimuli was delivered, increasing in 5 mA-steps. Mean value of PTP responses to first (red) and second (blue) stimulus. Error bars indicate the SD.

Comparison of Responses to Stimulation rate of 1/8 pps, 1 pps and 2 pps

Control responses to sustained stimulation with a stimulation rate (SR) of 1 pps or 2 pps were smaller compared to responses elicited by stimulation every 8 seconds. Table 4.2 and Figure 4.4 show results. Subject S1 was stimulated with stimulation intensity 55 mA, subject S2 was stimulated at 65 mA. Three responses at a SR of 1/8 pps were averaged, whereas responses at a SR of 1 or 2 pps were averaged over at least 10 responses.

Table 4.2: Mean PTP responses to stimulation with 1/8 pps, 1 pps and 2 pps. Mean values of PTP responses are presented in mV.

		SR 1/8 pps (S2)		SR 2 pps (S2)			SR 1 pps (S1)		SR 1/8 pps (S1)		
		Mean	SD	Mean	SD	Ratio	Mean	SD	Mean	SD	Ratio
Left Side	Q	2.80	0.03	1.55	0.21	55%	0.63	0.40	0.11	0.01	18%
	H	7.88	0.88	5.28	0.59	67%	4.36	0.22	2.51	0.08	57%
	TA	1.38	0.03	0.35	0.04	26%	0.58	0.02	0.23	0.02	39%
	TS	14.82	0.37	3.82	0.52	26%	5.66	0.32	1.72	0.22	30%
Right Side	Q	3.89	0.25	1.43	0.26	37%	0.36	0.24	0.12	0.03	34%
	H	4.61	0.11	1.92	0.42	42%	4.23	0.42	0.80	0.23	19%
	TA	1.81	0.01	0.77	0.12	42%	0.35	0.02	0.18	0.02	52%
	TS	17.31	0.33	7.80	0.90	45%	2.84	0.45	0.62	0.12	22%
Mean						**42%**					**34%**

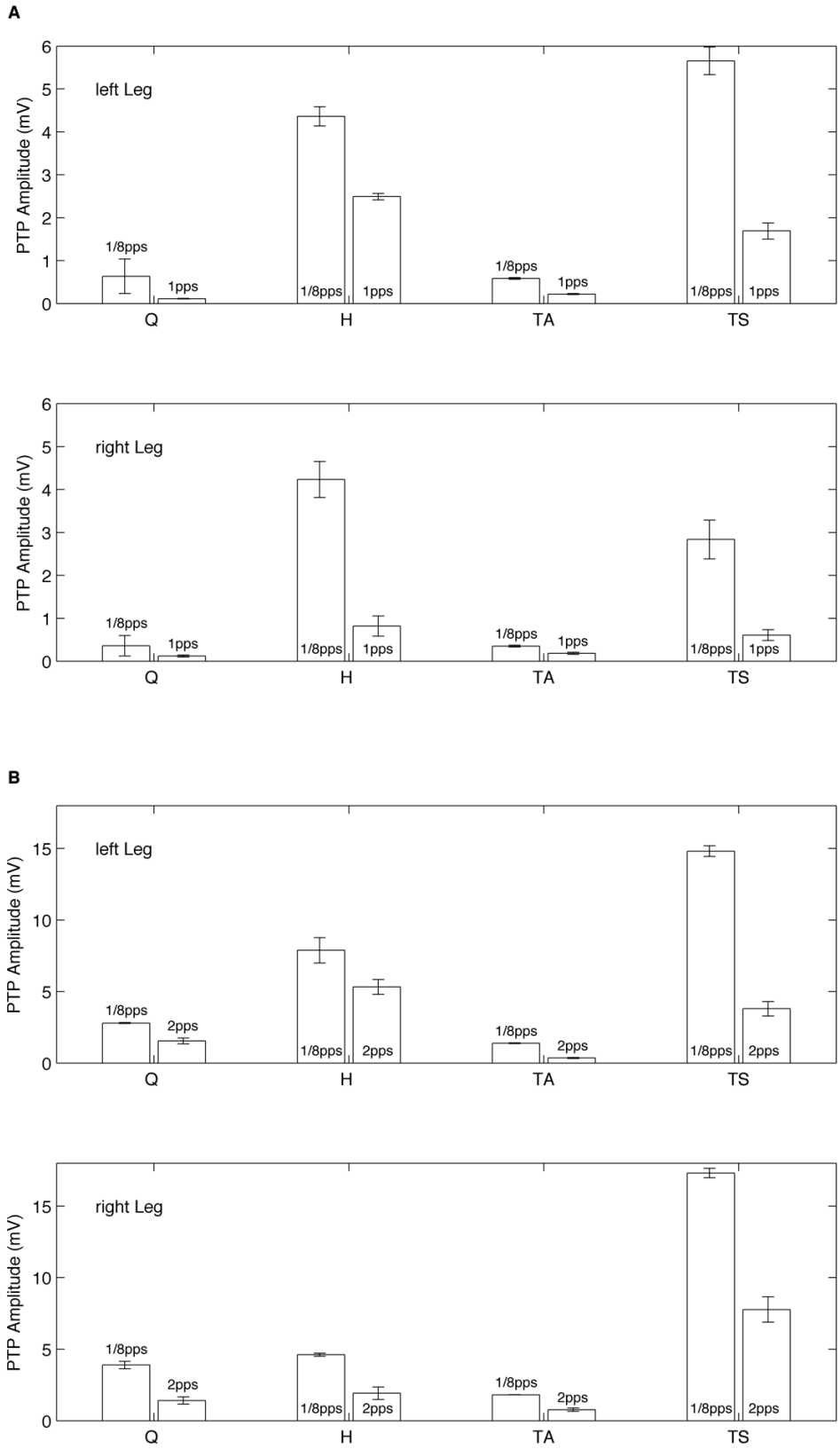

Figure 4.4: Mean PRR responses to stimulation with 1/8 pulse per second and 1 pulse per second in subject S1 (a). A stimulation intensity of 55 mA was applied. Mean responses to stimulation with 1/8 pps and 2 pps in subject S2 (b). Stimulation intensity: 65 mA. Recorded muscles were Quadriceps (Q), hamstrings (HM), tibialis anterior (TA), and triceps surae (TS) Error bars indicate the SD.

4.2 Modification of Reflex Responses by Motor Tasks

Control Responses to Sustained Stimulation

In four measurements (S1, S2a, S2b, S4), application of tSCS at a stimulation rate of 1 pps or 2 pps yielded responses with low variations of amplitudes and shape. Mean values and SD of 16 consecutive PTP responses are presented in Table 4.3.

The largest SD of the control responses was detected in hamstring muscle in all four participants. These variations were not correlated to any temporary muscle contraction, but rather showed a pattern in their amplitude that repeated every 4-5 s. This pattern is addressed in the last chapter.

Figure 4.5 depicts a series of 14 response spikes in subject S2 as example. Related mean and SD values are given in the third and fourth column of Table 4.3.

Table 4.3: PTP control responses to sustained stimulation in 4 subjects. Subjects were stimulated at a stimulation rate of 1 pps or 2 pps. Mean values and standard deviations were calculated from at least 16 responses and are presented in mV.

		S1 (SR 1 pps)[1)]		S2a (SR 2 pps)[2)]		S2b (SR 2 pps)[2)]		S4 (SR 2 pps)[3)]	
		Mean	SD	Mean	SD	Mean	SD	Mean	SD
Left Side	Q	0.11	0.01	1.54	0.20	0.07	0.01	0.17	0.03
	H	2.49	0.08	5.32	0.52	0.51	0.17	1.61	0.15
	TA	0.22	0.01	0.35	0.04	0.41	0.03	0.40	0.03
	TS	1.69	0.19	3.80	0.51	2.93	0.39	0.88	0.07
Right Side	Q	0.12	0.03	1.42	0.25	0.16	0.04	0.04	0.00
	H	0.82	0.24	1.92	0.43	0.83	0.12	0.36	0.18
	TA	0.18	0.03	0.77	0.12	1.02	0.07	0.33	0.06
	TS	0.61	0.13	7.77	0.89	3.79	0.28	0.85	0.11

Stimulation intensity: 1) 55 mA, 2) 65 mA, 3) 35 mA.

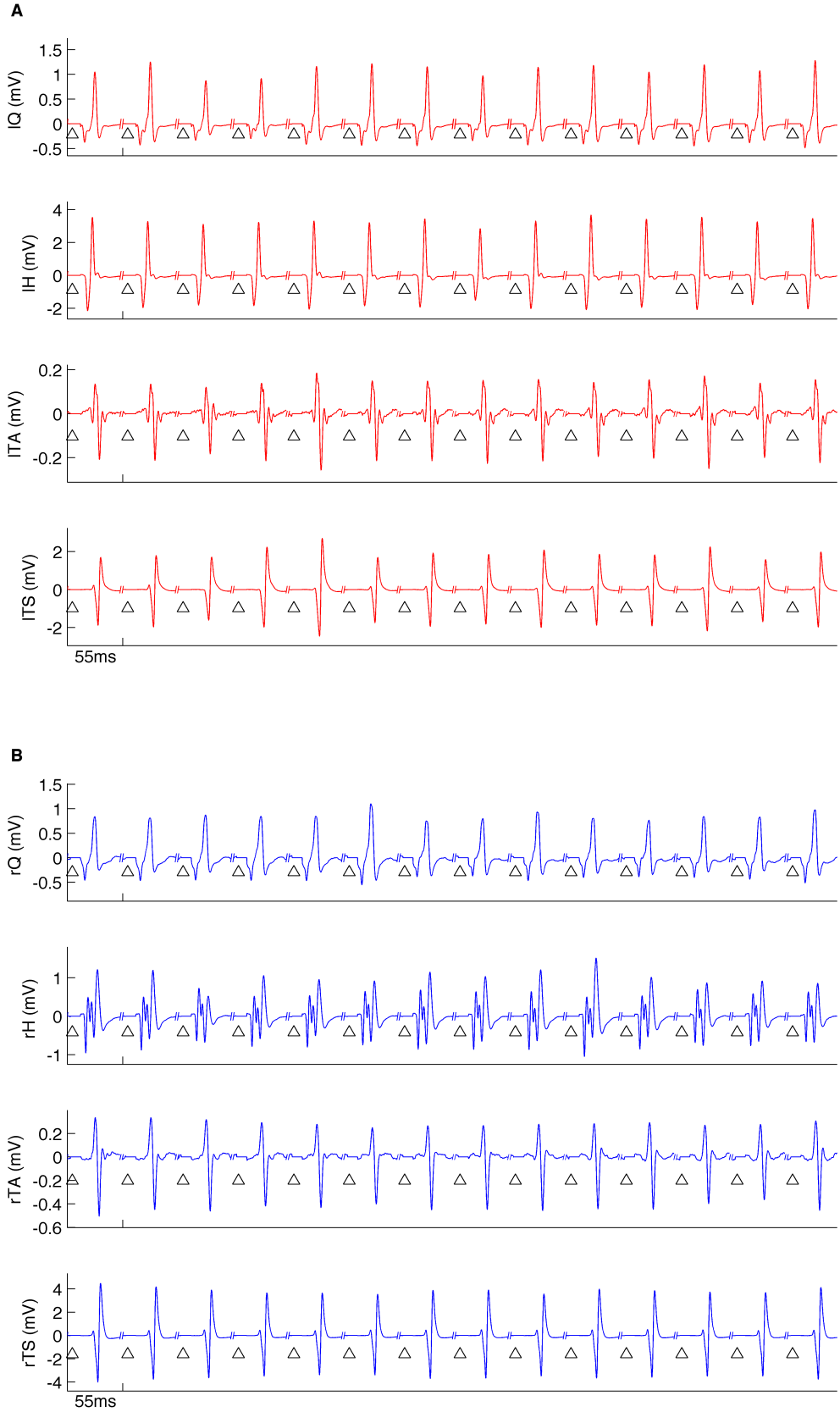

Figure 4.5: Example of control responses to sustained stimulation at a stimulation rate of 2 pps in subject S2. Stimulation intensity: 65 mA. Sections of -5 ms to 50 ms relating to stimulation are displayed. Black triangles indicate the stimulation. Muscles of the left leg are shown in (a), muscles of the right leg in (b).

Modification of Reflex Responses by Volitional Dorsiflexion

PRR responses to volitional unilateral dorsi- and plantar flexion were recorded in 4 subjects. 3 series of dorsiflexion and 3 series of plantar flexion were analyzed (each with 3 repetitions, example in Figure 4.6 and Figure 4.7).

Unilateral dorsiflexion lead to significant decrease of amplitude responses in the ipsilateral TS in every subject (Figure 4.6, Figure 4.8). Although PRR responses in the contralateral side also showed modifications during dorsiflexion, no overall tendency towards facilitation or suppression manifested. Response amplitudes during dorsiflexion were averaged and normalized to the mean unconditioned response.

Normalized mean amplitudes derived from the three measurements in the ipsilateral side were: Q 0.9 ± 0.1, H 0.9 ± 0.2, TA 0.9 ± 0.2, TS 0.5 ± 0.2. Table 4.4 presents the normalized data set for each measurement.

Table 4.4: Responses to unconditioned tSCS and to conditioning by unilateral dorsiflexion. Presented values are mean values of peak-to-peak response amplitudes in mV.

		Meas. 1[1)]		Meas. 2[2)]		Meas. 3[3)]		Ipsilat. side		Contralat. side	
		*L**	R	*L*	R	L	*R*	Mean (SD)		Mean (SD)	
Q	Unconditioned	0.08	0.04	0.11	0.15	1.69	1.44	0.54	0.78	0.63	0.92
	Dorsiflexion	0.07	0.04	0.10	0.13	1.73	1.18	0.45	0.63	0.63	0.95
	Ratio	89%	97%	96%	89%	102%	82%	89%	7%	96%	7%
H	Unconditioned	1.47	0.17	2.45	0.64	4.90	1.47	1.80	0.57	1.90	2.61
	Dorsiflexion	1.07	0.20	2.40	0.64	4.58	1.52	1.66	0.68	1.81	2.41
	Ratio	73%	114%	98%	101%	93%	103%	91%	16%	103%	10%
TA	Unconditioned	0.32	0.31	0.21	0.16	0.31	0.52	0.35	0.16	0.26	0.08
	Dorsiflexion	0.24	0.27	0.25	0.17	0.29	0.44	0.31	0.11	0.24	0.07
	Ratio	77%	89%	117%	104%	94%	85%	93%	21%	96%	8%
TS	Unconditioned	0.89	0.87	1.20	0.53	2.69	5.94	2.67	2.83	1.36	1.16
	Dorsiflexion	0.62	0.76	0.72	0.54	2.44	1.95	1.10	0.74	1.25	1.04
	Ratio	69%	88%	60%	101%	91%	33%	54%	19%	93%	7%

*Side of volitional motor task (italic). Stimulation intensity: 1) 35 mA, 2) 55 mA, 3) 65 mA.

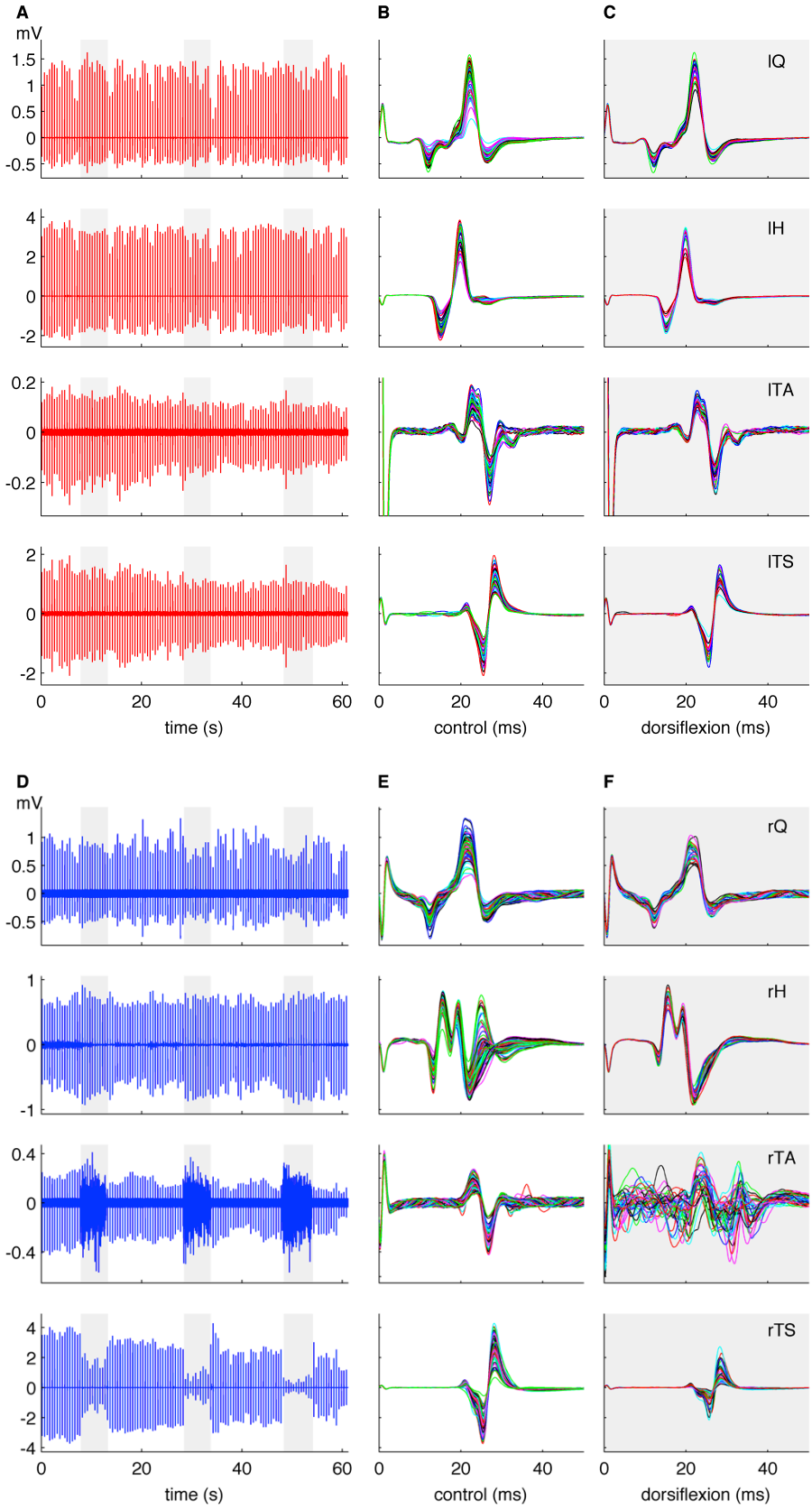

Figure 4.6: Example of PRR responses recorded in resting state and during volitional unilateral dorsiflexion in subject S2. Responses in muscle of the left leg are depicted in (a, b, c), responses in the right leg are shown in (d, e, f). Three repetitions of isotonic dorsiflexion (grey) at stimulation rate 2 pps were performed with the right leg. Responses were recorded in quadriceps (Q), hamstrings (H), tibialis anterior (TA), and triceps surae (TS). Overlaid trigger windows of unconditioned PRR responses (b, e). Overlaid trigger windows of conditioned PRR responses (c, f).

Modification of Reflex Responses by Volitional Plantar Flexion

Unilateral plantar flexion facilitated responses in ipsilateral TS, but also in ipsilateral TA and H. In all 3 measurements, co-activation of ipsilateral TA and H was seen. This muscular co-contraction during plantar flexion is addressed subsequently.

During the first measurement additional co-activation of ipsilateral quadriceps was observed. Therefore, the responses of the ipsilateral quadriceps were not taken into consideration for the evaluation of group results (Figure 4.8). The group results in the contracting leg were: Q 1.1 ± 0.1, H 1.3 ± 0.2, TA 1.6 ± 0.2, and TS 2.0 ± 0.5.

In all cases, no significant changes were measured in the muscles of the contralateral leg.

Table 4.5: PTP responses to unconditioned tSCS and to conditioning by unilateral plantar flexion. Presented values are mean values of peak-to-peak response amplitudes in mV.

		Meas. 1[1)]		Meas. 2[2)]		Meas. 3[1)]		Ipsilateral		Contralateral	
		*L**	R	*L*	R	L	*R*	Mean (SD)		Mean (SD)	
Q	Unconditioned	0.13	0.14	0.16	0.04	1.55	1.43	0.57	0.74	0.58	0.84
	Plantar flexion	0.25	0.14	0.17	0.05	1.84	1.74	0.72	0.89	0.68	1.01
	Ratio	195%[3)]	99%	107%	122%	119%	122%	114%	11%	113%	13%
H	Unconditioned	0.61	0.70	1.35	0.17	5.42	1.51	1.16	0.48	2.10	2.89
	Plantar flexion	0.81	0.61	1.89	0.19	5.50	1.58	1.43	0.56	2.10	2.95
	Ratio	134%	86%	140%	114%	102%	105%	126%	19%	100%	14%
TA	Unconditioned	0.31	0.98	0.40	0.32	0.33	0.62	0.45	0.16	0.54	0.38
	Plantar flexion	0.58	1.04	0.61	0.50	0.39	0.85	0.68	0.15	0.64	0.35
	Ratio	184%	106%	151%	156%	118%	138%	157%	24%	127%	26%
TS	Unconditioned	1.97	3.58	0.93	0.83	3.21	6.73	3.21	3.09	2.54	1.49
	Plantar flexion	4.97	3.77	1.61	1.22	3.87	11.62	6.07	5.09	2.96	1.50
	Ratio	252%	105%	173%	147%	120%	173%	199%	45%	124%	21%

*Side of volitional conditioning (italic), Stimulation intensity: 1) 65 mA, 2) 35 mA. 3) Value not taken into consideration for mean, SD and group results.

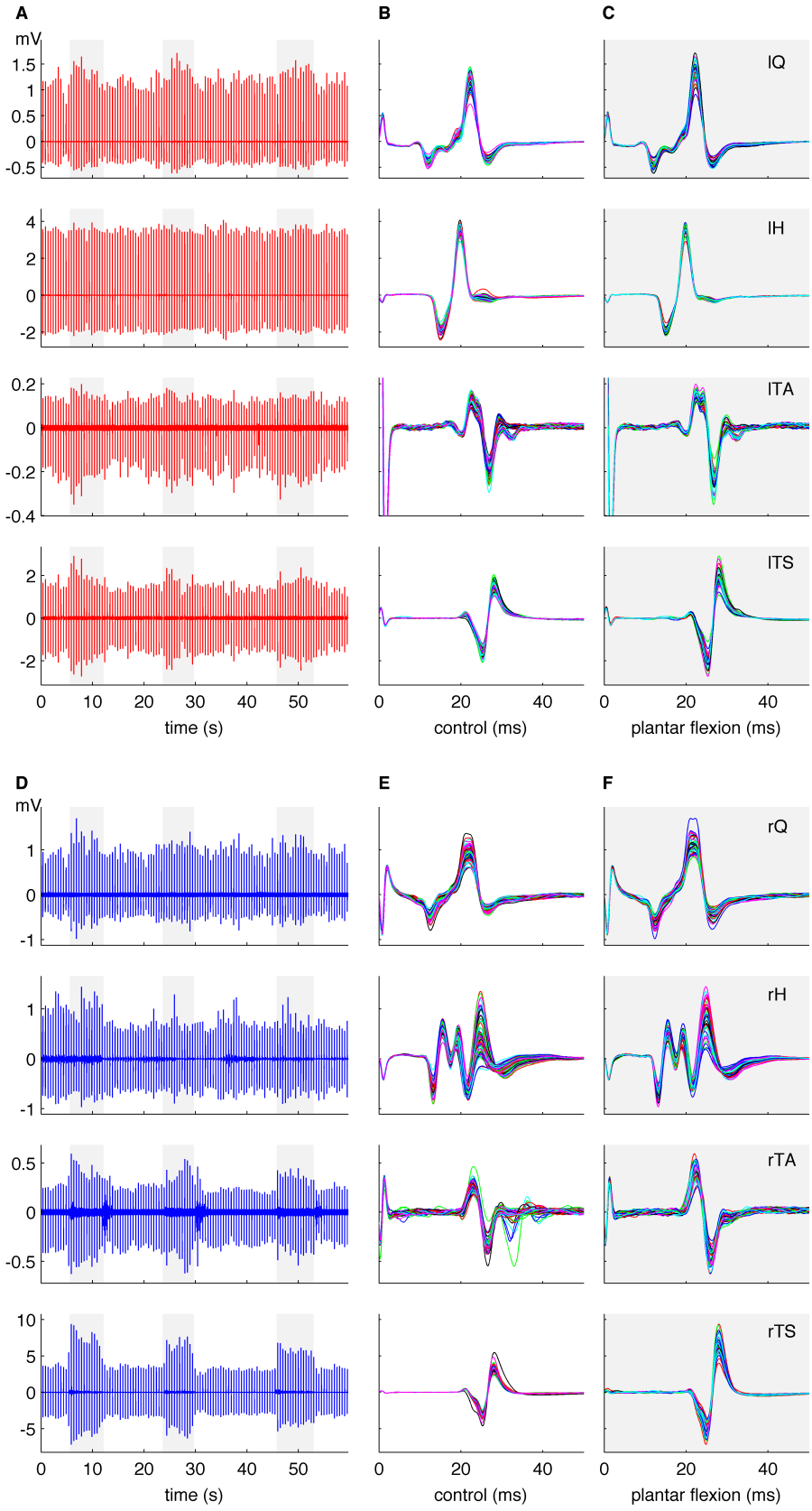

Figure 4.7: Example of PRR responses recorded in resting state and during volitional unilateral plantar flexion in subject S2. Responses in muscle of the left leg are depicted in (a, b, c), responses in the right leg are shown in (d, e, f). Three repetitions of isotonic plantar flexion (grey) at stimulation rate 2 pps were performed with the right leg. Responses were recorded in quadriceps (Q), hamstrings (H), tibialis anterior (TA), and triceps surae (TS). Overlaid trigger windows of unconditioned PRR responses (b, e). Overlaid trigger windows of conditioned PRR responses (c, f).

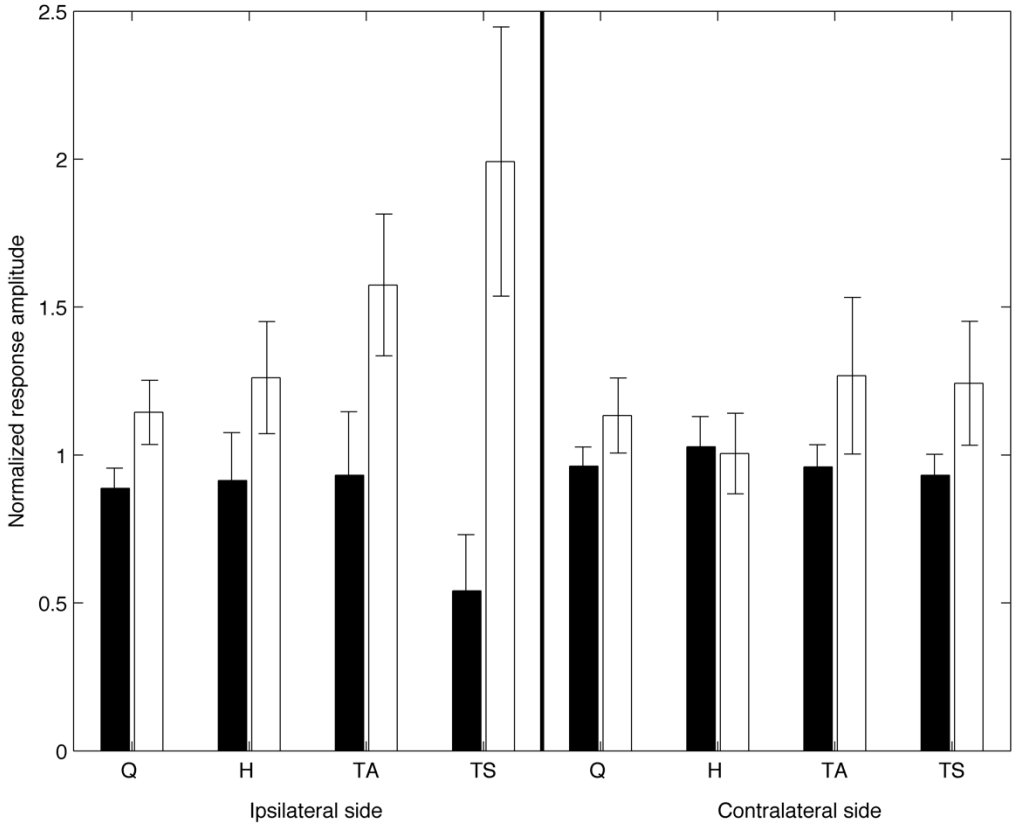

Figure 4.8: Group results for unilateral volitional dorsiflexion (black bars) and plantar flexion (white bars), with the test responses (PTP) normalized to the corresponding controls. Error bars indicate the SD.

Comparison of Responses to Weak and Strong Isotonic Dorsiflexion

In subject S1 conditioned PRR responses were measured at three levels of contraction force (weak, 1 kg and 3 kg). The generated muscle force was monitored with a spring balance mounted to the ball of the foot. In Figure 4.9 responses to the three conditioning test paradigms and control responses were superimposed and depicted in time window of 200 ms. After the PRR response a silent period (no EMG activity) was observed in the tibialis anterior. This silent period decreased with increasing contraction force. Contrary, the PRR response in ipsilateral TA was larger during higher contraction force (Table 4.6).

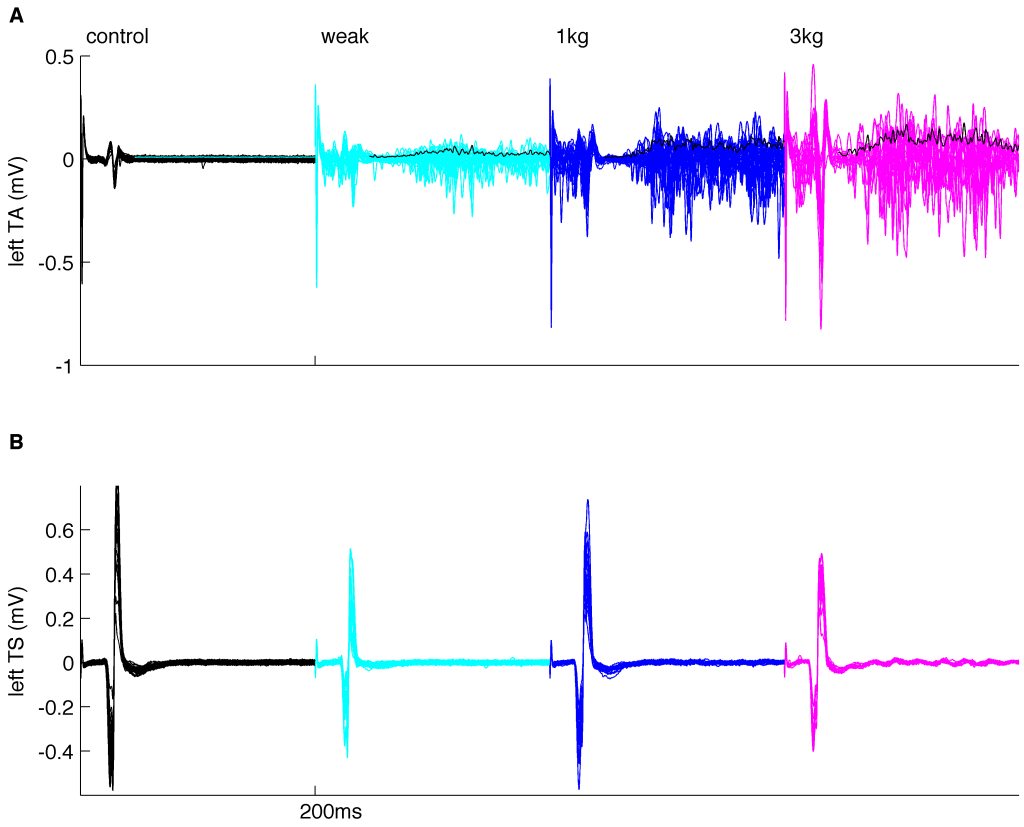

Figure 4.9: Comparison of PRR responses to weak and strong dorsiflexion in tibialis anterior (a) and triceps surae (b) in subject S1. Stimulation intensity: 55 mA. PRR responses to three conditioning paradigms were superimposed and plotted in time windows of 200 ms, with stimulation at time point zero. RMS curves were calculated for the time windows of 40 ms to 200 ms (cyan/black line).

Table 4.6: Responses to unconditioned tSCS, and to unilateral dorsiflexion with three different contraction forces. Mean RMS values were calculated by time averaging of the RMS curve of overlaid signal curves in a time window of 40 ms to 200 ms. All values are given in mV.

	Control (SD)		Weak (SD)		1kg (SD)		3kg (SD)	
Mean RMS value	0.009		0.026		0.057		0.085	
PRR response in TA (PTP)*	0.17	0.03	0.17	0.07	0.26	0.10	0.59	0.24
PRR response in TS (PTP)	1.03	0.23	0.48	0.20	0.77	0.19	0.69	0.13

*Predominantly posterior root reflex responses with a contribution of EMG activity of volitional contraction.

Muscular Co-Contractions during Plantar Flexion

For all subjects, a slight co-activation of ipsilateral H and TA was observed at least in one out of three repetitions. In subject S2 co-contraction of H and TA was seen as continuous EMG signal, interrupted by the PRR response pulse and a following silent period (Figure 4.10). In the contralateral side, PTP spikes of around 0.2 mV could be detected in the TS.

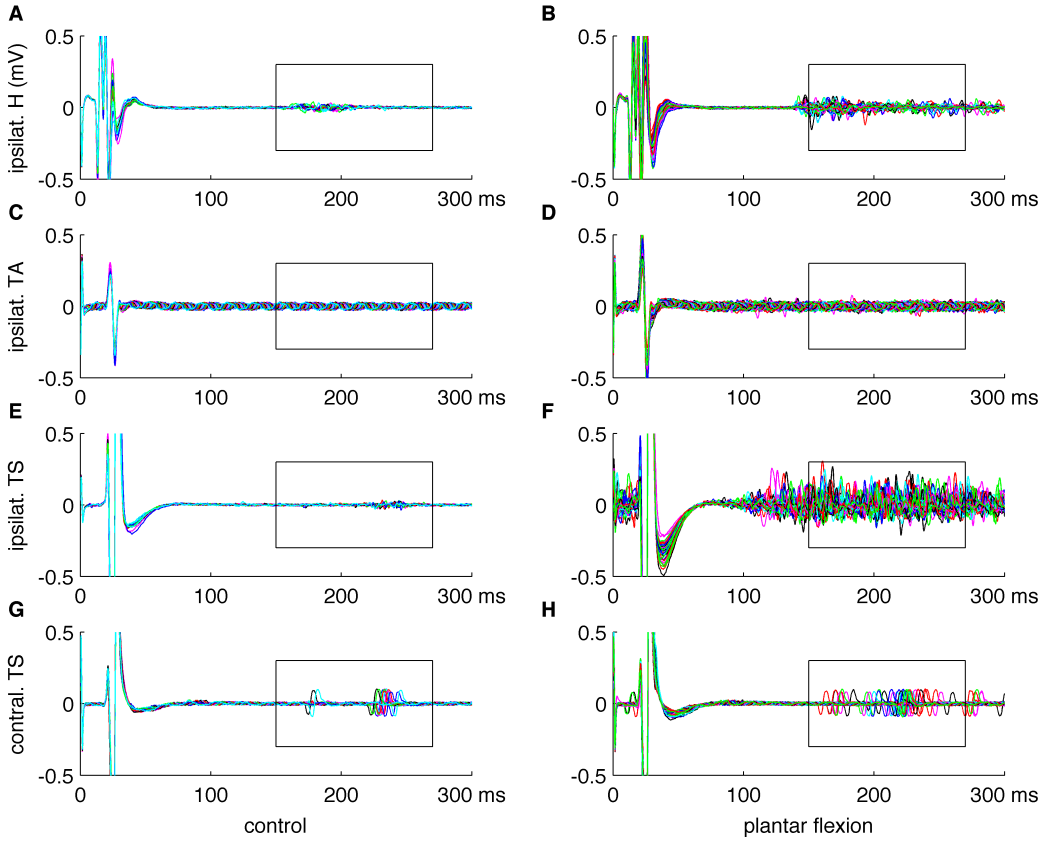

Figure 4.10: Contraction of various muscles during volitional unilateral plantar flexion. Superimposed control responses (a, c, e, g), and superimposed responses during plantar flexion (b, d, f, h). Root mean square values were calculated from the section indicated by the black rectangle.

Table 4.7: Muscular contraction measured with root mean square in a time frame of 150 ms to 270 ms after stimulus in subject S2. Three repetitions of plantar flexion were performed. Displayed values are given in µV.

		Control	Rep. 1	Rep. 2	Rep. 3	Mean (SD)		Ratio
Q	Ipsilat. side	30.2	29.1	29.7	30.7	29.8	0.8	99%
	Contralat. side	4.1	3.3	4.3	5.2	4.3	1.0	104%
H	Ipsilat. side	7.5	22.5	8.0	9.2	13.2	8.0	176%
	Contralat. side	5.5	5.3	5.4	5.3	5.3	0.0	97%
TA	Ipsilat. side	17.7	20.7	19.4	19.2	19.8	0.8	112%
	Contralat. side	5.7	5.8	5.7	5.8	5.8	0.1	103%
TS	Ipsilat. side	5.5	54.0	53.0	56.0	54.3	1.5	984%
	Contralat. side	15.3	18.2	16.3	17.3	17.3	1.0	113%

Time Evolution of Conditioned PRR Responses

Responses to sustained stimulation prior to, during, and after conditioning by a motor task were analyzed. Figure 4.11 shows an example of the time course of PTP response amplitudes to sustained stimulation with 1 pps (S1) and conditioning by dorsiflexion. Responses in TS decrease instantly to 40% of unconditioned responses at the onset of a dorsiflexion and slowly recover at hold phase and after offset. This recover could be seen in 3 of 7 measurements of dorsiflexion.

Figure 4.12 depicts an example of a time evolution during conditioning by unilateral plantar flexion at stimulation rate of 2 pps. At onset of plantar flexion, PTP responses in TA increased step-like by 58%, and responses in TS increased by 80%. In the ipsilateral side two maxima can be seen in the time evolution during hold phase, before response amplitudes return to the size in unconditioned state. These maxima were also detected in 2 other measurements of plantar flexion, and had the same time interval of approximately 4 s.

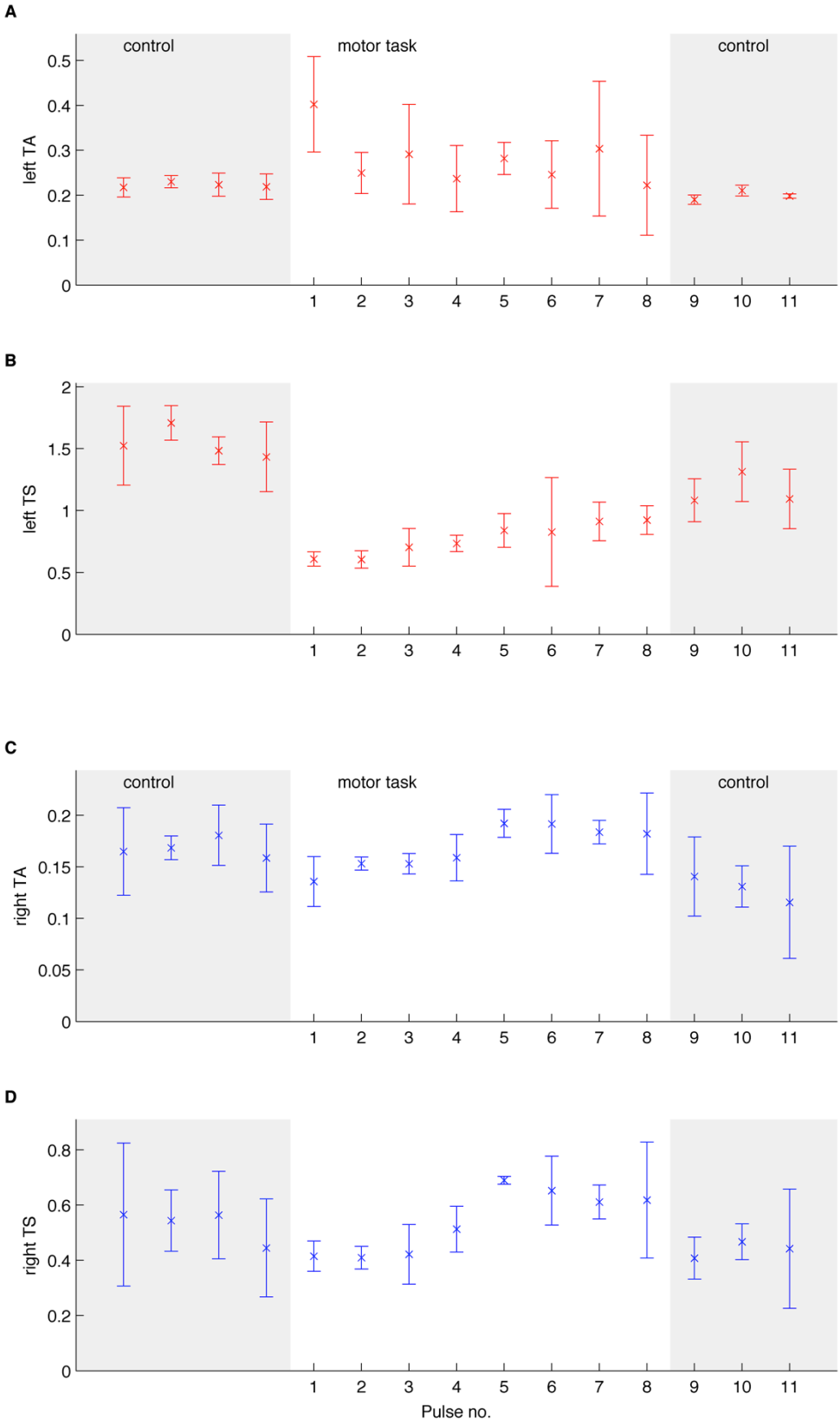

Figure 4.11: Example of the time evolution of PRR responses to conditioning by dorsiflexion with the left leg in subject S1 at stimulation rate 1 pps. PTP response amplitudes are averaged over three repetitions, and numbered, starting with the first pulse after onset of dorsiflexion. Response amplitudes in lower leg muscles of ipsilateral side are shown in (a, b), amplitudes in contralateral side in (c, d).

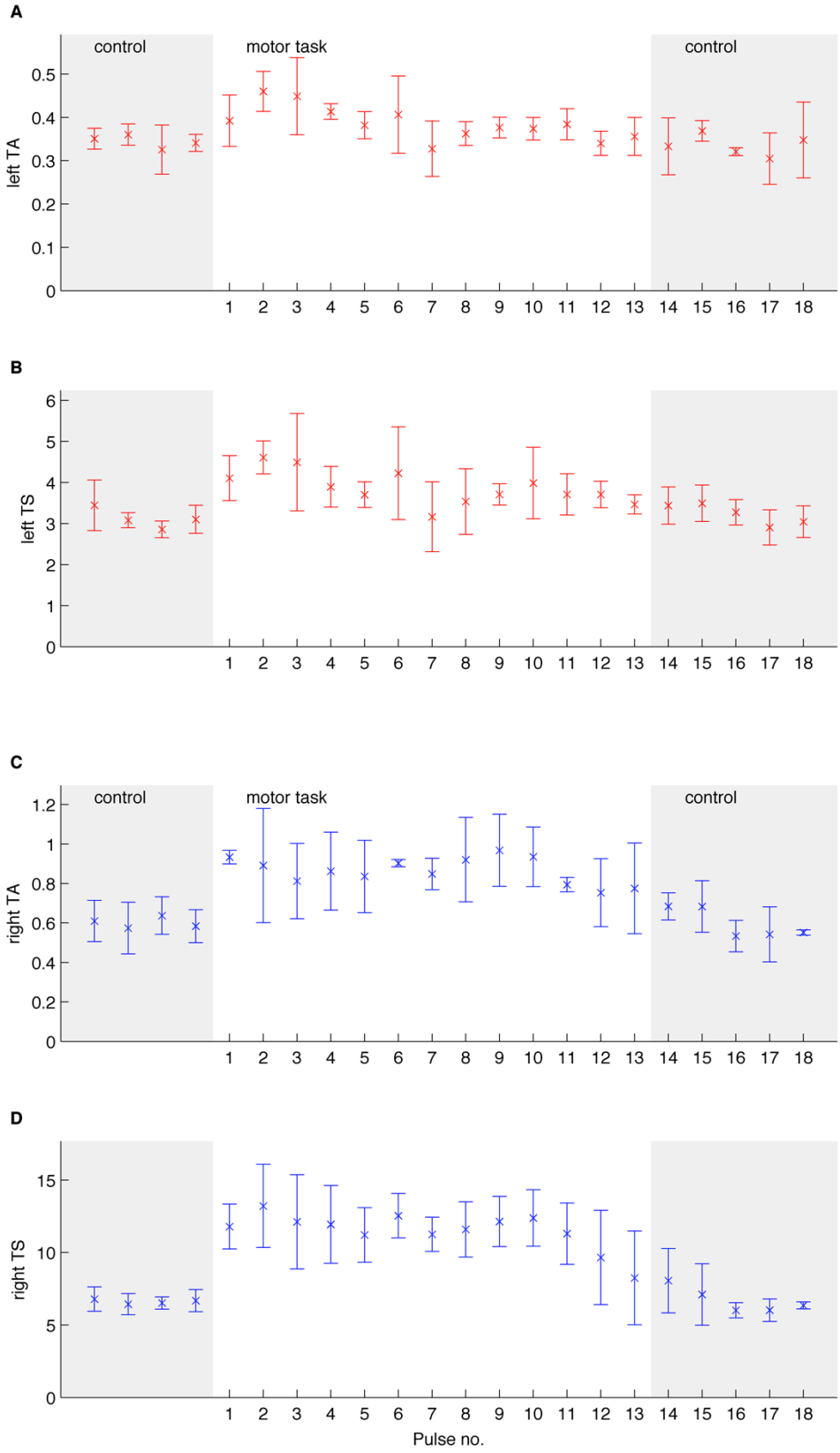

Figure 4.12: Example of the time evolution of PRR responses to conditioning by plantar flexion with the right leg in subject S2 at stimulation rate 2 pps. PTP response amplitudes are averaged over three repetitions, and numbered, starting with the first pulse after onset of plantar flexion. Response amplitudes in lower leg muscles of contralateral side are shown in (a, b), amplitudes in ipsilateral side in (c, d).

5

Discussion

In the present study, transcutaneous lumbosacral spinal cord stimulation could be utilized to elicit reflex responses in lower limb muscles. These spinal reflexes are called posterior root reflexes (PRR). The morphology of the response shows a monosynaptic reflex pathway. PRR are evoked in the quadriceps, hamstring, tibialis anterior, and triceps surae in both legs.

Biophysical Behavior of Electrical Stimulation

As described in simulation studies (Danner et al., 2011; Ladenbauer et al., 2010), the best location for depolarizing the posterior root fibers is at the entry point to the spinal cord. This hot spot is characterized by a strong curvature of the fiber and a change of electrical conductivity (cerebrospinal fluid to white matter). The positioning of the stimulating electrode proved to be essential for balanced reflex responses in all four recorded muscles. Displacement of the electrode to cranial direction facilitated recruitment in thigh muscles, whereas offset to caudal direction increased responses in TA and TS. A lateral displacement of the stimulating electrode towards the left side reduced the stimulation threshold intensities in the left leg compared to the right leg (Figure 4.2).

In general, a centrally placed electrode evoked slightly asymmetric responses in left and right lower limbs. These asymmetries are most probably due to the electrical field generated and anatomical asymmetries, as well as physiological left-right differences (Minassian, Hofstoetter, & Rattay, 2012).

In the presented PRR responses of five measurements, the response latencies were correlated to subject's height as previously described by Minassian et al. (2007).

Reflex Nature of the Responses

The reflex nature of the response was tested using a double stimuli paradigm. A strong depression of the responses to the second stimulus, with an inter-stimuli interval of 35 ms, proved the reflex character. This attenuation results from a prolonged refractory period of the reflex arc. In contrast, a large second response would be expected in case of direct activation of α-motoneurons in the ventral horn or anterior roots.

Recognizable responses to the second stimulus could be evoked at stimulation intensities over 120% of threshold intensity. According to Minassian et al. (2004), the refractory behavior of PRRs depends not only on the inter-stimuli-interval, but also on the stimulation strength. Therefore, the applied stimulation intensities are not dedicated to stimulate efferent fibers directly.

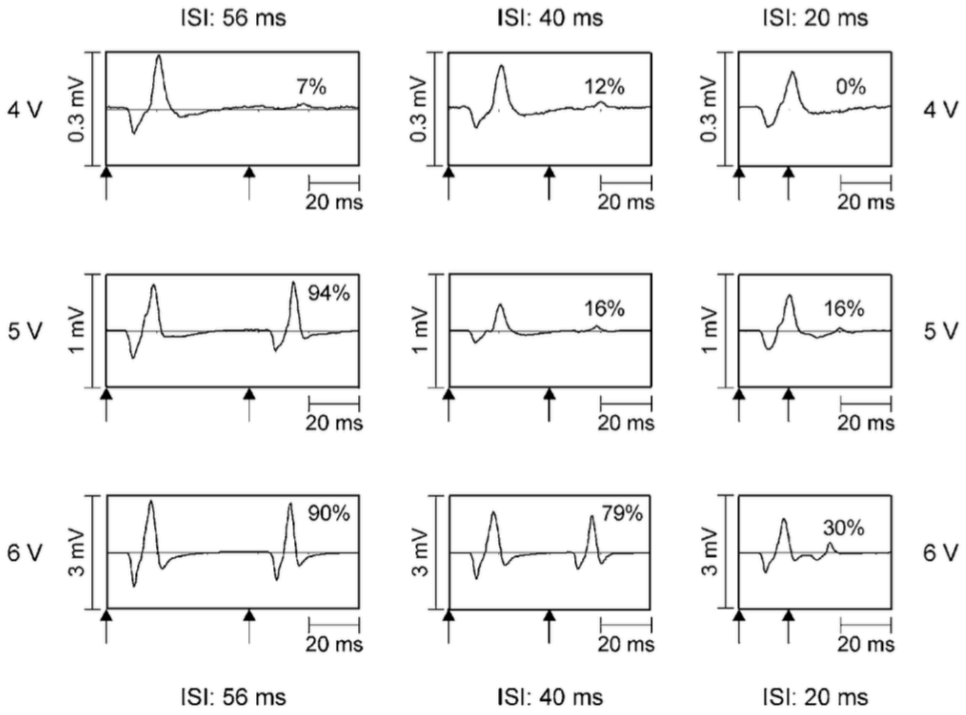

Figure 5.1: Results to measurements with pairs of stimuli from Minassian et al. (2004).

Variation in Control Responses

In three subjects the control responses to sustained stimulation revealed a remarkable pattern of increasing and decreasing PRR responses. These variations were mostly observable in hamstring and quadriceps (Figure 5.2). This pattern in PRR responses repeated every 4 and 5 s for all subjects, under a relaxed state of the subject.

According to Minassian et. al (2007) the first posterior root volley generated by a single pulse alters the excitability of the spinal neuronal circuitries. The altered excitability then affects following pulses, when applied in close succession. Excitability might be

reduced by presynaptic inhibition of Ia terminals, recurrent inhibition of motoneurons, and secondary contribution like from Golgi tendon organs activated by the first muscle twitch (Pierrot-Desiligny & Burke, 2012). Transcutaneous SCS recruits afferents of multiple posterior roots, therefore, facilitation of synergists or disynaptic inhibition from antagonists might also influence PRR responses (Delwaide, Cordonnier & Charlier, 1976). The recovery of the second response above 90% requires a minimum inter-stimuli interval of 5 s(Minassian et al., 2007).

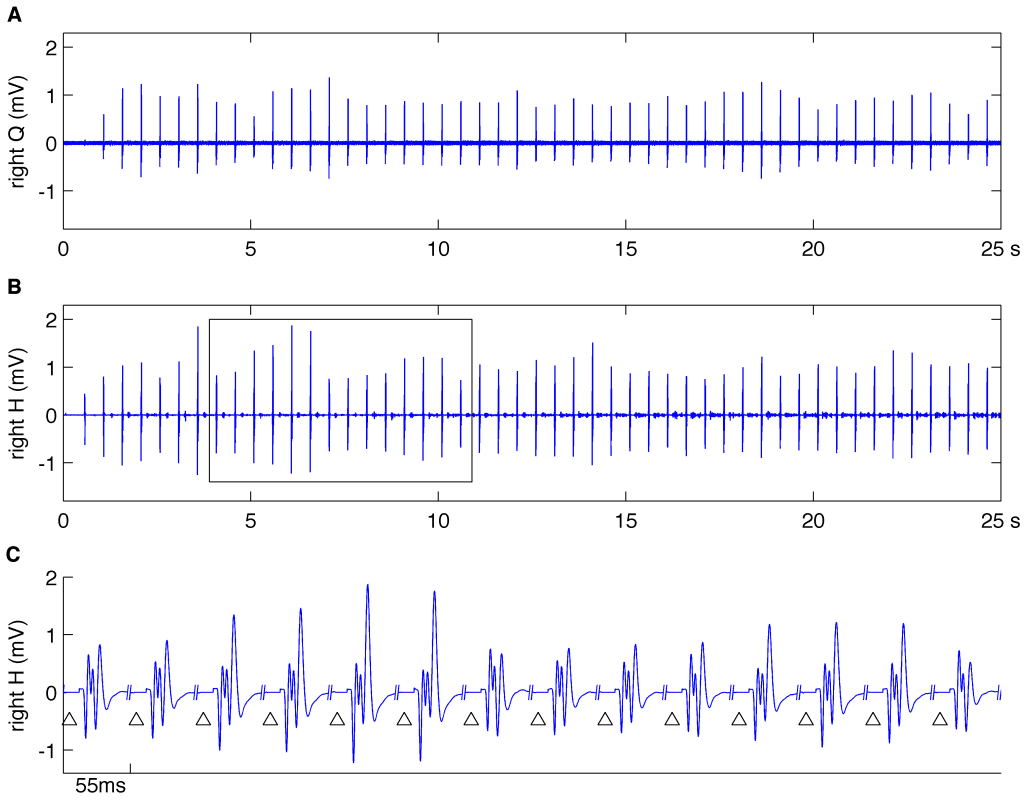

Figure 5.2: Pattern of PRR control responses at 2 pps in right quadriceps (a) and hamstring (b, c) of subject S2. The stimulation artifact was removed. The rectangular area in (b) is shown in (c). Furthermore in (c) only sections of -5 ms to 50 ms relating to stimulation are displayed, and stimulation is indicated by black triangles.

Modification of Responses to Sustained Stimulation

The recruitment curves showed, that the strength of applied sustained stimulation currents was within the recruitment window, limited downwards by the threshold intensity and upwards by saturation intensity.

However, control PRR responses to sustained stimulation at 1 pps or 2 pps were significantly attenuated, compared with responses to stimulation every 8 seconds (Table 4.2). This is attributed to an altered excitability of spinal neuronal circuitries, when stimuli are delivered with shorter inter-stimuli intervals.

Voluntary dorsiflexion inhibited responses in antagonistic TS corresponding to depression of soleus H reflex to tibial nerve stimulation, through activation of group Ia inhibitory pathways (Crone & Nielsen, 1989). We would generally expect facilitation of PRR responses in contracting muscles, due to monosynaptic Ia excitation (Pierrot-Deseiligny & Burke, 2012). Primary endings of muscle spindles have excitatory monosynaptic projections to homonymous and heteronymous motoneurons. Muscle spindles respond to muscular tension and contribute to facilitated muscle responses via the excitatory projections. Additionally, at dorsiflexion suppression of inhibitory pathways of the extensor side was expected (Shindo et al., 1984).
However, facilitation in TA during dorsiflexion was observed only in one subject. It is assumed that reflex pathways cannot facilitate responses in the contracting muscle, if the voluntary contraction already recruits all muscle fibers. This may result due to saturation of the response. Therefore, facilitation in TA was only detected, when the unconditioned response amplitudes were significantly smaller than the EMG signal amplitudes of voluntary dorsiflexion.
In addition, the results of modification of PRR by plantar flexion showed that TS never contracted to a level, where all muscle fibers were recruited. Here, for each subject a clear facilitation of agonist responses was observed. For further investigations, we propose recording of recruitment curves at sustained 1 pps or 2 pps, in order to determine the range of muscular recruitment of PRR.
At plantar flexion, antagonistic TA responses were also facilitated because a low co-contraction of TA was noticed in all measurements. Similarly, in ipsilateral hamstring facilitation of responses accompanied by muscular co-contraction was observed in two of three subjects. In that case, the influence of monosynaptic Ia excitation and suppression of inhibitory pathways could play a major role.

Another important factor is the crosstalk in the EMG recordings of the TA. The influence of TS responses was investigated in one subject by means of stimulation of afferents at level of the lumbar spine (electrode placed over the L4-L5 vertebral processes). We could elicit exclusively responses in TS and detected no interfering signals in the TA-recording channel. Nevertheless, the result of this sample cannot be generalized for all conducted experiments.

In all measurements no clear modifications of responses were observed in the muscles of the contralateral leg. This proved the constant stimulation conditions during volitional motor tasks.

Differences between Varied Forces of Isotonic TA Contraction

Lumbosacral cord stimulation evoked a short-latency depression of the EMG activity of volitional contraction. This silent region begins around 40 ms after stimulation and shortens with increasing contraction force. Petersen et al. (1998) stimulated the common peroneal nerve below motor threshold during volitional plantar flexion. They presented similar evoked depression in contracting TS, which also vanished for strong contractions. In a different study, Floeter (2003) characterized the term cutaneous silent period (CSP) as a brief interruption in voluntary contraction that follows strong electrical stimulation of a cutaneous nerve. The CSP is a protective reflex that is mediated by spinal inhibitory circuits and is reinforced in part by parallel modulation of the motor cortex (Floeter, 2003; Logician, Plotkin & Shefner, 1999).

Facilitation of TA reflex responses appeared with stronger contraction force. This facilitation can be attributed again to monosynaptic Ia excitation (Pierrot-Deseilligny & Burke, 2012) and to reduced disynaptic inhibition (Petersen et al., 1998).

Comments on the Method of tSCS

Transcutaneous spinal cord stimulation can be widely applied in motor control studies as well as for modification of movement after spinal cord injury or other neurological disorders (Minassian et al., 2012). The noninvasive stimulation technique depolarizes the posterior root fibers despite the large stimulating electrodes and the distant stimulation location (compared with epidural stimulation), due to the tissue heterogeneity of the volume conductor, and the curvature of posterior roots. In healthy subjects, however, local contraction of paravertebral muscle groups caused discomfort at high stimulation intensities and at high stimulation frequencies (above 10 pps). The discomfort limits the possible range of application of tSCS. Furthermore, electrical stimulation of the posterior roots always depolarizes afferents of multiple muscles simultaneously that in turn may influence each other through spinal networks.

Further studies applying the technique of transcutaneous spinal cord stimulation will contribute to understand neuronal networks of the spinal cord in more detail, and reveal, how far transcutaneous posterior root stimulation can modify the central state of excitability.

6

Conclusion

Transcutaneous electrical stimulation of afferent nerve fibers at the level of the lumbar spinal cord (stimulation site at T11-T12 interspinous space) was demonstrated to elicit reflexes, termed posterior root reflexes (PRR). These monosynaptic reflexes were observed bilaterally in quadriceps, hamstrings, triceps surae, and tibialis anterior. In the preliminary study, these reflexes were modified by unilateral voluntary dorsiflexion and plantar flexion, which supports previous experiments and simulation studies. The advantage of tSCS methodology compared to classical H reflex study is that a larger spinal network is recruited.

During voluntary performed dorsiflexion, the PRR responses in leg extensor muscles were significantly attenuated by disynaptic Ia inhibition. Absence of expected test response increase in contracting tibialis anterior indicated a saturated recruitment of its muscle fibers.

The PRR responses were facilitated during homonymous voluntary activation of the leg flexors and extensors when conditioned by plantar flexion. Generally, even weak muscle contraction facilitated PRR responses in activated muscle groups.

Here, the conditioning of reflex pathway was assessed using a train of stimuli of 1 pps or 2 pps. The high repetition rate leads to smaller responses but the assessment had a higher time resolution.

Overall, the presented new methodology is a first step to assess spinal networks in healthy and disabled subjects. This work can be used as a starting point for further studies, in order to analyze the supraspinal influence to the lumbosacral network.

References

Amaral, D. G. (2013). The functional organization of perception and movement. *Principles of Neural Science*, 356–369.

Benarroch, E. E. (1993). The Central Autonomic Network: Functional Organization, Dysfunction, and Perspective. *Mayo Clinic Proceedings*, *68*(10), 988–1001. http://doi.org/10.1016/S0025-6196(12)62272-1

Brodal, P. (2010). *The central nervous system*. *structure and function*.

Coventry, M. B., Ghormley, R. K., & Kernohan, J. W. (1945). The Intervertebral Disc: Its Microscopic Anatomy And Pathology. Part I. Anatomy, Development, and Physiology. *The Journal of Bone & Joint Surgery*, *27*(1), 105–112.

Crone, C. (1993). Reciprocal inhibition in man. *Danish Medical Bulletin*, *40*(5), 571–81.

Crone, C., Hultborn, H., Jespersen, B., & Nielsen, J. (1987). Reciprocal Ia inhibition between ankle flexors and extensors in man. *The Journal of Physiology*, *389*, 163–85. http://doi.org/10.1113/jphysiol.1987.sp016652

Crone, C., & Nielsen, J. B. (1989). Spinal mechanisms in man contributing to reciprocal inhibition during voluntary dorsiflexion of the foot. *The Journal of Physiology*, *416*, 255–272.

Danner, S. M., Hofstoetter, U. S., Ladenbauer, J., Rattay, F., & Minassian, K. (2011). Can the human lumbar posterior columns be stimulated by transcutaneous spinal cord stimulation? A modeling study. *Artificial Organs*, *35*(3), 257–62. http://doi.org/10.1111/j.1525-1594.2011.01213.

Davidoff, R. a. (1992). Skeletal muscle tone and the misunderstood stretch reflex. *Neurology*. http://doi.org/10.1212/WNL.42.5.951

Delwaide, P. J., Cordonnier, M., & Charlier, M. (1976). Functional relationships between myotatic reflex arcs of the lower limb in man: investigation by excitability curves. *Journal of Neurology, Neurosurgery, and Psychiatry*, *39*(6), 545–54. http://doi.org/10.1136/jnnp.39.6.545

Dimitrijevic, M. R., Gerasimenko, Y., & Pinter, M. M. (1998). Evidence for a Spinal Central Pattern Generator in Humansa. *Annals of the New York Academy of Sciences*, *860*(1), 360–376. http://doi.org/10.1111/j.1749-6632.1998.tb09062.x

Dramer, G. D. (2014). *Clinical Anatomy of the Spine, Spinal Cord, and Ans*. *Clinical Anatomy of the Spine, Spinal Cord, and Ans*. http://doi.org/10.1016/B978-0-323-07954-9.00005-0

Dy, C. J., Gerasimenko, Y. P., Edgerton, V. R., Dyhre-Poulsen, P., Courtine, G., & Harkema, S. J. (2010). Phase-dependent modulation of percutaneously elicited multisegmental muscle responses after spinal cord injury. *Journal of Neurophysiology*, *103*(5), 2808–2820. http://doi.org/10.1152/jn.00316.2009

Ebrall, P. (2007). Thieme Atlas of Anatomy (Head and Neuroanatomy). *The Journal of Chiropractic Education*, *21*(2), 162–163. http://doi.org/10.3174/ajnr.A0733

Eccles, J. C., Kostyuk, P. G., & Schmidt, R. F. (1962). Presynaptic Inhibition of the Central Actions of Flexor Reflex Afferents. *J Physiol.*, *161*, 258–281.

Floeter, M. K. (2003). Cutaneous silent periods. *Muscle and Nerve*. http://doi.org/10.1002/mus.10447

Gerasimenko, Y., Roy, R. R., & Edgerton, V. R. (2008). Epidural stimulation: Comparison of the spinal circuits that generate and control locomotion in rats, cats and humans. *Experimental Neurology*. http://doi.org/10.1016/j.expneurol.2007.07.015

Gray, H. (1918). *Anatomy of the human body*. *Bartleby.Com, May 2000*.

Graziano, M. S. a, Aflalo, T. N. S., & Cooke, D. F. (2005). Arm movements evoked by electrical stimulation in the motor cortex of monkeys. *Journal of Neurophysiology*, *94*(6), 4209–23. http://doi.org/10.1152/jn.01303.2004

Henneman, E., Somjen, G., & Carpenter, D. O. (1965). Functional Significance of Cell Size in Spinal Motoneurons. *Journal of Neurophysiology*, *28*, 560–580.

Hofstoetter, U. S., Hofer, C., Kern, H., Danner, S. M., Mayr, W., Dimitrijevic, M. R., & Minassian, K. (2013). Effects of transcutaneous spinal cord stimulation on voluntary locomotor activity in an incomplete spinal cord injured individual. *Biomedizinische Technik*, *58*(SUPPL. 1 TRACK-A). http://doi.org/10.1515/bmt-2013-4014

Humzah, M. D., & Soames, R. W. (1988). Human intervertebral disc: structure and function. *The Anatomical Record*, *220*(4), 337–56. http://doi.org/10.1002/ar.1092200402

Hunt, C. C. (1990). Mammalian muscle spindle: peripheral mechanisms. *Physiological Reviews*, *70*(3), 643–663.

Iles, J. F. (1986). Reciprocal inhibition during agonist and antagonist contraction. *Experimental Brain Research*, *62*(1), 212–214. http://doi.org/10.1007/BF00237419

Issever, A. S., Walsh, A., Lu, Y., Burghardt, A., Lotz, J. C., & Majumdar, S. (2003). Micro-computed tomography evaluation of trabecular bone structure on loaded mice tail vertebrae. *Spine*, *28*(2), 123–8. http://doi.org/10.1097/01.BRS.0000041588.39440.64

Kandel, E. R., Schwartz, J. H., & Jessell, T. M. (2000). *Principles of Neural Science*. *Neurology* (Vol. 3). http://doi.org/10.1036/0838577016

Krames, E. S., Hunter Peckham, P., Rezai, A., & Aboelsaad, F. (2009). What Is Neuromodulation? *Neuromodulation*, 3–8.

Ladenbauer, J., Minassian, K., Hofstoetter, U. S., Dimitrijevic, M. R., & Rattay, F. (2010). Stimulation of the human lumbar spinal cord with implanted and surface electrodes: a computer simulation study. *IEEE Transactions on Neural Systems and Rehabilitation Engineering : A Publication of the IEEE Engineering in Medicine and Biology Society*, *18*(6), 637–645. http://doi.org/10.1109/TNSRE.2010.2054112

Logician, E. L., Plotkin, G. M., & Shefner, J. M. (1999). The cutaneous silent period is mediated by spinal inhibitory reflex. *Muscle and Nerve*, *22*(4), 467–472. http://doi.org/10.1002/(SICI)1097-4598(199904)22:4<467::AID-MUS7>3.0.CO;2-Y

Lundberg, A. (1970). The excitatory control of the Ia inhibitory pathway. *Excitatory Synaptic Mechanisms*, 333–340.

McCrea, D. A., & Rybak, I. A. (2008). Organization of mammalian locomotor rhythm and pattern generation. *Brain Research Reviews*, *57*(1), 134–46. http://doi.org/10.1016/j.brainresrev.2007.08.006

Minassian, K., Hofstoetter, U., & Rattay, F. (2012). Transcutaneous Lumbar Posterior Root Stimulation for Motor Control Studies and Modification of Motor Activity after Spinal Cord Injury. In *Restorative Neurology of Spinal Cord Injury*. http://doi.org/10.1093/acprof:oso/9780199746507.003.0010

Minassian, K., Jilge, B., Rattay, F., Pinter, M. M., Binder, H., Gerstenbrand, F., & Dimitrijevic, M. R. (2004). Stepping-like movements in humans with complete spinal cord injury induced by epidural stimulation of the lumbar cord: electromyographic study of compound muscle action potentials. *Spinal Cord : The Official Journal of the International Medical Society of Paraplegia*, *42*(7), 401–416. http://doi.org/10.1038/sj.sc.3101615

Minassian, K., Persy, I., Rattay, F., Dimitrijevic, M. R., Hofer, C., & Kern, H. (2007). Posterior root-muscle preflexes elicited by transcutaneous stimulation of the human lumbosacral cord. *Muscle and Nerve*, *35*(3), 327–336. http://doi.org/10.1002/mus.20700

Mosekilde, L. (1989). Sex differences in age-related loss of vertebral trabecular bone mass and structure--biomechanical consequences. *Bone*, *10*(6), 425–32.

Murg, M., Binder, H., & Dimitrijevic, M. R. (2000). Epidural electric stimulation of posterior structures of the human lumbar spinal cord: 1. muscle twitches - a functional method to define the site of stimulation. *Spinal Cord*, *38*(7), 394–402. http://doi.org/10.1038/sj.sc.3101038

Netter, F. H. (2006). *Atlas of human anatomy*. *Exp Neurol* (Vol. 97).

Nielsen, J., Kagamihara, Y., Crone, C., & Hultborn, H. (1992). Central facilitation of Ia inhibition during tonic ankle dorsiflexion revealed after blockade of peripheral feedback. *Experimental Brain Research*, *88*(3), 651–656. http://doi.org/10.1007/BF00228194

Nielsen, J., Sinkjær, T., Toft, E., & Kagamihara, Y. (1994). Segmental reflexes and ankle joint stiffness during co-contraction of antagonistic ankle muscles in man. *Experimental Brain Research*, *102*(2), 350–358. http://doi.org/10.1007/BF00227521

Pal, G. P., Cosio, L., & Routal, R. V. (1988). Trajectory architecture of the trabecular bone between the body and the neural arch in human vertebrae. *The Anatomical Record*, *222*(4), 418–425. http://doi.org/10.1002/ar.1092220414

Penfield, W., & Rasmussen, T. (1950). The Cerebral Cortex of Man. A Clinical Study of Localization of Function.pdf. *Academic Medicine*. http://doi.org/10.1097/00001888-195009000-00037

Petersen, N., Morita, H., & Nielsen, J. (1998). Evaluation of reciprocal inhibition of the soleus H-reflex during tonic plantar flexion in man. *Journal of Neuroscience Methods*, *84*(1-2), 1–8. http://doi.org/10.1016/S0165-0270(98)00044-2

Pierrot-Desiligny, E., & Burke, D. (2012). *The Circuitry of the Human Spinal Cord: Spinal and Corticospinal Mechanisms of Movement* (1st ed.). Cambridge University Press.

Purves D, Augustine GJ, Fitzpatrick D, et al., E. (2001). Neuroscience. *Sunderland (MA): Sinauer Associates*.

Rexed, B. (1952). The cytoarchitectonic organization of the spinal cord in the cat. *The Journal of Comparative Neurology*, *96*, 414–495. http://doi.org/10.1002/cne.900960303

Rhoades, R., & Bell, D. (2012). *Medical Physiology: Principles for Clinical Medicine*. *Vasa*.

Ribot, C., Tremollieres, F., Pouilles, J. M., Louvet, J. P., & Guiraud, R. (1988). Influence of the menopause and aging on spinal density in French women. *Bone and Mineral*, *5*(1), 89–97.

Roy, F. D., Gibson, G., & Stein, R. B. (2012). Effect of percutaneous stimulation at different spinal levels on the activation of sensory and motor roots. *Experimental Brain Research*, *223*(2), 281–289. http://doi.org/10.1007/s00221-012-3258-6

Sherrington, C. S. (1906). *The Integrative Action of the Nervous System.* New York: Charles Scribner's Sons.

Shindo, M., Harayama, H., Kondo, K., Yanagisawa, N., & Tanaka, R. (1984). Changes in reciprocal ia inhibition during voluntary contraction in man. *Experimental Brain Research*, *53*(2), 400–408. http://doi.org/10.1007/BF00238170

Skedros, J. G., Mason, M. W., & Bloebaum, R. D. (1994). Differences in osteonal micromorphology between tensile and compressive cortices of a bending skeletal system: Indications of potential strain- specific differences in bone microstructure. *Anatomical Record*, *239*(4), 405–413. http://doi.org/10.1002/ar.1092390407

Standring, S. (2008). *Gray's Anatomy: The Anatomical Basis of Clinical Practice*. *Development* (Vol. 10). http://doi.org/10.1097/ACM.0b013e31819391e2

Uhrenholt, L., Hauge, E., Charles, a V., & Gregersen, M. (2008). Degenerative and traumatic changes in the lower cervical spine facet joints. *Scandinavian Journal of Rheumatology*, *37*(5), 375–84. http://doi.org/10.1080/03009740801998770

Appendix

Visualization of the Dataset

For visualization and analysis of datasets that were recorded at single stimuli and pairs of stimuli the following m-file was written, and executed in Matlab version R2013b. Imported data was the .asc output file from the recording software Dasylab 11.0. Calculated value vectors were exported to Microsoft Excel 14.2.3. Additional ratios, mean values and standard deviations were calculated in Excel.

```
%% Read in data

DataPath = '/Users/...';
PlotPath = '/Users/...';

% Function ListDirectory_v1 shows all files in DataPath folder, in
% order to run the code through all asc-files. With TAKEFILE a
% single, specific file of these can be selected
FNAME = ListDirectory_v1(DataPath,'asc');
TAKEFILE = 'RC';

for fIT = 1:length(FNAME)
    if ~isempty(strfind(FNAME(fIT).name,TAKEFILE))

        FNAMEtxt = FNAME(fIT).name;
        disp(['---------------- ' FNAMEtxt ' --------------------']);

        % Import file
        newData1 = importdata([DataPath FNAME(fIT).name]);

        % Create new variables in the base workspace.
        vars = fieldnames(newData1);
        for i = 1:length(vars)
            assignin('base', vars{i}, newData1.(vars{i}));
        end
```

```
% Data of 3200 frames were recorded per stimulation
% trigger (800 prior and 2399 after stimulation trigger).
% Here the raw data is split into a 3D-vector with frames,
% recorded channels, and trigger repetitions.
REP = round(length(data(:,1))/3200);
disp(['Repetitions: ' num2str(REP)]);

Data = zeros(3200,8,REP);

for rep = 1:REP
    Data(:,:,rep) = data(((1:3200)+(rep-1)*3200),2:9);
end
```

```
%% Subtract fitted sine function

% Find minimum, maximum, and zero crossing of interfered
% baseline in an interval between -40 to -10ms before
% stimulation, to generate a fitted sine function
temp1 = [0,1,0,-1,0,1];
for rep = 1:REP
 for ch =1:8
  for pIT = 1:length(Data(:,ch,rep))
      if Data(pIT,ch,rep) <= temp1(2)  && ...
              pIT/8-100 > -40 && pIT/8-100 < -10;
         temp1(1:2) = [pIT/8-100,Data(pIT,ch,rep)];
      end
      if Data(pIT,ch,rep) >= temp1(4) && ...
              pIT/8-100 > -40 && pIT/8-100 < -10;
         temp1(3:4) = [pIT/8-100,Data(pIT,ch,rep)];
      end
      if Data(pIT,ch,rep) >= -0.001 && ...
              Data(pIT,ch,rep) <= 0.001 && pIT/8-1
         temp1(5:6) = [pIT/8-100,Data(pIT,ch,rep)];
      end
  end
 values(rep,ch,1:6) = temp1;
 temp1 = [0,1,0,-1,0,1];
 end
end

% Generate and subtract a fitted sine function of the style
% P(t)=(max-min)/2*sin((t-t0)*2pi*f). The if-function checks
% the sine phase (if sin((tmax-t0)*2pi*f)>0) and shifts the
% phase by pi, if necessary
for rep = 1:REP
 for ch = 1:8
```

```
  for pIT = 1:length(Data(:,ch,rep))
      if sin((values(rep,ch,3)-values(rep,ch,5))/...
              20*2*pi()) > 0

         SData(pIT,ch,rep) = Data(pIT,ch,rep)-...
              (values(rep,ch,4)-values(rep,ch,2))/2*...
              sin((((pIT/8)-100))-values(rep,ch,5)))/...
              20*2*pi();
      else
         SData(pIT,ch,rep) = Data(pIT,ch,rep)-...
              (values(rep,ch,4)-values(rep,ch,2))/2*...
              sin(-(((pIT/8)-100))-values(rep,ch,5)))/...
              20*2*pi();
      end
   end
  end
end
```

%% **Find peaks**

```
% Seek for response peaks within the interval 10-33ms, and
% within the interval 45-80ms (for pairs of stimuli), and
% calculate their peak-to-peak amplitude
PeakR=(10+100)*8:(33+100)*8;
PeakR2=(45+100)*8:(80+100)*8;

for rep=1:REP;
 for ch=1:8
     peaks(:,ch,rep)=[min(SData(PeakR,ch,rep)) ...
         max(SData(PeakR,ch,rep)) min(SData(PeakR2,ch,...
         rep)) max(SData(PeakR2,ch,rep))];
     PTP(:,ch,rep) = [peaks(2,ch,rep)-peaks(1,ch,rep);...
         peaks(4,ch,rep)-peaks(3,ch,rep)];
 end
end
```

%% **Plot example of responses**

```
% A single repetition is selected with Actrep, the x-axis is
% defined as time in ms (-100 to 300ms related to
% stimulation), and ORD is a vector to arrange the subplots
% of left leg muscles on the left and right leg muscles on
% the right
time = (0:3199)/8-100;
Actrep = [19];

figure(1), FigureMaximize_v1; % Maximize figure window
```

```
ORD=[1 3 5 7 2 4 6 8];
muscles = {'left Q (mV)  ','left H (mV)  ','left TA ...
        (mV) ','left TS (mV) ','right Q (mV) ','right H...
        (mV) ','right TA (mV)','right TS (mV)'}

for ch = 1:8
 for rep = Actrep
     subplot(4,2,ORD(ch)), hold on,
     plot(time,SData(:,ch,rep),'m'),
     plot(0:0.1:80,0);
     xlim([0 80]); ylabel(muscles(ch));
     if ORD(ch)<7, set(gca,'xticklabel',[]);end
     if (ch) == 4, set(gca,'xtick',[0 20 40 60 80],...
           'xticklabel',{'0','20','40','60','80 ms'}, end
     if (ch) == 8, set(gca,'xtick',[0 20 40 60 80],...
           'xticklabel',{'0','20','40','60','80 ms'}, end
 end
end

% Save figure as high-resolution png-file
print(1,'-dpng', '-r600',[PlotPath 'example.png'])
```

```
%% Plot recruitment curves

% For recruitment curves one pair of stimuli and two single
% stimuli were delivered, and then stimulation intensity was
% increased in 5mA-increments. Stimulation intensities were
% recorded in channel 14 and are stored in xint. For each
% intensity step, PTP-amplitudes of the first of the pair of
% pulses and of the two single pulses are averaged (mean,
% standard deviation) and plotted against xint. Additionally
% PTP-amplitude of the second of the pair of pulses is
% written into the vector dp and plotted against xint.
i=1;
for ch = 1:8
 for rep=1:3:REP
     xint(i) = data(3150*rep,14) % Intensity steps
     mean(i,ch)=(PTP(1,ch,rep)+PTP(1,ch,rep+1)+...
           PTP(1,ch,rep+2))/3;
     sd(i,ch)=std(PTP(1,ch,rep:rep+2));
     dp(i,ch)=PTP(2,ch,rep);
     i=i+1;
 end
 i=1;
end

figure(2), FigureMaximize_v1;
```

```
        for ch = 1:8
            subplot(4,2,ORD(ch)), hold on,
            errorbar(xint,mean(:,ch),sd(:,ch),'r');
            plot(xint,dp(:,ch),'--ob','markersize',2);
            xlim([28,72]); ylabel(muscles(ch))
            if ORD(ch)<7, set(gca,'xticklabel',[]);end
            if (ch) == 4, xlabel('Stimulation intensity (mA)'), end
            if (ch) == 8, xlabel('Stimulation intensity (mA)'), end
        end

        print(2,'-dpng', '-r600',[PlotPath FNAMEtxt 'RC.png'])
```

```
    end
end
```

Analysis of Modification of PRR

For datasets that were recorded at sustained stimulation, the following fundamental m-file was written. For further analysis of control responses, muscular contraction signal, and the time evolution, the presented code was used as basis and adapted.

```
%% Read in data

% Reading in of data is identical with reading in data of
% single/pairs of stimuli shown before, but is not split into
% repetitions of stimulation triggers in this step
DataPath = '/Users/...';
PlotPath = '/Users/...';

FNAME = ListDirectory_v1(DataPath,'asc');

TAKEFILE = 'Dorsi_EMG';

for fIT = 1:length(FNAME)
    if ~isempty(strfind(FNAME(fIT).name,TAKEFILE))

        FNAMEtxt = FNAME(fIT).name;
        disp(['---------------- ' FNAMEtxt ' --------------------']);

        % Import file
        newData1 = importdata([DataPath FNAME(fIT).name]);

        % Create new variables in the base workspace.
        vars = fieldnames(newData1);
        for i = 1:length(vars)
```

```
    assignin('base', vars{i}, newData1.(vars{i}));
end

% Define samplerate from file
txtSampletime = textdata{5,1};
ind1 = strfind(txtSampletime, '0.00');
ind2 = strfind(txtSampletime, ' sec');
Sampletime = str2double(txtSampletime(ind1:ind2));
Samplerate = 1/Sampletime;
 disp(['Samplerate = ' num2str(Samplerate)]);
```

%% Cut Axes

```
% Data of the left leg channels are plotted in fig 101, and
% the section of interest is selected via clicks. Cut data
% are stored as Cdata
xCUT = [0 data(end,1)];
muscles = {'left Q (mV)  ','left H (mV)  ','left TA ...
        (mV) ','left TS (mV) ','right Q (mV) ','right H...
        (mV) ','right TA (mV)','right TS (mV)'}

figure(101),
for ch=2:5
    subplot(4,1,ch-1), plot(data(:,1),data(:,ch),'k');
    xlim(xCUT), ylabel(muscles(ch-1,:));
end

% Function to select min and max by clicks
[i,x1,y1]=ClickInGraph_v1(101);
[i,x2,y2]=ClickInGraph_v1(101);

xmin = find(data(:,1) >= x1,1);
xmax = find(data(:,1) >= x2,1);
close 101

Cdata = data(xmin:xmax,:);
xCUT = [Cdata(1,1) Cdata(end,1)];
```

%% Generate Marker Signal

```
% The marker signal that tags responses, which are
% conditioned by motor tasks, is set manually, or taken from
% recorded data (channel 15)
TIME = Cdata(:,1);

MP=[19.11 23.31 39.54 44.55 60.91 71]
```

```
T1 = find(TIME > MP(1),1);
T2 = find(TIME > MP(2),1);
T3 = find(TIME > MP(3),1);
T4 = find(TIME > MP(4),1);
T5 = find(TIME > MP(5),1);
T6 = find(TIME > MP(6),1);

Manual=Cdata(:,15)*0;
Manual(T1:T2) = 5*ones(size(T1:T2));
Manual(T3:T4) = 5*ones(size(T3:T4));
Manual(T5:T6) = 5*ones(size(T5:T6));

MARKERSignal = Manual; % Manually defined marker
MARKERSignal2 = Cdata(:,15); % Recorded marker

% Set range for y-axis of each channel for further plots.
% Limits of the y-axis are the global signal minimum and
% maximum found in the interval between 5s and the end of
% Cdata
Range = 5*Samplerate:length(Cdata);
for ch=2:9
YRange(ch,1:2)=[min(Cdata(Range,ch)) max(Cdata(Range,ch))];
end
```

```
%% Apply notch filter

% Notch filter is only applied to improve data view, but
% not for further calculations, since it distorts peak-to-
% peak-amplitudes of responses. Notch-filtered data is
% stored as Ndata
fspec  = fdesign.notch('N,F0,Q,Ap',6,50,10,1,Samplerate);
d=design(fspec);
Ndata=Cdata;
Ndata(:,2:9)= filter(d,Cdata(:,2:9));
```

```
%% Detect stimulation artifact

% Stimulation pulses are defined with the aid of stimulation
% artifacts that were recorded with the trigger electrodes
% in the chest area (channel 13). Absolute values of the
% trigger channel are compared to a threshold to find the
% artifacts
Trigger = Cdata(:,13);
THRESHOLD = 1;
StimPulseIndex = find(abs(Trigger) >= THRESHOLD);
```

```
% Calculate the stimulation rate from detected stimulation
% pulses
StimRate = 10/round(max(diff(StimPulseIndex))/800);

disp(['Stimulation Rate: ' num2str(StimRate) ' pps'])
StimRateCount = Samplerate/StimRate;

% Stimulation pulses are now defined at the rising slope of
% the artifacts. The next stimulation pulse is seeked after
% a refractory period of tmp > 0.8*stimulation rate (to
% eliminate points at the descending slope of the artifact)
tmp = find(diff(StimPulseIndex)>StimRateCount*0.8);
StimPulseIndex = [StimPulseIndex(1); StimPulseIndex(tmp+1)];

% Set stimulation points are plotted together with the
% artifacts and checked
figure, plot(abs(Trigger));
hold on, plot(StimPulseIndex, abs(Trigger...
            (StimPulseIndex))*0.000001+THRESHOLD, 'r+');
```

```
%% Plot trigger windows

col='rgbcmky';
NumOfPulses = length(StimPulseIndex);
plotRange = -40:400; % Interval -5ms to 50ms
plotRangeTime = plotRange/8;
SPO = [1 3 5 7 2 4 6 8];

tmp1=nan(length(plotRange), length(data(1,:)),NumOfPulses);
tmp2=nan(length(plotRange), length(data(1,:)),NumOfPulses);

% Data is split into trigger windows of -5 to 50ms
% (plotRange) with regard to the stimulation pulses and
% further distinguished between unconditioned responses, and
% responses, conditioned by motor tasks
for ch = 2:9
 for pIT = 1:NumOfPulses-1
     if MARKERSignal(StimPulseIndex(pIT)) > 2.5
     tmp1(:,ch,pIT)=Cdata(plotRange+StimPulseIndex(pIT),ch);
     else
     tmp2(:,ch,pIT)=Cdata(plotRange+StimPulseIndex(pIT),ch);
     end
  end
```

```
 end

% For each channel, unconditioned and conditioned case,
% trigger windows are overlaid and plotted in various
% colors. Figure 101 shows channels of the left leg
figure (101), FigureMaximize_v1;
for ch = 2:5
 for pIT = 1:NumOfPulses-1
     subplot(4,3,SPO(ch+3)), hold on,
     plot(plotRangeTime,tmp1(:,ch,pIT),col(mod(pIT,6)+1));
     ylim(YRange(ch,:));
     if ch == 5, xlabel('conditioned'); end

     subplot(4,3,SPO(ch-1)), hold on,
     plot(plotRangeTime, tmp2(:,ch,pIT),col(mod(pIT,6)+1));
     ylim(YRange(ch,:));
     ylabel(muscles(ch-1,:));
     if ch == 5, xlabel('unconditioned'); end
 end
end

figure (102), FigureMaximize_v1; % Channels of the right leg
for ch = 6:9
 for pIT = 1:NumOfPulses-1
     subplot(4,3,SPO(ch-1)), hold on,
     plot(plotRangeTime,tmp1(:,ch,pIT),col(mod(pIT,6)+1));
     ylim(YRange(ch,:));
     if ch == 5, xlabel('conditioned'); end

     subplot(4,3,SPO(ch-5)), hold on,
     plot(plotRangeTime,tmp2(:,ch,pIT),col(mod(pIT,6)+1));
     ylim(YRange(ch,:));
     ylabel(muscles(ch-1,:));
     if ch == 5, xlabel('unconditioned'); end
  end
 end

print(101,'-dpng', '-r600',[PlotPath 'trigg_L.png'])
print(102,'-dpng', '-r600',[PlotPath 'trigg_R.png'])
```

```
%% Calculate mean/sd curve

SPO2 = [1 3 5 7 2 4 6 8];
```

```
% From the overlaid curves a mean curve and standard
% deviation is calculated, for unconditioned and conditioned
% case separately.
figure (103), FigureMaximize_v1;
for ch = 2:9
    MEAN1 = nanmean(tmp1(:,ch,:),3); % Conditioned pulses
    SD1 = nanstd(tmp1(:,ch,:),1,3);
    MEAN2 = nanmean(tmp2(:,ch,:),3); % Unconditioned pulses
    STD2 = nanstd(tmp2(:,ch,:),1,3);

    % Seek reflex response maximum and minimum in the mean
    % curve within an interval of 8ms to 50ms and calculate
    % the peak-to-peak amplitude
    PeakR = (8+5)*8:length(tmp1);
    for pIT=1:NumOfPulses
        Amp(ch-1,1:3)=[max(MEAN2)-min(MEAN2) max(MEAN1)-...
              min(MEAN1)
    end

   % Plot mean curve and standard deviation curves
   subplot(4,2,SPO2(ch-1))
   hold on, plot(plotRangeTime,MEAN1,'r'),
   ylabel(muscles(ch-1,:)); ylim(YRange(ch,:));
          plot(plotRangeTime,MEAN1-STD1, ':m');
          plot(plotRangeTime,MEAN1+STD1,':m');
   plot(plotRangeTime,MEAN2,'b');
          plot(plotRangeTime,MEAN2-STD2,':c');
          plot(plotRangeTime,MEAN2+STD2,':c');
end
print(103,'-dpng', '-r600',[PlotPath 'means.png'])
```

```
%% Delete stimulation artifact

% For a clear view of the whole dataset, the simulation
% artifacts are deleted from the overall signal curve.
% Therefore the signal is set to zero in a range from -2ms to
% 8ms for every stimulation pulse
delArtRange = -16:64;
for pIT = 1:NumOfPulses
    Cdata(delArtRange+StimPulseIndex(pIT),2:9)=0;
end
```

```
%% Plot all data

        figure(201), FigureMaximize_v1;
        for ch = 2:9 % Plot channels of left leg
            if ch<6, subplot(5,2,SPO2(ch-1)), plot(Cdata(:,1),...
                  Cdata(:,ch),'r'),
            xlim(xCUT),
            ylim(YRange(ch,:)),
            ylabel(muscles(ch-1,:));

        else % Plot channels of right leg
            subplot(5,2,SPO2(ch-1)), plot(Cdata(:,1),...
                  Cdata(:,ch),'b'),
            xlim(xCUT),
            ylim(YRange(ch,:));
        end

        % Plot marker signal
        for p=9:10 subplot(5,2,p), plot(Cdata(:,1),...
                    MARKERSignal,'r'),
            if p==9, ylabel('Marker'); end,
            xlim(xCUT),
            ylim([-0.5 5.5]),
            xlabel('time (s)');
        end

        print(201,'-dpng', '-r600',[PlotPath 'all.png'])

%% Calculate RMS of contraction signal

        % Muscular contraction is evaluated in an interval of 150ms
        % to 270ms after stimulus.
        RMSRange=2800:3760;

        % Create vector with conditioned pulses only
        i=1;
        for pIT=1:NumOfPulses
            if MARKERSignal(StimPulseIndex(pIT))>2.5
               condPulses(i)=pIT;
               i=i+1;
            end
        end

        % Root mean square curves of muscular contraction will be
```

```
        % calculated for each of the three repetitions of a motor
        % task separately. Therefore the stimulation pulses at the
        % six edges of the marker signal are seeked.
        i=2;
        edges(1,1)= condPulses(1); edges (3,2)= condPulses(end);
        for pIT=1:length(condPulses)-1
            if condPulses(pIT+1) > condPulses(pIT)+5,
            edges(i,1)=condPulses(pIT+1);
            edges(i-1,2)=condPulses(pIT)
            i=i+1;
            end;
        end

        % Calculation of root mean square curves of muscular
        % contraction for all three repetitions of motor tasks and
        % for control responses
        for ch= 2:9
            RMS1(:,ch)=sqrt(nanmean(tmp1(RMSRange,ch,edges(1,1):...
                  edges(1,2)).^2,3));
            RMS2(:,ch)=sqrt(nanmean(tmp1(RMSRange,ch,edges(2,1):...
                  edges(2,2)).^2,3));
            RMS3(:,ch)=sqrt(nanmean(tmp1(RMSRange,ch,edges(3,1):...
                  edges(3,2)).^2,3));
            RMSc(:,ch)=sqrt(nanmean(tmp3(RMSRange,ch,:).^2,3));

            % Calculation of time average of RMS curves
            RMSmeans(ch-1,:)=[nanmean(RMSc(:,ch),1) ...
                  nanmean(RMS1(:,ch),1) nanmean(RMS2(:,ch),1) ...
                  nanmean(RMS3(:,ch),1)];
        end
    end
end
```